

NASE Natural Sciences and Engineering Bulletin



e-ISSN: 3023-8293



Journal Owner

Gaziantep University

Editor-in-Chief

Prof. Dr. ıgdem AYKAÇ
Gaziantep University, Gaziantep, Türkiye
Director of Graduate School of Natural and Applied Sciences
editornase@gaziantep.edu.tr

Associate Editors

Prof. Dr. Tolgay KARA
Gaziantep University, Gaziantep, Türkiye
editoreng@gaziantep.edu.tr

Assoc. Prof. Dr. Mine MENEKŞE YILMAZ
Gaziantep University, Gaziantep, Türkiye
editornat@gaziantep.edu.tr

Language Editor

Prof. Dr. Emrah CİNKARA
Gaziantep University, Gaziantep, Türkiye

Technical and Ethic Editors

Dr. Esra ÜNLÜ
Sibel TUTAR

Section Editors

| | |
|---|---|
| Prof. Dr. Ali Coşkun DALGIÇ | Gaziantep University Food Engineering |
| Prof. Dr. İlkey GÜVEN | Gaziantep University Department of Mathematics |
| Prof. Dr. Mustafa ÖZAKÇA | Gaziantep University Civil Engineering |
| Prof. Dr. Necla KARA TOĞUN | Gaziantep University Mechanical Engineering |
| Prof. Dr. Nuran DOĞRU | Gaziantep University Electrical and Electronics Engineering |
| Prof. Dr. Serap ULUSAM SEÇKİNER | Gaziantep University Industrial Engineering |
| Prof. Dr. Vural Emir KAFADAR | Gaziantep University Physics Engineering |
| Prof. Dr. Züleyha DEĞİRMENCİ | Gaziantep University Textile Engineering |
| Assoc. Prof. Dr. Adile AKPINAR | Gaziantep University Department of Biology |
| Assoc. Prof. Dr. Derya KAPUSUZ YAVUZ | Gaziantep University Material Science and Engineering |
| Assoc. Prof. Dr. Meriç ŞİMŞEK ASLANOĞLU | Osmaniye Korkut Ata University Food Engineering |
| Assist. Prof. Dr. Abdullah KARGIN | Gaziantep University Department of Mathematics |
| Assist. Prof. Dr. Dilek BÜYÜKBEŞE YAYLA | Gaziantep University Department of Chemistry |
| Assist. Prof. Dr. Emre KARA | Gaziantep University Aerospace Engineering |

Scientific Board

| | |
|--|---|
| Prof. Dr. Ali Fırat ÇABALAR | Gaziantep University Civil Engineering |
| Prof. Dr. Ali Hussien Mary KİNANİ | University of Baghdad Mechatronics Engineering |
| Prof. Dr. Ayşegül İYİDOĞAN | Gaziantep University Department of Chemistry |
| Prof. Dr. Canan CAN | Gaziantep University Department of Biology |
| Prof. Dr. Deniz ÇEKMECELİOĞLU | Penn State University Agricultural and Biological Engineering |
| Prof. Dr. Hüseyin TOKTAMIŞ | Gaziantep University Optic Engineering |
| Prof. Dr. İbrahim BÜYÜKYAZICI | Ankara University Department of Mathematics |
| Prof. Dr. Osman ERKMEN | İstanbul Arel University Department of Nutrition and Dietetics |
| Prof. Dr. Ömer EYERCİOĞLU | Gaziantep University Mechanical Engineering |
| Prof. Dr. Recep YUMRUTAŞ | Gaziantep University Mechanical Engineering |
| Prof. Dr. Remziye Aysun KEPEKÇİ | Gaziantep University Department of Biology |
| Prof. Dr. Sedat SAYAR | Mersin University Food Engineering |
| Prof. Dr. Sema KAYHAN | Gaziantep University Electrical and Electronics Engineering |
| Prof. Dr. Uğur GÜL | Hacettepe University Department of Mathematics |
| Assoc. Prof. Dr. Abdul Hafez ABDUL HAFEZ | Hasan Kalyoncu University Software Engineering |
| Assoc. Prof. Dr. Hüseyin YAĞLI | Gaziantep University Mechanical Engineering |
| Assoc. Prof. Dr. Mustafa Güven GÖK | Gaziantep University Material Science and Engineering |
| Assist. Prof. Dr. Muhammad Umair KHAN | Pakistan National University of Technology Computer Engineering |

EDITORIAL



I am excited to announce the second issue of Natural Sciences and Engineering Bulletin (NASE) which started to publish in May 2024, as the journal of Graduate School of Natural and Applied Sciences of Gaziantep University.

The positive feedback we received after our first issue has confirmed that we are on the right path and has motivated us to further improve the journal. One of the main goals of our journal is to provide medium for sharing and disseminating technological developments, new ideas and research results in the fields of natural sciences and engineering, within the rules

of ethics and scientific understanding, as an indexed journal. We believe that we are one step closer to this goal with this issue.

The issue contains five articles from the disciplines of metallurgical and materials engineering, industrial engineering, electrical and electronics engineering and food engineering. All articles have been peer-reviewed using the double-blind review system. As the Editor-in-Chief, I would like to express my gratitude to all authors and reviewers who contributed to this issue. I would like to extend my special thanks to NASE Associate Editors Assoc. Prof. Dr. Mine MENEKŞE YILMAZ and Prof. Dr. Tolgay KARA for their valuable efforts. I would also like to thank Prof. Dr. Emrah CİNKARA, NASE Language Editor, and Dr. Esra ÜNLÜ and Sibel TUTAR, Technical and Ethical Editors, for their valuable contributions.

I would like to invite you to submit your original research papers to NASE in the future so that this journal can fulfill its mission and benefit the scientific community. On behalf of the editorial board, authors and reviewers, I would like to welcome you to our second NASE issue.

Prof. Dr. Çiğdem AYKAÇ

Editor-in-Chief

Director of Graduate School of Natural and Applied Sciences of Gaziantep University

CONTENTS

Research Article

- 1-16 Mn-Cu Based Coating on Graphite Cycling in Alkaline and Neutral Electrolytes for Flexible Supercapacitor Applications**
Abdulcabbar YAVUZ, Hüseyin FAAL
- 17-26 Leveraging Latent Dirichlet Allocation and Fuzzy Clustering for Identifying Key UAV Applications in Disaster Response**
Zeynep YÜKSEL, Nazmiye ELİGÜZEL, Süleyman METE
- 27-37 Sensitive Microwave Sensor for Adulteration Detection in Olive Oil**
Hüseyin KORKMAZ, Uğur Cem HASAR
- 38-56 Understanding Consumer Preferences in Kahramanmaraş for Bulgur and Bulgur Products**
Reyyan ŞİMŞEK, Sevim KAYA
- 57-77 A Hybrid Plant-Soil Electrical Analogy and Control Engineering Framework for Dynamically Modeling Cancer Cell Growth in an Elastic Environment**
Bayram Arda KUŞ, Mustafa GÜRBÜZ

Mn-Cu Based Coating on Graphite Cycling in Alkaline and Neutral Electrolytes for Flexible Supercapacitor Applications

Abdulcabbar YAVUZ^{1*}, Hüseyin FAAL²

Keywords

*Flexible Electrode,
Energy Storage,
Ionic Liquid,
Deep Eutectic
Solvent,
Potential Window*

Abstract – Notable advancements have been made in the advancement of technologies utilizing flexible screens and sensors. However, the progress in the field of flexible energy storage devices has been comparatively restricted. Research on flexible energy storage electrodes is necessary because of the crucial role of flexibility and stretchability in wearable, biomedical, and portable electronic devices. This study examines the electrochemical characteristics of graphite filaments covered with alloy which possesses flexibility. Electrochemical synthesis of Mn-Cu-based modified graphite was achieved using a deep eutectic solvent at varying static voltages. Analyzed in this study was the electrochemical deposition performance of films in Ethaline deep eutectic solvent, as well as the subsequent cycling of the resultant electrodes in a KOH, Na₂SO₄ and the mixture of KOH and Na₂SO₄ electrolytes. The potential window used for this analysis was increased to 1.5 V. The graphite substrate, coated with Mn-Cu through the application of a voltage of -1.9 V, exhibited a length capacitance of 109 mF cm⁻² when cycling electrolyte is the mixture of KOH and Na₂SO₄. The film exhibited extensive surface covering and showed promise for utilization in energy storage applications.


1. Introduction

As we approach the end of the first quarter of the twenty-first century, it is obvious that the increase in energy and electricity consumption has produced a serious issue. Rapid population increase and changing consumer habits are the two main causes of this global problem because a rapid population could spend more energy. Additionally, daily life in many countries has been changed due to technological improvement. Almost all technological devices (mobile phones, computers, electric vehicles, household goods, etc.) are based on energy consumption. A sizeable amount of the total energy consumption is jointly accounted for by the industrial, transportation, and construction sectors. Global energy demand could be anticipated to double by 2050 and triple by the end of the century. Increasing the efficiency of the current traditional energy systems alone might not be sufficient to meet this demand sustainably (Guney and Tepe, 2017; Mitali et al., 2022).

It seems that conventional energy sources have harmful environmental effects that lead to ecological problems such as acid rain, ground-level ozone production, air and water pollution, global warming, and ozone layer depletion. The quick depletion of available fossil fuel resources has also compelled energy supply firms around the world to think about ways to increase the efficiency and economy of the use of current energy sources, as well as to take action to develop new energy resources. Renewable energy sources were created as a result of overcoming these difficulties and improving the sustainability of energy storage techniques, and they offer significant advantages both economically and environmentally (Hannan et al., 2021; Yang et al., 2018).

In terms of energy usage and power management, energy storage technologies are crucial. It contributes to a sustainable, safe, and clean way of future energy needs. There are numerous techniques for energy storage

^{1*}**Corresponding Author.** Gaziantep University, Faculty of Engineering, Department of Metallurgical and Materials Engineering, Sehitkamil, 27310 Gaziantep, Turkey. E-mail: ayavuz@gantep.edu.tr  ORCID: 0000-0002-7216-0586

²Gaziantep University, Graduate School of Natural and Applied Sciences, Materials Science and Engineering, Sehitkamil, 27310 Gaziantep, Turkey. E-mail: faal720@gmail.com  ORCID: 0009-0004-7171-8308

Citation: Yavuz, A. and Faal, H. (2024). Mn-Cu based coating on graphite cycling in alkaline and neutral electrolytes for flexible supercapacitor applications. *Natural Sciences and Engineering Bulletin*, 1(2), 1-16.

including capacitors and supercapacitors (Luo et al., 2015; Sharma et al., 2019); sodium-sulfur (NaS), lithium-ion, nickel-cadmium (Ni-Cd) and lead-acid batteries (Kalhammer and Schneider, 1976); fuel cells, mechanically pumped hydropower (Luo et al., 2015), compressed air energy storage systems (CAES), and flywheels. Supercapacitor technologies with fast charge-discharge capabilities have become increasingly prominent as a case of the need for high-power applications, maintaining energy quality, and satisfying continuous energy demand (Ho et al., 2010). They have the potential to serve as a more eco-friendly form of energy storage, as they generally contain fewer chemicals that are harmful to the environment and can be recycled. However, it is important to note that while they may reduce the presence of toxic substances, this does not entirely eliminate the possibility of such chemicals being present in certain formulations (Wen et al., 2015). Supercapacitors might, therefore, be crucial components of energy storage systems in the future (González et al., 2016). Some supercapacitors are based on the principle of electrostatic storage, which is achieved by applying a voltage between two electrodes. These kinds of supercapacitors are referred to as electric double-layer capacitors (EDLC). Energy could be stored through an electrolyte solution between two solid electrolytes. Pseudocapacitors and hybrid supercapacitors (their details are given in Section 2) are other main categories of supercapacitors within the context of energy storage techniques (Li et al., 2008).

Electric double-layer capacitors (EDLCs) improve storage capacities by increasing electrical conductivity, increasing the surface area of the electrodes, and reducing pore size (Arumugam et al., 2023). Pseudocapacitors store energy by reversible multi-electron redox faradaic reactions (Sahin et al., 2020). Pseudocapacitors could have higher specific capacitance values, while EDLCs generally exhibit greater cyclic stability and superior power density and energy density performance. As the name implies, hybrid systems also give the option of combining the power source of a capacitor-like electrode (EDLC structure) with the energy source of a battery-like electrode (pseudocapacitor) in the same cell (Iro et al., 2016). The EDLC generally consist of carbon-based materials. The materials of pseudocapacitors are hydroxide, sulphide and oxide-based metals/alloys such as Mn (Mohanty et al., 2023) and Cu (Sayyed et al., 2023). Additionally, conducting polymers are also the material of pseudocapacitors. When different materials belonging to EDLC and pseudocapacitors are combined, hybrid supercapacitors can be obtained.

The main components with a significant impact on the performance of supercapacitors are electrodes and electrolytes (Yavuz et al., 2022). The elements that store and release this energy are identified as electrodes (Baig et al., 2023). Electrolytes are defined as those that provide energy storage and release processes at the interface and facilitate the movement of ions. Therefore, the selection of the correct electrolyte and electrode is important for supercapacitors' performance and efficiency (Iro et al., 2016). Therefore, we have focused on the combination of both electrodes and electrolytes in this study.

The material, structure, conductivity, surface area and electrochemical properties of the electrode are critical factors that influence the electrode's selection. For instance, a combination of EDLC and pseudocapacitive materials could be fabricated for high-performance supercapacitors. In this study, active alloy-coated flexible graphite electrodes have been studied to analyse supercapacitor performance. These coatings could create a larger surface area of the electrode and increase the interaction with the electrolyte. Thus, electrode selection could increase the energy storage capacity by enabling more interaction on the electrolyte interface of the electrodes (Arumugam et al., 2023).

Deep eutectic solvents (DESs) and ionic liquids (ILs) have shared characteristics, such as being liquid at very low temperatures and exhibiting little volatility; they are classified as separate categories of solutions. Ionic liquids are purely ionic compounds, usually consisting of a sizable organic cation and an inorganic or organic anion. Deep eutectic solvents are created by the interaction of a hydrogen bond donor and a hydrogen bond acceptor. This often leads to the formation of a mixture consisting of a quaternary ammonium salt and a hydrogen bond donor, such as urea or aromatic acid. By causing a depression in the melting point, this interaction results in the formation of a eutectic mixture. Contrary to ILs, DESs are not completely ionic and are, hence, more convenient and cost-effective to manufacture. Various electrolytes such as DESs, sodium sulfate (Na_2SO_4) (Purushothaman et al., 2012), potassium hydroxide (KOH) (Brisse et al., 2018), a mixture of sodium sulfate + potassium hydroxide ($\text{Na}_2\text{SO}_4 + \text{KOH}$) (HCl) (Niknam et al., 2022) and hydrochloric acid could be used for electrodeposition and cycling of electrodes.

The main aim of the study is to analyze the interactions between selected electrodes and electrolytes and how their variations could influence supercapacitor performance. This could be used for the development and optimization of supercapacitor technology. In this research, electrodes, electrolytes, and the interactions between these two components were investigated. The resulting data could be used to evaluate the parameters affecting supercapacitor properties. This research could contribute to our understanding of how these electrolytes and electrodes could affect supercapacitor performance. Mn-Cu-based electrodes were electrodeposited on the graphite layer. After the coating process, modified electrodes were transferred to various electrolytes such as sodium sulfate (Na_2SO_4), potassium hydroxide (KOH), sodium sulfate and potassium hydroxide mixture ($\text{Na}_2\text{SO}_4 + \text{KOH}$) and hydrochloric acid (HCl) in order to compare their electrochemical performance. This study is the first to electrodeposit Mn-Cu alloy onto a graphite layer using a deep eutectic solvent. Furthermore, it is the first to investigate the electrochemical performance of this alloy in various electrolytes, including alkaline, acidic, and neutral solutions, with a particular focus on the novel $\text{Na}_2\text{SO}_4 + \text{KOH}$ mixture.

2. Materials and Methods

A solution of Ethaline deep eutectic solvent was created by combining two parts ethylene glycol with one part choline chloride, then heating the mixture at a temperature of 65°C for a duration of 45 minutes. A solution containing 0.5 M MnCl_2 and 0.5 M CuCl_2 was produced using an Ethaline deep eutectic solvent. Due to the rapid solubility of both metal chlorides in Ethaline deep eutectic solvent, the mixing duration was limited to a short period of time (usually 10 minutes). A solution was prepared by combining equal quantities of 1 M MnCl_2 and 1 M CuCl_2 in a glass beaker at a temperature of 65°C . The resulting solution contained 0.5 M MnCl_2 and 0.5 M CuCl_2 . The graphite electrodes were directly submerged in Ethaline in order to electrodeposit Mn-Cu alloys. No pretreatment step was applied. Cyclic voltammogram curves were generated for the deposition baths containing pure Ethaline, Ethaline with Mn^{2+} ions, and Ethaline with Cu^{2+} ions. These curves were used to analyze the electrochemical deposition behaviour of pure Ethaline, Mn, Cu, and Mn-Cu in Ethaline on graphite electrodes. Three distinct static voltages (-1.6 V, -1.9 V, and -2.2 V) were individually supplied to the graphite electrodes for a duration of 300 seconds at a temperature of 65°C in order to produce the alloys.

A three-electrode system was used for the growth and electrochemical characterisation of the electrodes. The reference electrode containing an AgCl layer covered on Ag wire and a saturated potassium chloride electrolyte in a glass body is used in aqueous solutions. In deep eutectic solvents (DESSs), a silver wire is used as a direct reference electrode. The counter electrode was titanium-coated ruthenium mesh. Graphite-coated tape was used as a working electrode. The potentiostat was controlled using a VersaSTAT 3, Princeton Applied Research model potentiostat manufactured by AMATEK Company (USA). The list of chemicals utilized to produce the findings in this study is manganese (II) chloride dihydrate ($\text{MnCl}_2 \cdot 2\text{H}_2\text{O}$, >99, Merck), copper (II) chloride dihydrate ($\text{CuCl}_2 \cdot 2\text{H}_2\text{O}$, >99, Merck), choline chloride ($\text{HOC}_2\text{H}_2\text{N}(\text{CH}_3)_3\text{Cl}$, >99, Alfa Aesar), mono ethylene glycol, >99, Nebioğlu), potassium hydroxide (KOH, >90, Tekkim), sodium sulfate (Na_2SO_4 , >90, Merck).

The preparation of the graphite-coated flexible tape electrode is presented in Figure 1. The first step in cleaning the surface of the bulk graphite substrate is to carefully wipe the main graphite surface from which the samples will be taken with a clean napkin. This process ensures that any visible dirt, dust, or debris on the surface is removed (Figure 1a). After the cleaning process is completed, 600 mesh sandpaper is used to make the surface smoother. At this stage, the graphite surface is carefully sandpapered until it has a flat structure like a transom. In this way, the substrate surface gains a smooth and homogeneous structure (Figure 1b). After the sanding process, the graphite surface reaches a clean and flat structure. Now, for basic processing, transparent tape is used to cover the substrate surface and prepare it for further processing. This tape is carefully placed on the graphite surface, and the taping process is performed (Figure 1c). The tape is adhered to the graphite surface by pressing lightly. This pre-bonding step ensures that the tape adheres properly to the surface. The tape is well adhered to the graphite surface. This step ensures that the tape adheres more firmly to the surface and eliminates possible air bubbles. Finally, the tape is completely adhered to the graphite surface, leaving no loose edges or gaps. This step allows the tape to form a tight bond with the graphite surface (Figure 1d). As a result of the banding process, the graphite surface is covered with tape, and a flexible graphite film is formed. This flexible graphite film is removed from the graphite surface to obtain a thin, flexible substrate (Figure 1e & 1f). The samples are prepared

by measuring and cutting the flexible graphite-coated tape (Figure 1g) to the desired size (1 cm²). These samples have been used as current collectors (Figure 1h & 1i).

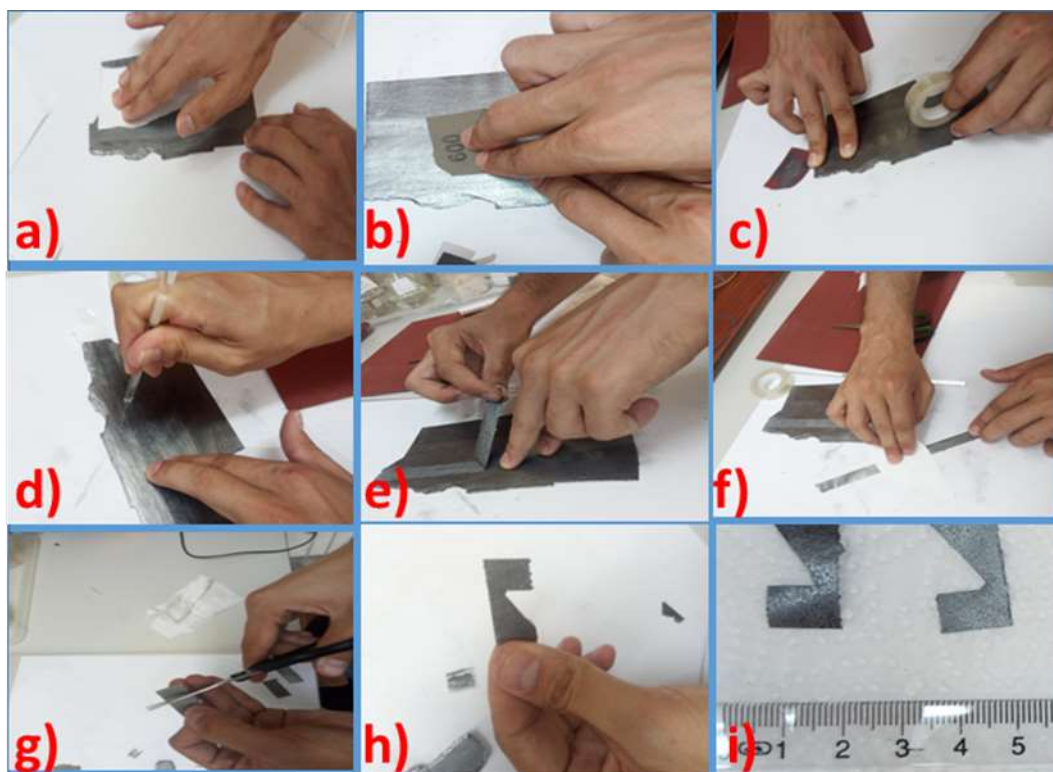


Figure 1. Photographs showing the preparation of flexible tape graphite substrate; a) Cleaning the surface of the graphite; b) Sandpapering the surface of the graphite; c) Covering the substrate surface with a tape; d) Adhered to the graphite surface by pressing lightly with glass rod; e) Removing thin flexible graphite film from the graphite surface; f) Homogenising the surface of the graphite tape; g) Cutting the flexible graphite tape; h) Obtaining a graphite film sample of 1 cm² size; i) The obtained samples are preserved for the electrode coating test steps after quality standard control.

Once all the sodium sulfate (Na₂SO₄) or potassium hydroxide (KOH) were completely dissolved in the water, 1 M Na₂SO₄ and 1 M KOH solutions were obtained. As a final step, the equal volumes of these two solutions were mixed in a new beaker, resulting in an electrolyte solution consisting of 0.5 M KOH + 0.5 M Na₂SO₄. This meticulously prepared electrolyte solution was then ready for use in the experimental procedures. The modified electrodes were then submerged in solutions containing potassium hydroxide (KOH) and sodium sulfate (Na₂SO₄), as well as solutions containing combinations of these two electrolytes in equal amounts, to reveal their electrochemical behaviours. By utilizing chronocoulometric, chronoamperometric, cyclic voltammetric, and cyclic polarisation techniques, the electrochemical properties of both pure graphite and coated graphite electrodes were examined. These attributes included capacitance calculations, stability, energy storage capabilities, and rate-limiting reactions.

3. Results and Discussion

3.1. Growth of electrodes

The chronocoulometric analysis method was used to apply -1.6 V, -1.9 V, and -2.2 V potentials to graphite-based samples in an Ethaline solution containing 0.5 M MnCl₂ + CuCl₂ at 60 °C for 150 seconds. This allowed us to determine the growth of manganese and copper alloys by electrochemical deposition on the graphite electrode. The red line in Figure 2a is the cyclic voltammogram responses of graphite in Ethaline, including Cu²⁺ ions. Oxidation and reduction of copper are observed at around -0.5 V. Redox reactions of Mn²⁺ in the electrolyte have been observed (see green line of Figure 2a) with the reduction of Mn starting at around -1.5 V, which could be associated with the initial stages of Mn deposition and growth. These peaks do not belong to the

graphite electrode as the black line in Figure 2b, which is a cyclic voltammogram of graphite in pure Ethaline, does not illustrate redox peaks. Oxidation and reduction peaks of Ethaline having both ions (Cu^{2+} and Mn^{2+}) appear (see blue line in Figure 2b). The application of a potential less than 1.5 V could cause the growth of Mn-Cu alloy. The growth of a manganese and copper alloy on a graphite electrode over 150 seconds at potentials of -1.6 V, -1.9 V, and -2.2 V, as well as the alloy's capacity and charging period. The electrochemical plating procedure can be optimized using this data to produce the optimum manganese copper alloy for graphite electrodes. Chronocoulometric results were obtained by the integration of chronoamperometry data.

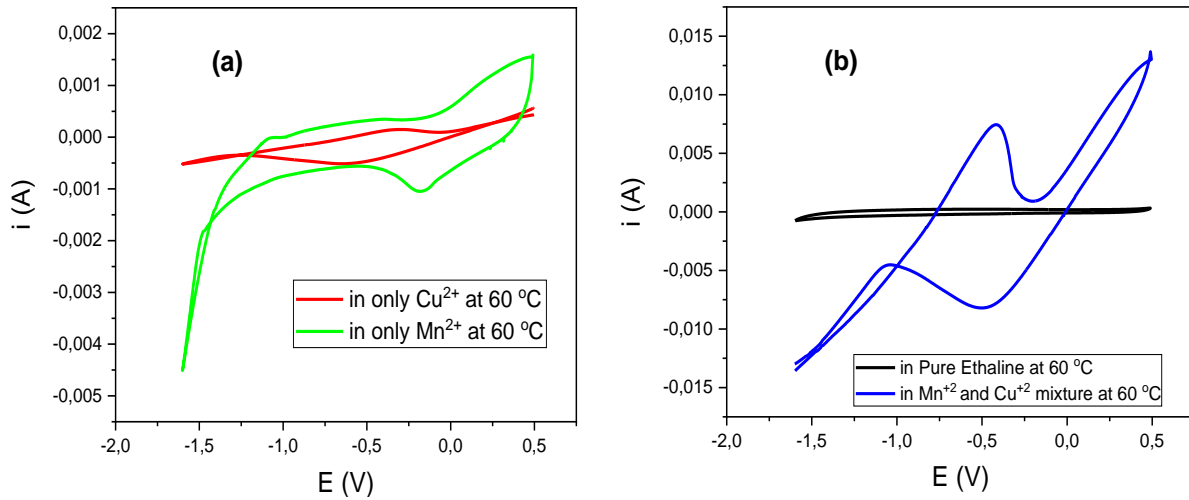


Figure 2. Cyclic voltammogram results of bare graphite in a) Ethaline having CuCl_2 (red line) and Ethaline having MnCl_2 (red line) and b) pure Ethaline (black line) and Ethaline having both CuCl_2 and MnCl_2 (blue line). The scan rate and temperature of the experiments are 50 mV s^{-1} and $60 \text{ }^\circ\text{C}$.

The chronoamperometry method was employed for electrodeposition of manganese and copper metals onto graphite tapes (Figure 3a). Chronocoulometric data of the electrochemical deposition of a manganese-copper-based layer on the graphite electrode in Figure 3b. The charge change will be, accordingly, a stabilized line over time if the current flux approaches a constant value with time. This shows that the electrochemical reaction has reached equilibrium, and the current is stable.

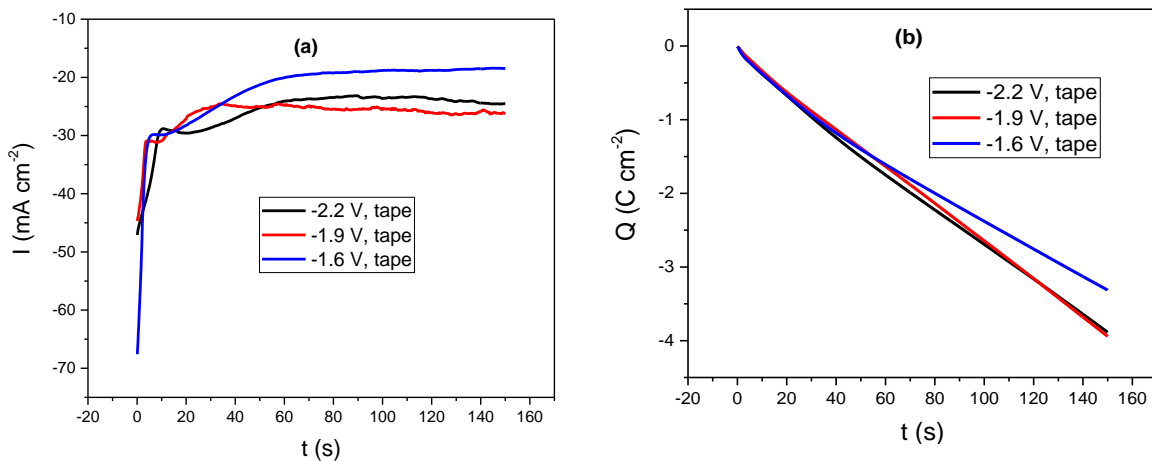


Figure 3. The chronoamperometry and chronocoulometry responses of Mn-Cu growth at $60 \text{ }^\circ\text{C}$ for 150 seconds a) chronoamperometry data of Mn-Cu alloy growth on graphite coated tape by application of -2.2 V (black line), -1.9 V (red line) and -1.6 V (blue line), and b) chronocoulometry data of the growth given in panel a.

It is known that the current graph expresses the change in the amount of charge (coulomb) carried in a certain time. For this reason, over time, a constant current results in a steady build-up of charge. When the current is high, the charge accumulation starts quickly and then increases more quickly over time. This indicates that the electrochemical process is proceeding steadily and that the current does not change with time.

3.2. Electrochemical Characterisation of the Electrodes

3.2.1. Mn-Cu electrodeposited by application of -1.6 V

In the initial stage, graphite surfaces were coated with Mn-Cu films under a constant potential of -1.6 V using a solution containing 0.5 M Mn^{+2} and 0.5 M Cu^{+2} ions in Ethaline. This process enabled the deposition of metal alloys onto the graphite surfaces. Then, the electrodes were immersed in different electrolyte liquids determined as 1 M Na_2SO_4 and 1 M HCl in the range of -1 to 0.5 V with the same scanning rate. Cyclic voltammetry tests were performed at the same scanning rate to examine their electrochemical behaviour. Upon evaluating the results of the cyclic voltammetry tests, as depicted in Figure 4a and 4c, the current density in the HCl-based electrolyte decreases upon cycling and reduction-oxidation peaks become stable after tens of cycling, and current ranged from -0.5 mA cm^{-2} to $+0.5 \text{ mA cm}^{-2}$. Additionally, in the Na_2SO_4 electrolyte, this value corresponds to peaks within the range of -4 mA cm^{-2} to $+1 \text{ mA cm}^{-2}$. The current graph is stable, meaning that this electrolyte could be used for cycling in the area of energy storage devices. Moreover, upon reviewing Figure 4b and 4d, it became evident that the cyclic stability of HCl acid was lower compared to that of Na_2SO_4 electrolyte, and cyclic stability did not establish quickly. Therefore, we concluded that HCl acid is not suitable for electrochemical tests.

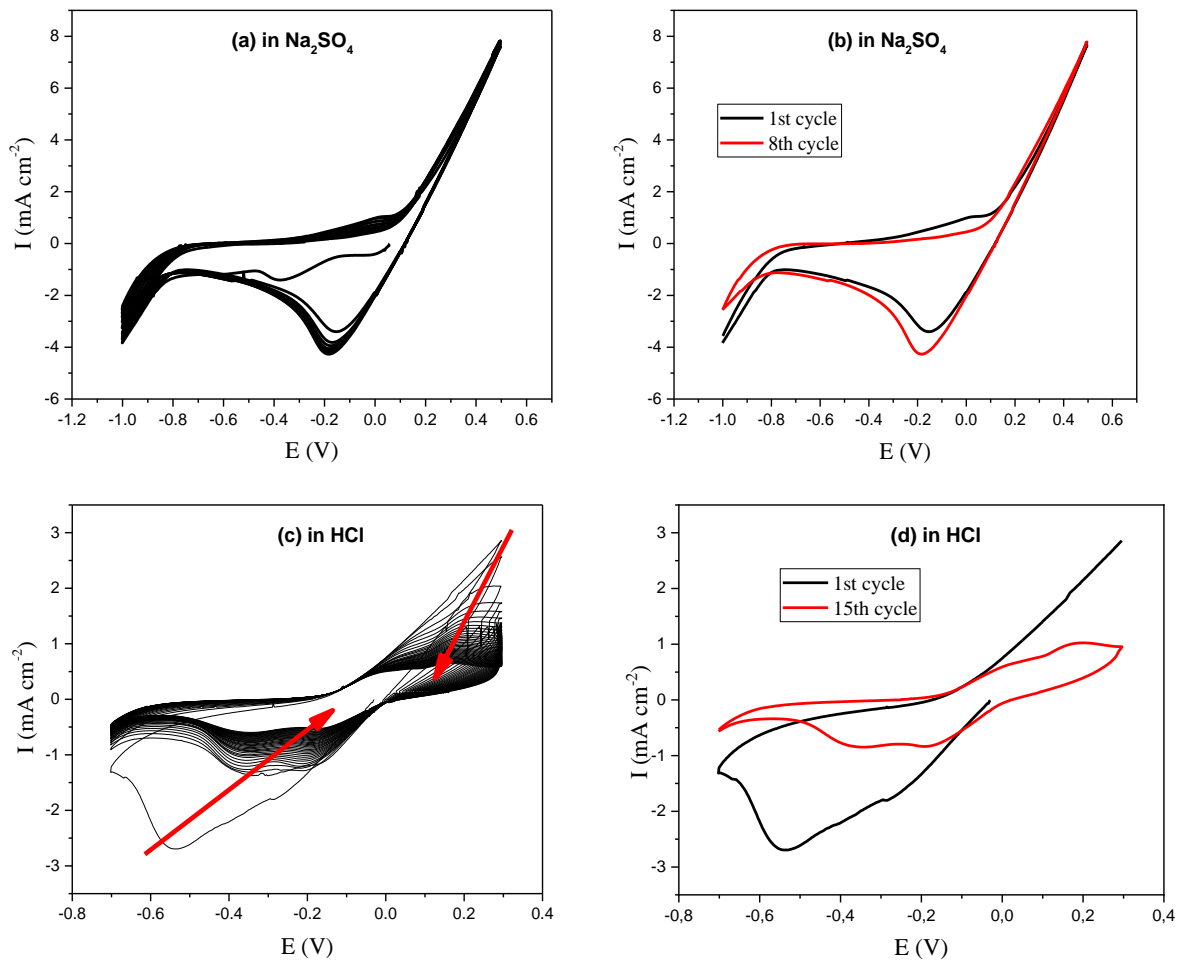


Figure 4. a) The cyclic voltammety responses of Mn-Cu alloys cycling in 1 M Na_2SO_4 . b) 1st and 8th cycle of Mn-Cu alloy in 1 M Na_2SO_4 . c) Cyclic voltammety responses of Mn-Cu alloys cycling in 1 M HCl. d) first and 15th cycle of Mn-Cu alloy in 1 M HCl. The electrodes were electrodeposited by application of -1.6 V in Ethaline containing Mn^{2+} and Cu^{2+} ions.

Furthermore, with insights gained from the results of cyclic voltammetry tests conducted in various electrolytes, an important role of electrolyte selection in influencing electrochemical properties and energy storage capacity has been discovered. The coating process, which was carried out by applying a potential of -2.2 V to the graphite surfaces by using an Ethaline solution containing 0.5 M Mn^{+2} and 0.5 M Cu^{+2} , was completed. Figure 5 illustrates the decrease of current upon cycling. However, the current responses evolve and become stable. Figure 5c illustrates the area under the current-voltage curve of the mixing electrolyte is higher than that of the other electrolyte. Figure 5c confirms that the mixed electrolyte is a more efficient option in terms of charge storage capacity.

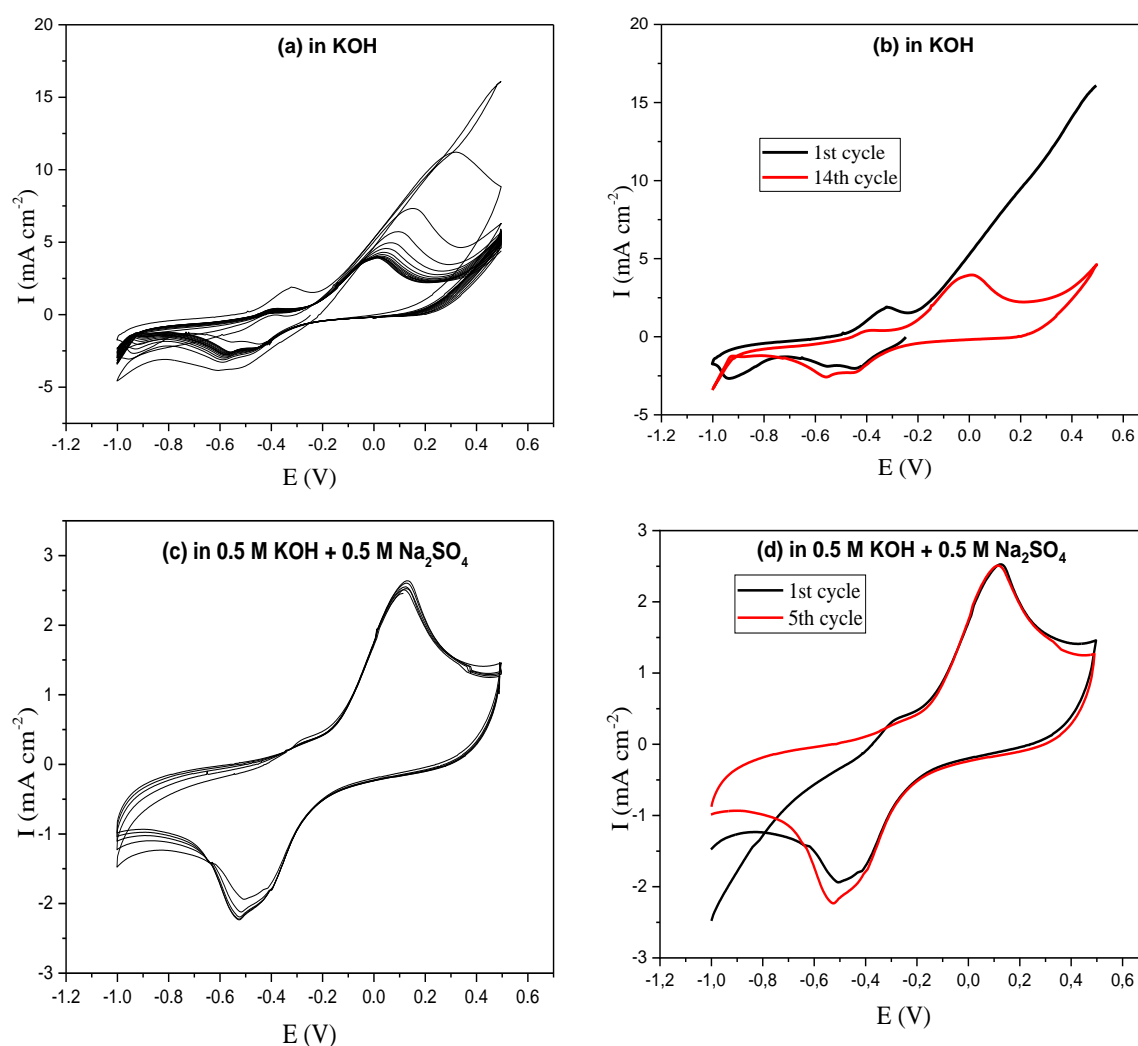


Figure 5. a) The cyclic voltammetry responses of Mn-Cu alloys cycling in 1 M KOH. b) 1st and 14th cycle of Mn-Cu alloy in 1 M KOH. c) cyclic voltammetry responses of Mn-Cu alloys cycling in 0.5 M Na_2SO_4 + 0.5 M KOH. d) 1st and 5th cycle of Mn-Cu alloy in 0.5 M Na_2SO_4 + 0.5 M KOH. The electrodes were electrodeposited by application of -2.2 V in Ethaline containing Mn^{2+} and Cu^{2+} ions

A preliminary study was conducted to determine the effects of different solution compositions and voltage levels on the electrochemical performance of Mn-Cu coatings and approach optimal values. In this preliminary study, processes were carried out using different solutions with varying compositions and concentrations, such as KOH, Na_2SO_4 , and 0.5 M KOH + 0.5 M Na_2SO_4 , employing three uniform voltage levels (-1.6, -1.9, and -2.2 V) for each solution. In this case, consistent voltage levels were applied for each solution. As a result of these processes, it was observed that the coating had a significant impact on the electrochemical performance of the electrodes (in Figure 6). Particularly, in processes conducted within 1 M KOH, 1 M Na_2SO_4 , and 0.5 M KOH + 0.5 M Na_2SO_4

mixed solutions, it was noted that the different voltage levels (-1.6, -1.9, and -2.2 V) did not yield the same. The cyclic voltammogram responses of the alloy-based coatings were examined by comparing the current values of bare graphite and Mn-Cu coated graphite in the solutions of 1 M KOH, 1 M Na₂SO₄, and the mixture of 0.5 M KOH + 0.5 M Na₂SO₄ in Figure 6. The current value given by bare graphite in three solutions is approximately 0.4 mA (in Figure 6a, b, c). Mn-Cu coated graphite has been observed to provide around 4 mA in 1 M KOH solution (in Figure 6a) and about 6 mA in 1 M Na₂SO₄ solution (in Figure 6b). However, the current value generated by Mn-Cu coated graphite tapes at a potential of -1.9 V in a mixture of solution of 0.5 M KOH and 0.5 M Na₂SO₄ was calculated to be around 6.5 mA (in Figure 6c).

As a result of the cyclic voltammogram data, it was observed that the electrochemical performance of Mn-Cu-coated graphite was significantly higher compared to that of bare graphite. In this context, it was determined that the optimal operating voltage was -1.9 V, and it was planned to continue the experiments using three different solvents. These experiments are important steps toward further optimizing the electrochemical performance.

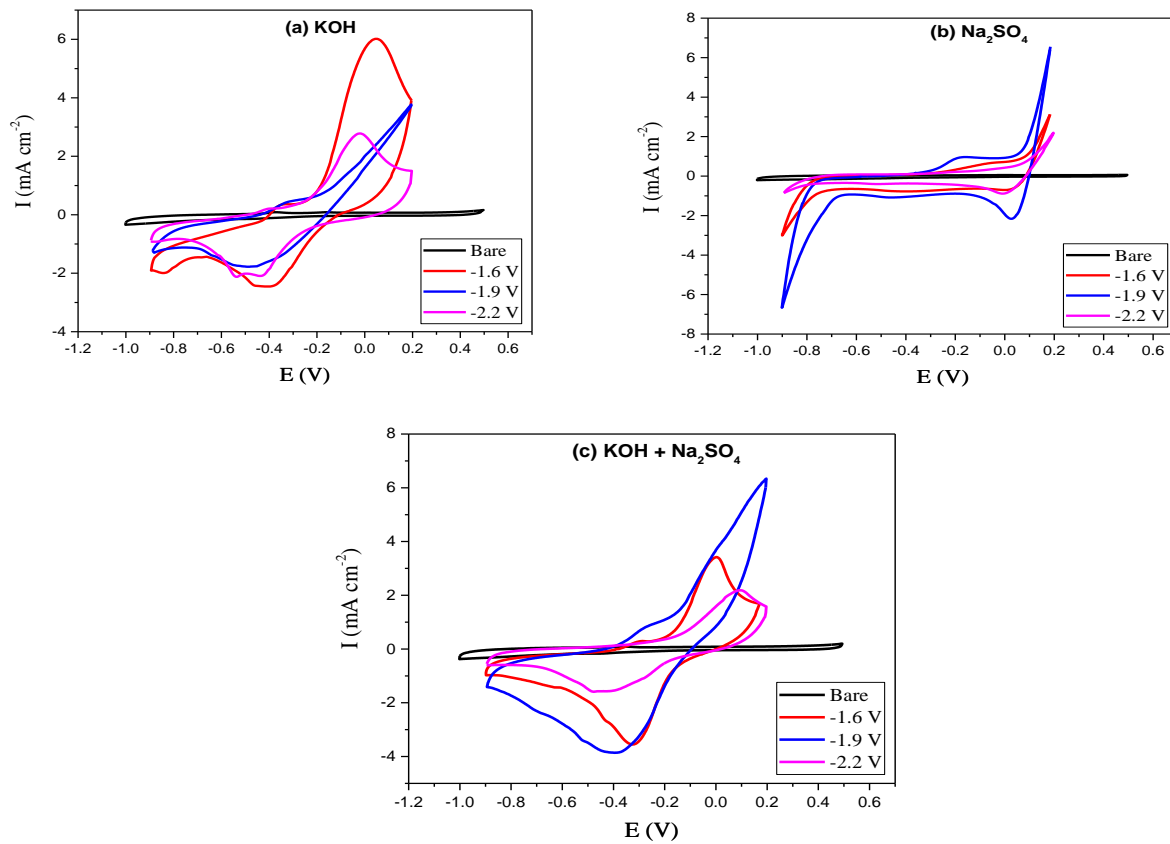


Figure 6. The cyclic voltammogram results of all types of graphite films cycled a) in 1 M KOH ($v = 50 \text{ mV s}^{-1}$). b) 1 M Na₂SO₄ ($v = 50 \text{ mV s}^{-1}$). c) 0.5 M Na₂SO₄ + 0.5 M KOH ($v = 50 \text{ mV s}^{-1}$)

Figure 7 is obtained when the experiment was carried out by taking Mn-Cu coated graphite samples obtained by applying -1.6 V potential using Ethaline. Then, the samples were subjected to cyclic voltammetry experiments in three different electrolyte solutions with electrode potentials ranging from -0.9 V to 0.2 V. Different scan rates (100 mV/s, 50 mV/s, 25 mV/s, and 10 mV/s) were used for these studies.

All graphs in Figure 7 show the increase in the current density of Mn-Cu alloys obtained at different electrode potentials with the increase in scanning speed. These observations explain that the current density in electrochemical reactions is a reflection of the rate of charge transfer. As the scanning speed increases, the amount of charge transfer per unit time increases, increasing current density. The data shown in Figure 7b, however, also show a distinct scenario. Current density maxima are observed in these figures at -3 and 3 mA cm⁻². Comparatively to Figures 7a and 7c, this figure's area under the curve is noticeably smaller. This implies that

the electrolyte in Figure 7b has less storage capacity and electrochemical capacity than the covered surfaces of the other samples.

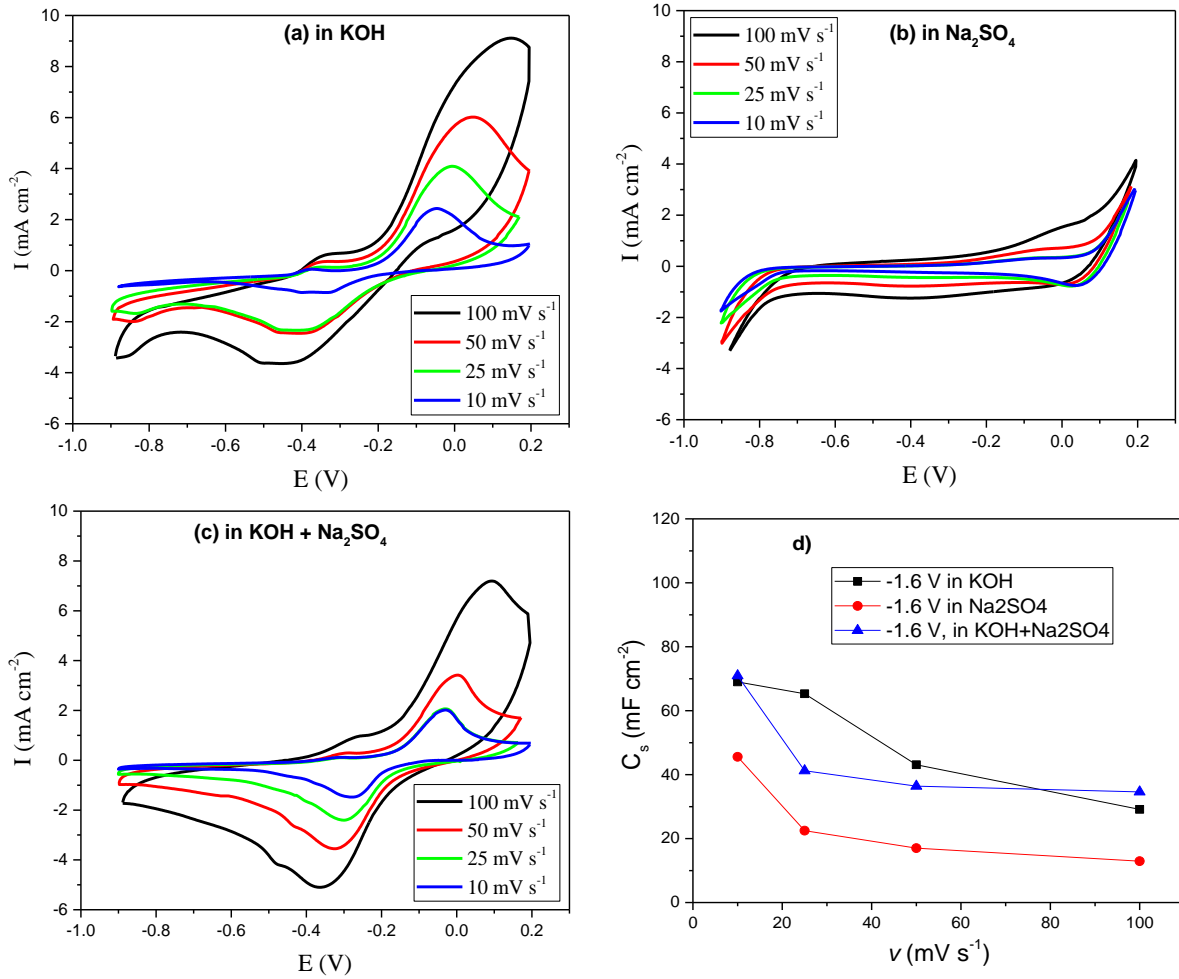


Figure 7. The cyclic voltammetry data Mn-Cu coated from Ethaline Deep Eutectic Solvent on graphite by application of -1.6 V and now cycling in a) 1 M KOH; b) 1 M Na₂SO₄ and c) an electrolyte consisting of 0.5 M KOH and 0.5 M Na₂SO₄. The scan rates are given in the panels. d) Plot of the area capacitance of the electrodes given in panel a, panel b, and panel c depending on scanning speed.

The specific capacitance (C) is generally expressed using the following formula:

$$C = \frac{2}{A \cdot \Delta V} \int \frac{I dV}{v} \quad (1)$$

Where:

- C is the specific capacitance ($F \text{ cm}^{-2}$),
- I represents the current density ($A \text{ cm}^{-2}$),
- ΔV stands for the potential difference (V),
- v signifies the scan rate (mV s^{-1}),
- A is the area of active materials of the working electrode (cm^2)

Specific capacitance refers to the amount of charge stored on an electrode surface during an electrochemical process. The scanning rate, on the other hand, indicates the speed of the electrode potential in voltammetry

experiments. Referring to Figure 7, the relationship between specific capacitance and scan rate is inversely proportional. That is, as the scanning speed increases, the specific capacitance decreases.

Table 1. Specific capacitance values of Mn-Cu coated graphite tapes electrodeposited at -1.6 V potential depending on the varying scanning rates in different electrolyte solutions

| Scan Rate (mV s ⁻¹) | Specific Capacitance in KOH (mF cm ⁻²) | Specific Capacitance in Na ₂ SO ₄ (mF cm ⁻²) | Specific Capacitance in KOH + Na ₂ SO ₄ (mF cm ⁻²) |
|------------------------------------|--|--|--|
| 100 | 29 | 13 | 35 |
| 50 | 43 | 17 | 36 |
| 25 | 65 | 23 | 41 |
| 10 | 69 | 46 | 71 |

The same conclusion may be drawn about this by looking at the experimental data in Table 1. At higher scan rates (e.g., 100 mV/s), the measured specific capacitance value in the KOH electrolyte is 29 mF cm⁻². As the scan rate decreases (e.g., 10 mV/s), the specific capacitance value increases, reaching 69 mF cm⁻². This indicates that slower scan rates (higher time scale) allow for greater charge storage capacity on the electrode surface. Decreasing the scan rate allows for more charge storage on the electrode surface, leading to higher capacitance values. Moreover, different electrolyte solutions exhibit similar trends, with capacitance values increasing as the scan rate decreases.

3.2.2. Mn-Cu electrodeposited by application of -1.9 V

When comparing the graphs in Figure 8 and results in Table 2, a distinct difference in the data obtained from the common electrolytes is observed. For instance, the current density values at a scan rate of 100 mV/s generally range between -2 and 4 mA cm⁻² on average in Figure 8. In the Na₂SO₄ electrolyte, the current density values vary between -1 and 7 mA cm⁻². Furthermore, in the 1 M KOH + 1 M Na₂SO₄ electrolyte, the values span from -4 to 8 mA cm⁻².

Table 2. Specific capacitance values of Mn-Cu coated graphite tapes at -1.9 V potential depending on the varying scanning rates in different electrolyte solutions

| Scan Rate (mV s ⁻¹) | Specific Capacitance (mF cm ⁻²) in KOH | Specific Capacitance (mF cm ⁻²) in Na ₂ SO ₄ | Specific Capacitance (mF cm ⁻²) in KOH + Na ₂ SO ₄ |
|------------------------------------|--|--|--|
| 100 | 12 | 22 | 29 |
| 50 | 18 | 31 | 50 |
| 25 | 28 | 42 | 61 |
| 10 | 43 | 81 | 109 |

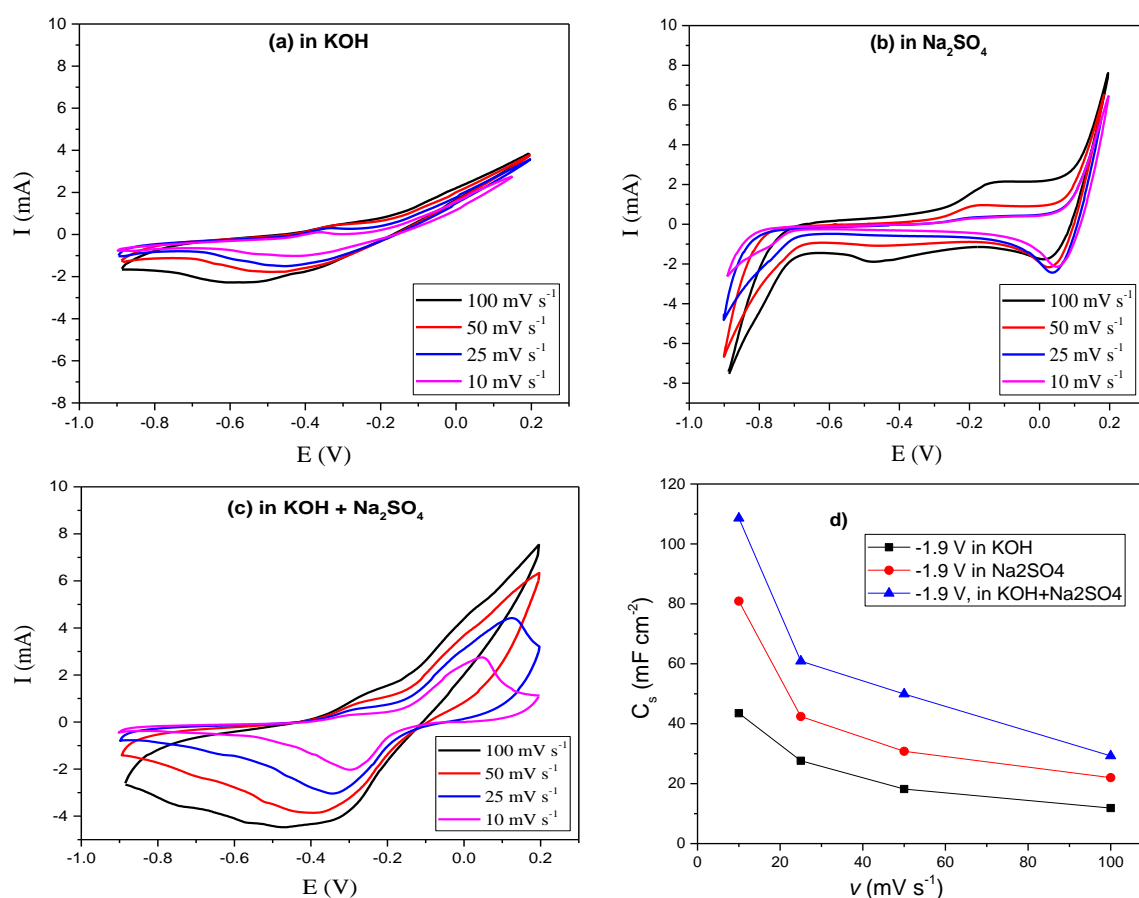


Figure 8. The cyclic voltammograms of Mn-Cu alloy in a) 1 M KOH, b) 1 M Na_2SO_4 and c) an electrolyte consisting of 0.5 M KOH and 0.5 M Na_2SO_4 . Mn-Cu alloy coating on graphite tapes was obtained in Ethaline deep eutectic solvent by applying a constant voltage of -1.9 V. d) Plot of the area capacitance of the electrodes given in panel a, panel b, and panel c depending on scanning speed.

3.2.3. Mn-Cu electrodeposited by application of -2.2 V

The photographs of the Mn-Cu coating of graphite are presented in Figure 9. The current density values range from -3 to 4 mA cm^{-2} in the KOH electrolyte. In the Na_2SO_4 electrolyte, these values vary between -1 and 2 mA cm^{-2} . For the 1 M KOH + 1 M Na_2SO_4 electrolyte, the values fall within the range of -2.5 to 3 mA cm^{-2} . Exploring the factors underlying these discrepancies, we find that at higher scan rates, the time allocated to the redox reaction diminishes, resulting in higher peak current values, especially at higher voltages.

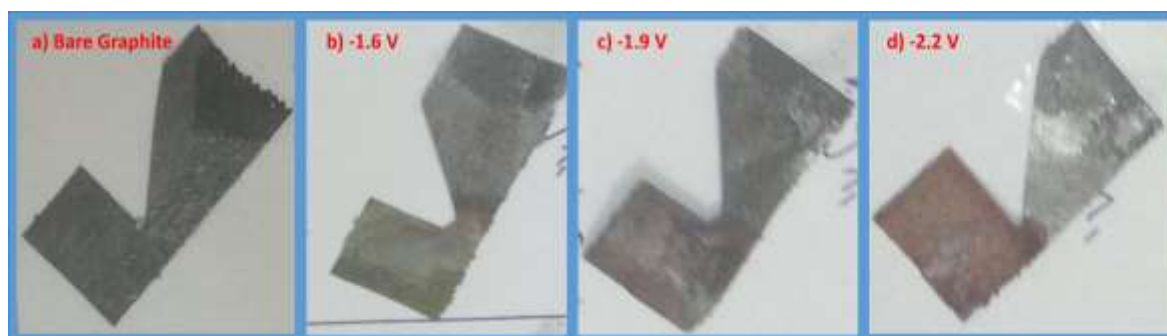


Figure 9. Photograph of a) bare graphite; b) Mn-Cu alloy coating on graphite tapes obtained in Ethaline deep eutectic solvent by applying a constant voltage of -1.6V; c) Mn-Cu alloy coating on graphite tapes obtained in Ethaline deep eutectic solvent by applying a constant voltage of -1.9 V; d) Mn-Cu alloy coating on graphite tapes obtained in a deep eutectic solvent by applying a constant voltage of -2.2 V

Additionally, considering the alloy deposition process, we note that lower negative voltage values generally lead to sparser and thinner coating layers (Figure 9). As ions are gradually transported to the surface, the coating layer becomes more irregular and filled with voids. However, at higher negative voltages, denser and more compact coating layers were observed (Figure 9c and 9d). Faster ion transport at higher voltages seems to yield a more homogeneous layer. All these processes, supported by our graphical data, collectively highlight the effects of different voltage levels and scan rates on the electrochemical coating process.

Comparing previous experimental figures by analyzing the graphs of Figure 10, in contrast to what was anticipated under the same scanning speed and electrolyte conditions, the flexible graphite samples coated at higher voltage exhibit lower current peaks. Numerous predictable and unforeseen causes can be responsible for this behaviour, and it might be related to how electro-coating works. Because they carry more energy at higher voltages, the ions in the electrolyte could move to the surface layer more quickly. A more compact and dense coating layer may have occurred as a result. On the other hand, a coating layer may have become thinner and thinner because the ions carry less energy at lower voltages.

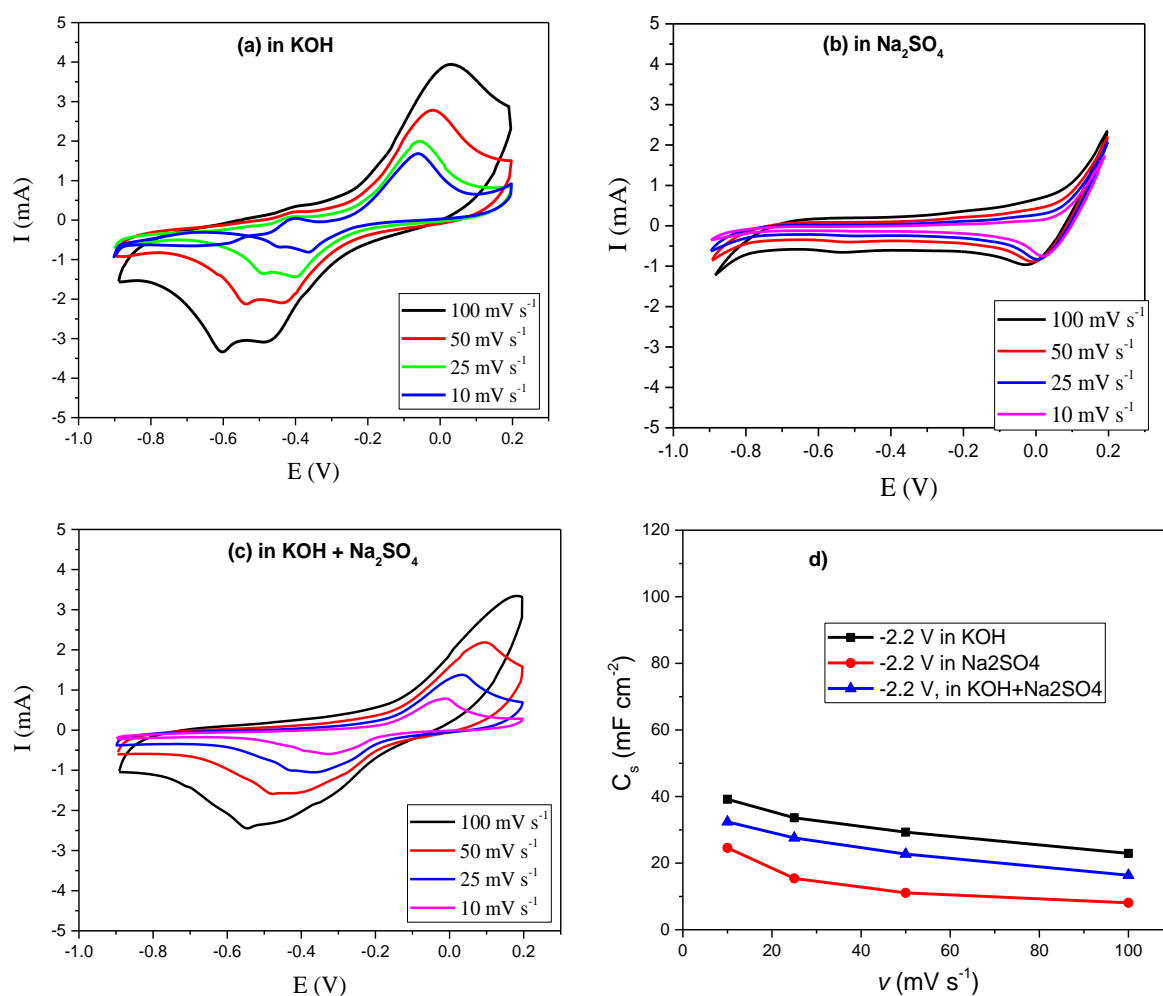


Figure 10. The cyclic voltammograms of Mn-Cu alloy in a) 1 M KOH, b) 1 M Na₂SO₄ and c) an electrolyte consisting of 0.5 M KOH and 0.5 M Na₂SO₄. Mn-Cu alloy coating on graphite tapes was obtained in Ethaline deep eutectic solvent by applying a constant voltage of -2.2 V. d) Plot of the areal capacitance of the electrodes given in panel a, panel b, and panel c depending on scanning speed.

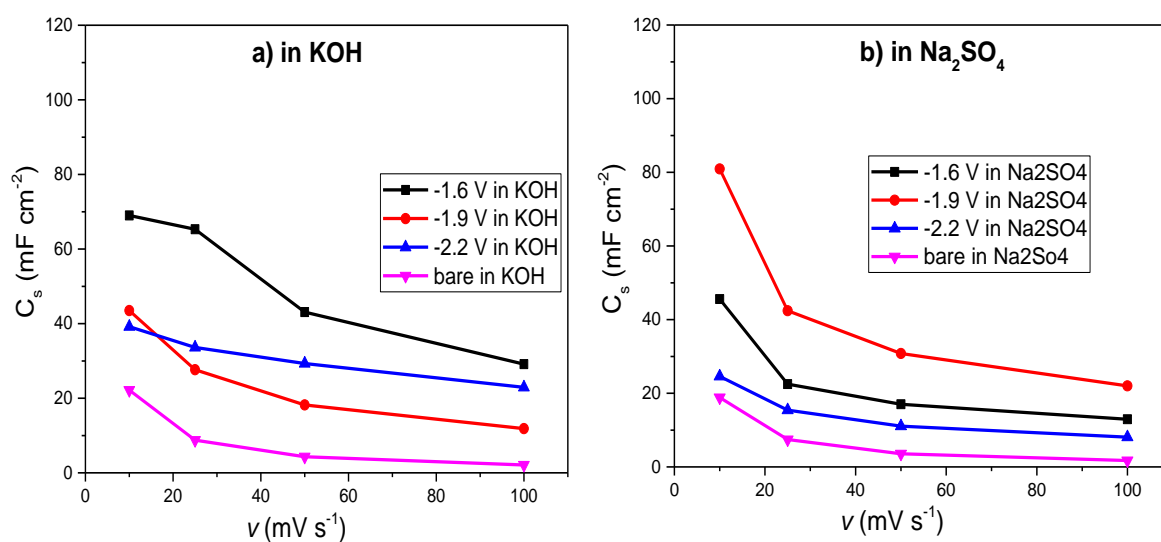
Figure 10 and Table 3 present specific capacitance values obtained at various scanning rates in different electrolyte solutions: KOH, Na₂SO₄, and a mixture of KOH + Na₂SO₄. These data provide valuable insights into the relationship between electrolyte compositions, scanning rates, and specific capacitance values. Upon examination, a clear trend emerges in the specific capacitance values across the different electrolyte solutions.

Table 3. Specific capacitance values of Mn-Cu coated graphite tapes at -2.2 V potential depending on the varying scanning rates in different electrolyte solutions

| Scan Rate (mV s ⁻¹) | Specific Capacitance (mF cm ⁻²) in KOH | Specific Capacitance (mF cm ⁻²) in Na ₂ SO ₄ | Specific Capacitance (mF cm ⁻²) in KOH + Na ₂ SO ₄ |
|------------------------------------|--|--|--|
| 100 | 23 | 8 | 16 |
| 50 | 29 | 11 | 23 |
| 25 | 34 | 15 | 28 |
| 10 | 39 | 25 | 32 |

When examining the graphs in Figure 10 individually, the results obtained under different coating voltages offer valuable insights. Firstly, the KOH electrolyte data acquired at -1.6 V coating voltage greatly outperforms the data obtained at other coating voltages (Figure 10a). These results demonstrate how the electrolyte and the coating voltage of -1.6 V improve and increase the electrode's capacitance properties. Notably, even better results were obtained in comparison to the uncoated graphite-specific capacitance values and the -1.9 V and -2.2 V coatings. This demonstrates the potential of slower scan speeds to accommodate a higher capacity for charge storage on the electrode surface and highlights the critical importance of selecting the right electrolyte.

Analysis of the data acquired under a coating voltage of -1.9 V similarly reveals a tendency similar to the data shown in Figure 11a. The reported specific capacitance value in the KOH electrolyte is 12 mF cm⁻² at higher scan rates (for example, 100 mV/s). The specific capacitance value rises to a maximum of 43 mF cm⁻² when the scan rate falls (for example, to 10 mV/s). When evaluating the results acquired in the Na₂SO₄ electrolyte under a -1.9 V coating voltage, the same pattern is observed. Higher specific capacitance values are produced when the scan rate is reduced. For instance, the specific capacitance is 22 mF cm⁻² at a scan rate of 100 mV/s but increases to 81 mF cm⁻² with a scan rate of 10 mV/s (Figure 11b).



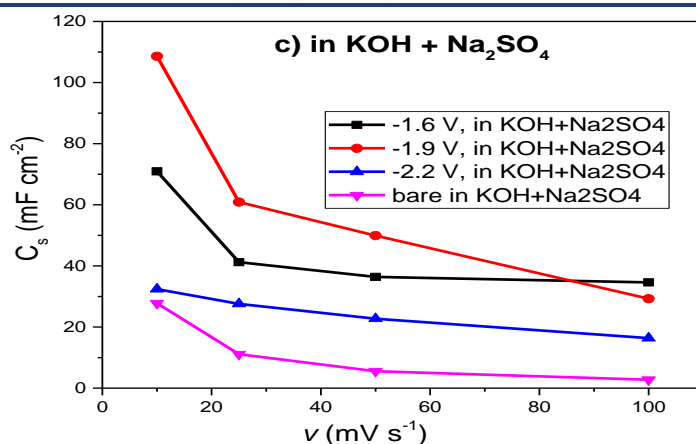


Figure 11. Specific capacitance of Mn-Cu based alloy on graphite depending on the applied coating voltage at different values a) cycled in 1 M KOH; b) cycled 1 M Na₂SO₄ and; c) cycled in the mixture of 0.5 M KOH and 0.5 M Na₂SO₄ at various scanning speed.

A comparison of the capacitances of metal-based supercapacitor electrodes, as reported in the literature, is provided in Table 4. The study of data obtained using the mixed KOH + Na₂SO₄ electrolyte also yielded similar results. It is obvious that for scan rate measurements, the best results are obtained with a constant -1.9 V coating voltage. For instance, the specific capacitance value is 29 mF cm⁻² at a scan rate of 100 mV/s, but it increases to 109 mF cm⁻² with a scan rate of 10 mV/s (in Figure 11c).

Additionally, the high capacitance characteristics of the 0.5 M KOH + 0.5 M Na₂SO₄ concentrated electrolyte are supported by the capacitance values under the -1.6 V coating voltage. These experimental graphs demonstrate, in conclusion, how important electrolyte composition and scan rate are in determining certain capacitance values. The complicated nature of these systems' energy storage mechanisms is underlined by the relationship between ion conductivity and surface response kinetics.

The electrolytes used in this study, specifically KOH, Na₂SO₄, and their mixture, play a crucial role in influencing the cyclic performance of the electrodes due to their distinct ionic characteristics. The size of the ions, their mobility within the electrolyte, and their chemical interactions with the electrode surface significantly impact the overall electrochemical behaviour. Moreover, the structural and compositional properties of the electrodes themselves, particularly in terms of their material composition and surface morphology, also contribute to the cyclic performance observed. In addition, the applied voltages during the electrochemical deposition process are critical in determining the specific capacitance values achieved. Varying the deposition voltage directly influences the nucleation and growth dynamics of the Mn-Cu film on the graphite substrate. Specifically, the applied growth voltages can significantly influence the deposition rates, the uniformity of the deposited particles, and the resulting surface area available for charge storage. These factors, in turn, play an important role in determining the capacitance, as variations in deposition conditions directly affect the microstructural properties of the electrode surface and its capacity for efficient charge accumulation.

Table 4. Comparison of electrode capacitances for supercapacitors as reported in the literature

| Electrode Material | Method | Specific Capacitance (mF cm ⁻²) | Electrolyte | Reference |
|----------------------|----------------------------|---|---------------------------------------|----------------------|
| MnO ₂ | Electrodeposition | 13 | Na ₂ SO ₄ | (Tran et al., 2020) |
| CuO/rGO | Hydrothermal | 80 | Na ₂ SO ₄ | (Bu and Huang, 2017) |
| NiO-TiO ₂ | Potentiostatic anodization | 46 | NaOH | (Xie et al., 2009) |
| Ni(OH) ₂ | Facile hydrothermal | 36 | PVA-KOH | (Dong et al., 2014) |
| Mn-Cu | Electrodeposition | 109 | KOH + Na ₂ SO ₄ | This work |

4. Conclusion

The development of technologies that make use of flexible screens and sensors has seen significant progress in recent years. On the other hand, the development of flexible energy storage technologies has been somewhat slow in comparison to other areas of research. It is essential to do research on flexible energy storage electrodes because of the significant role that flexibility and stretchability play in the development of wearable, biomedical, and portable electrical electronic devices. Within the scope of this research work, the electrochemical properties of graphite filaments that have been coated with an alloy and exhibit flexibility are investigated. The electrochemical synthesis of modified graphite based on manganese and copper was accomplished in a deep eutectic solvent ionic liquid, which altered the static voltage levels. The performance of electrochemical deposition of films in Ethaline deep eutectic solvent was analyzed in this study. The alloy was obtained from Mn and Cu-based chloride salts in an Ethaline ionic liquid. The growth potentials were -1.6, -1.9 and -2.2 V. The subsequent cycling of the resultant electrodes in a KOH, Na₂SO₄, and the mixture of KOH and Na₂SO₄ electrolytes was also analyzed. An increase to 1.5 V was made to the potential window that was utilized for this investigation. It was determined how much the areal capacitance of the flexible electrodes that were manufactured was. It is possible to exert control over the performance of the electrode by modifying the structure of the material through alterations in the conditions under which the deposition takes place. After being coated with Mn-Cu by means of an application of a voltage of -1.9V, the graphite substrate displayed a length capacitance of 109 mF cm⁻² when the cycling electrolyte was a mixture of potassium hydroxide and sodium sulfate. There was a significant amount of surface covering on the film, which indicates that it has the potential to be deployed in energy storage applications.

Acknowledgments

The authors thank the Scientific Research Project Unit at Gaziantep University (MF.ALT.22.18).

Ethics Permissions

In studies requiring ethics committee permission, information about the permission (committee name, date and issue number) should be given in the method section and also on the last page of the article.

Author Contributions

Abdulcabbar Yavuz and Hüseyin Faal contributed to the study's conception and design. Material preparation, data collection, and analysis were performed by Abdulcabbar Yavuz and Hüseyin Faal. The calculations were performed by Hüseyin Faal. Abdulcabbar Yavuz supervised the project. Hüseyin Faal wrote the first draft of the manuscript, and Abdulcabbar Yavuz commented on previous versions of the manuscript. All authors read and approved the final manuscript.

Conflict of Interest

Authors declare that there is no conflict of interest for this paper.

References

- Arumugam, B., Mayakrishnan, G., Subburayan Manickavasagam, S. K., Kim, S. C., and Vanaraj, R. (2023). An overview of active electrode materials for the efficient high-performance supercapacitor application. *Crystals*, 13(7), 1118.
- Baig, M. M., Khan, M. A., Gul, I. H., Rehman, S. U., Shahid, M., Javaid, S., and Baig, S. M. (2023). A review of advanced electrode materials for supercapacitors: challenges and opportunities. *Journal of Electronic Materials*, 52(9), 5775–5794.
- Brisse, A. L., Stevens, P., Toussaint, G., Crosnier, O., and Brousse, T. (2018). Ni(OH)₂ and NiO based composites: Battery type electrode materials for hybrid supercapacitor devices. *Materials*, 11(7), 1178.
- Bu, I. Y. Y., and Huang, R. (2017). Fabrication of CuO-decorated reduced graphene oxide nanosheets for supercapacitor applications. *Ceramics International*, 43(1), 45–50.
- Dong, X., Guo, Z., Song, Y., Hou, M., Wang, J., Wang, Y., and Xia, Y. (2014). Flexible and wire-shaped micro-supercapacitor based on Ni(OH)₂-nanowire and ordered mesoporous carbon electrodes. *Advanced Functional Materials*, 24(22), 3405–3412.

- González, A., Goikolea, E., Barrera, J. A., and Mysyk, R. (2016). Review on supercapacitors: Technologies and materials. *Renewable and Sustainable Energy Reviews*, 58, 1189–1206.
- Guney, M. S., and Tepe, Y. (2017). Classification and assessment of energy storage systems. *Renewable and Sustainable Energy Reviews*, 75, 1187–1197.
- Hannan, M. A., Wali, S. B., Ker, P. J., Abd Rahman, M. S., Mansor, M., Ramachandaramurthy, V. K., Muttaqi, K. M., Mahlia, T. M. I., and Dong, Z. Y. (2021). Battery energy-storage system: A review of technologies, optimization objectives, constraints, approaches, and outstanding issues. *Journal of Energy Storage*, 42, 103023.
- Ho, J., Jow, T. R., and Boggs, S. (2010). Historical introduction to capacitor technology. *IEEE Electrical Insulation Magazine*, 26(1), 20–25.
- Iro, Z. S., Subramani, C., and Dash, S. S. (2016). A brief review on electrode materials for supercapacitor. *International Journal of Electrochemical Science*, 11(12), 10628–10643.
- Kalhammer, F. R., and Schneider, T. R. (1976). Energy storage. *Annual Review of Energy*, 1(1), 311–343.
- Li, H. Q., Wang, Y. G., Wang, C. X., and Xia, Y. Y. (2008). A competitive candidate material for aqueous supercapacitors: High surface-area graphite. *Journal of Power Sources*, 185(2), 1557–1562.
- Luo, X., Wang, J., Dooner, M., and Clarke, J. (2015). Overview of current development in electrical energy storage technologies and the application potential in power system operation. *Applied Energy*, 137, 511–536.
- Mitali, J., Dhinakaran, S., and Mohamad, A. A. (2022). Energy storage systems: A review. *Energy Storage and Saving*, 1(3), 166–216.
- Mohanty, R. I., Mukherjee, A., Bhanja, P., and Jena, B. K. (2023). Novel microporous manganese phosphonate-derived metal oxides as prospective cathode materials for superior flexible asymmetric micro-supercapacitor device. *Journal of Energy Storage*, 72, 108730.
- Niknam, E., Naffakh-Moosavy, H., and Afshar, M. G. (2022). Electrochemical performance of nickel foam electrode in potassium hydroxide and sodium sulfate electrolytes for supercapacitor applications. *Journal of Composites and Compounds*, 4(12), 149–152.
- Purushothaman, K. K., Cuba, M., and Muralidharan, G. (2012). Supercapacitor behavior of α -MnMoO₄ nanorods on different electrolytes. *Materials Research Bulletin*, 47(11), 3348–3351.
- Sahin, M. E., Blaabjerg, F., and Sangwongwanich, A. (2020). A review on supercapacitor materials and developments. *Turkish Journal of Materials*, 5(2), 10–24.
- Sayed, S. G., Shaikh, A. V., Shinde, U. P., Hiremath, P., and Naik, N. (2023). Copper oxide-based high-performance symmetric flexible supercapacitor: Potentiodynamic deposition. *Journal of Materials Science: Materials in Electronics*, 34(17), 1361.
- Sharma, K., Arora, A., and Tripathi, S. K. (2019). Review of supercapacitors: Materials and devices. *Journal of Energy Storage*, 21, 801–825.
- Tran, C. C. H., Santos-Peña, J., and Damas, C. (2020). Electrodeposited manganese oxide supercapacitor microelectrodes with enhanced performance in neutral aqueous electrolyte. *Electrochimica Acta*, 335, 135564.
- Wen, Q., Chen, J. X., Tang, Y. L., Wang, J., and Yang, Z. (2015). Assessing the toxicity and biodegradability of deep eutectic solvents. *Chemosphere*, 132, 63–69.
- Xie, Y., Huang, C., Zhou, L., Liu, Y., and Huang, H. (2009). Supercapacitor application of nickel oxide–titania nanocomposites. *Composites Science and Technology*, 69(13), 2108–2114.
- Yang, Y., Bremner, S., Menictas, C., and Kay, M. (2018). Battery energy storage system size determination in renewable energy systems: A review. *Renewable and Sustainable Energy Reviews*, 91, 109–125.
- Yavuz, A., Artan, M., and Yilmaz, N. F. (2022). The effect of growth potential on the self-discharge behavior of Cu–Ni based alloy electrodes. *Journal of Physics and Chemistry of Solids*, 169, 110872.

Leveraging Latent Dirichlet Allocation and Fuzzy Clustering for Identifying Key UAV Applications in Disaster Response

Zeynep YÜKSEL¹, Nazmiye ELİGÜZEL², Süleyman METE^{3*}


Keywords


*Drone,
Fuzzy c-means,
LDA,
Post-disaster,
Unmanned aerial
vehicle*


Abstract – Over the past few decades, there has been a significant increase in the occurrence of natural disasters, such as earthquakes and landslides, presenting a grave risk to the safety of people's lives and their possessions. Drones, also known as unmanned aerial systems (UAVs), are increasingly attracting the attention of organizations engaged in disaster events, especially in the context of post-disaster emergency response. This research aims to assess the use of UAV applications in the post-disaster phase through a descriptive literature analysis. The evaluation is conducted using the Latent Dirichlet Allocation (LDA) topic modelling and clustering approach, namely the fuzzy c-means algorithm. A total of 433 papers are extracted from the Scopus database. The analysis offers valuable insights into three primary domains: imaging-based damage assessment, emergency communication networks, and vehicle routing optimization. These findings emphasize the significance of technology and streamlined systems in effectively handling complex situations, such as disaster response and network management. By integrating UAVs into disaster response strategies, policymakers can significantly enhance the agility and efficiency of their operations, ultimately saving lives and minimizing the impact of natural disasters on communities. This study can assist in achieving these goals by providing valuable insights and guidance.

1. Introduction

Drones or unmanned aerial vehicles (UAVs) are aircraft capable of autonomous flight without human intervention (Calamoneri et al., 2024). UAVs can capture aerial images that are valuable for analyzing large areas of land using geospatial techniques. UAVs are encompassed within the realm of remote sensing (Garnica-Peña and Alcántara-Ayala, 2021). They have gained growing attention from organizations engaged in disaster response activities. They serve a variety of purposes in post-disaster activities, including damage assessment using UAV images (Zou et al., 2024), bushfire detection (Qadir et al., 2024), network communication (Lei et al., 2024; Wu et al., 2024), and vehicle routing issues (Faiz et al., 2024; Zhang et al., 2022). The literature we reviewed contained a paper that addressed the use of UAVs in the aftermath of a disaster. The following are some of them: Freeman et al. (2021) outlined the findings of a comprehensive examination of the utilization of aerial robotic technology in the field of civil engineering. Civil engineering applications can be categorized into three primary areas: (i) monitoring and inspecting civil infrastructure; (ii) managing sites, constructing using robots, and maintaining structures; and (iii) conducting surveys and assessing damage quickly after a disaster. The authors conducted a review focusing on these issues. Mohd Daud et al. (2022) seek to assess the current viability of drone projects and address various obstacles associated with deploying drones in large-scale disasters, with the intention of empowering and motivating potential future endeavors. According to the identified papers, the use of drones in disasters was categorized into four main areas: (1) mapping or disaster management, (2) search and rescue, (3) transportation, and (4) training. Lozano and Tien (2023) concentrated on the tools,

¹Gaziantep Islam Science and Technology University, Faculty of Engineering, Department of Industrial Engineering, Gaziantep, Türkiye. E-mail: zeynep.yuksel@gibtu.edu.tr  ORCID: 0009-0006-8201-372X

²Gaziantep Islam Science and Technology University, Faculty of Engineering, Department of Industrial Engineering, Gaziantep, Türkiye. E-mail: nazmiye.eliguzel@gibtu.edu.tr  ORCID: 0000-0001-6354-8215

^{3*}**Corresponding Author.** Gaziantep University, Faculty of Engineering, Department of Industrial Engineering, Gaziantep, Türkiye. E-mail: smete@gantep.edu.tr  ORCID: 0000-0001-7631-5584

Citation: Yüksel, Z., Eligüzel, N., Mete, S. (2024). Leveraging Latent Dirichlet Allocation and Fuzzy Clustering for Identifying Key UAV Applications in Disaster Response. *Natural Sciences and Engineering Bulletin*, 1(2), 17-26.

including UAVs, employed to evaluate the physical harm in lifeline networks and structures. The tools provided encompass several lifeline networks, such as water, gas, transportation, power, and building infrastructure. They also cover a wide range of hazards, such as earthquakes, flooding caused by hurricanes, and heavy rainfall. The paper provided a comprehensive evaluation of each tool, examining important factors such as scope, accuracy, and long-term accessibility. Their analysis aimed to facilitate the integration of datasets across different tools and pinpoint any deficiencies in current data collection methods. Phadke and Medrano (2023) investigated a wide range of application scenarios for UAV swarms in order to highlight the various components that collaborate to enhance the overall resilience of the swarm. Swarm applications are classified using a three-category system. Although systemic resilience is a complex topic, most practical implementations of UAV swarm research primarily aim to enhance the resilience of certain components against unexpected events. Ishiwatari (2024) investigated the function of drones in disaster management by studying different uses of drones in reaction to the Noto Peninsula earthquake in January 2024. Multiple concerns were identified, such as the necessity to integrate drone capabilities into disaster management plans, formulate suitable laws and regulations, establish coordination mechanisms between the public and private sectors, tackle technological limitations arising from advancements in technology, and implement specialized training programs for drone operators. Garnica-Pena and Alcantara-Ayala (2021) seek to examine the role of the global landslide research community in reducing the risk and managing the consequences of disasters, specifically focusing on the utilization of UAVs, as discussed in the existing literature. The initial section highlighted the significance of research contributions on disaster risk for the execution of initiatives and strategies related to disaster risk management. The second half focused on providing background information and discussing the present applications of drones in the field of hazards and risk. Zhang et al. (2024) presented a classification scheme for the drone cooperative delivery problem (TDCDP) and provided a comprehensive summary of the relevant studies. The analysis focused on the detailed examination of the effects of changes in clients and environments on truck and drone delivery modalities. The suggested taxonomy categorized the delivery modes in TDCDP into four types: Parallel delivery, mixed delivery, drone delivery with truck-assisting, and truck delivery with drone-assisting.

UAVs have gained prominence as a cutting-edge technology for disaster management. Their capabilities in aerial imaging, communication, and navigation make them ideal for enhancing disaster response efforts. In recent literature, the utilization of UAVs in disaster management has been extensively explored across various domains, including infrastructure monitoring, disaster response, and hazard assessment. However, our study distinguishes itself by offering a comprehensive descriptive literature review that specifically assesses UAV applications in post-disaster scenarios. Unlike previous works, which often emphasize specific applications or technologies, our research applies the LDA topic modelling to systematically identify and categorize the main topics and trends within the literature related to UAV applications in disaster response. Furthermore, by employing the fuzzy c-means algorithm, we provide a nuanced analysis of UAV applications, clustering them to offer insights into their effectiveness and potential for future enhancements. This dual approach of topic modelling and clustering not only enriches the understanding of current UAV applications but also highlights emerging trends and gaps, setting the stage for more targeted and effective disaster response strategies.

The subsequent sections of the paper are structured in the following manner: Section 2 outlines the methodology that is relevant to the topic. Section 3 provides a concise overview of the findings and the subsequent discussions. Section 4 serves as the conclusion of the study.

2. Materials and Methods

This section outlines the process of identifying the most important publications in the dataset using LDA topic modelling combined with the fuzzy c-means algorithm. The search syntax is provided in Table 1.

Table 1. Search strings on Scopus

| Database | Search strings |
|------------------------|---|
| Scopus (July 17, 2024) | (TITLE-ABS-KEY ("drone") OR TITLE-ABS-KEY ("unmanned aerial vehicles") AND TITLE-ABS-KEY ("post-disaster") |

The search yields 433 papers. The abstracts of all publications are examined. The pre-processing stage, which involves the cleansing and preparation of data for subsequent operations, is implemented on the data set using the MATLAB R2021a software. URLs (Uniform Resource Locators), also referred to as web addresses, have been eliminated due to their tendency to cause text misclassification. Punctuations and search strings (such as “drone”, “unmanned aerial vehicles”, “UAVs”, and “post disaster”) are eliminated. Finally, tokenization is implemented, which involves the division of sequences into distinct tokens. After the pre-processing stage, the LDA procedure is implemented on the dataset. The fuzzy c-means algorithm is implemented after the LDA to acquire center documents.

2.1. Latent Dirichlet allocation (LDA)

Blei et al. (2003) introduced the LDA, a probabilistic model that generates a corpus. The fundamental concept is that documents are represented as stochastic combinations of latent topics, with each subject being defined by a probability distribution of words.

$$p(D|\alpha, \beta) = \prod_{d=1}^M \int P(\theta_d | \alpha) \left(\prod_{n=1}^{N_d} \sum_{z_{dn}} p(z_{dn} | \theta_d) p(w_{dn} | z_{dn}, \beta) \right) d\theta_d \quad (1)$$

The concentration parameter of the Dirichlet prior for the topic distribution of each document is denoted by α in (1), while β represents the same parameter for the word distribution within each topic. z_{dn} represents the topic assignment for the n th word in document d , w_{dn} represents the n th word in document d , and θ_d represents the topic distribution for document d . The total number of words in the document is denoted by N , the number of documents being analyzed is denoted by M , and the corpus of M documents is represented by D .

2.2. Fuzzy c-means

Bezdek et al. (1984) introduced the renowned fuzzy c -means clustering algorithm, which differs from the classic k -means approach by enabling a sample to be assigned to multiple clusters rather than a single one. The fuzzification factor, which determines the degree of fuzziness within the clusters, is used to assign membership values to data items for the clusters within a range of 0 to 1. The objective function is minimized by the methodology. The fuzzy c -means model is as follows (Mao and Xu, 2024):

$$\sum_{i=1}^N \sum_{j=1}^C \mu_{ij}^m \|x_i - v_j\|^2 \quad (2)$$

$$\mu_{ij} \geq 0, \sum_{j=1}^C \mu_{ij} = 1, 0 < \sum_{i=1}^N \mu_{ij} < N \quad (3)$$

where x_i represents the i th data point from the dataset X , which is a set of real numbers in an n -dimensional space. v_j represents the j th prototype of the cluster in this context. μ_{ij} is the membership grade of the individual data point x_i belonging to v_j . As a coefficient, the fuzzification factor is represented by the scalar “ m ” (where $m > 1$). The parameter m , known as the fuzzification factor, has a substantial influence on the formation of clusters during the process. (2) and (3) require that the overall sum of membership grades for each data point in all clusters is 1. Each cluster must contain at least one data point, although no cluster may completely dominate all data points. (4) determines the degree to which a data point is associated with a cluster by evaluating its distance from the cluster's prototype. (5) adjusts the cluster prototypes with the weighted sum of data points' membership grades, adjusted by the fuzzification factor. The objective function described above is minimized by iteratively computing modifications to the membership degree and prototypes, specifically,

$$\mu_{ij} = \frac{1}{\sum_{k=1}^C \left(\frac{\|x_i - v_j\|}{\|x_i - v_k\|} \right)^{\frac{2}{m-1}}} \quad (4)$$

$$v_j = \frac{\sum_{i=1}^N (x_i \mu_{ij}^m)}{\sum_{i=1}^N \mu_{ij}^m} \quad (5)$$

3. Results and Discussion

By using 433 papers, the LDA process is implemented to gather important topics and their probabilities. Figure 1 helps to determine the appropriate number of topics.

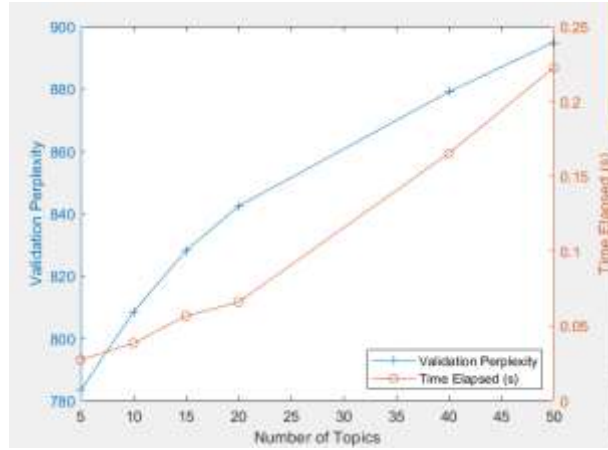


Figure 1. Relationship between the number of topics, validation perplexity and time elapsed

Figure 1 shows the relationship between the number of topics and two metrics: validation perplexity and time elapsed. Taking the Figure 1 into account, we determined the number of topics as 7. At 7 topics, there's a good balance between model complexity and efficiency. The perplexity is relatively low, ensuring clearer topic distinction. The time required for processing is minimal, making the model computationally efficient.

After the LDA process, a matrix with dimensions of 433x7 is acquired. This matrix displays the probability of 7 significant topics across 433 documents. The number of clusters is computed using the elbow approach based on the data from the resulting matrix. Figure 2 demonstrates the results of the elbow method.

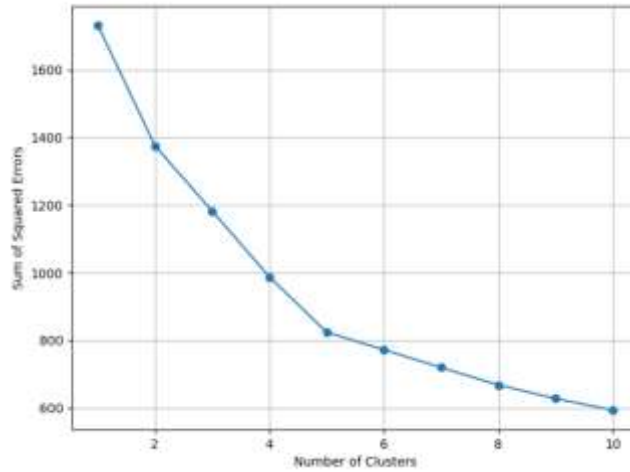


Figure 2. Results of the elbow method

The Figure 2 suggests an "elbow" around 3-5 clusters. This is where the rate of decrease in the sum of squared errors starts to slow, indicating a potential optimal number of clusters. We selected a cluster count of 5 to observe the range of variety. However, in this case, three of the five clusters overlapped at the same point. Consequently, we gather three clusters. The center coordinates of the clusters are obtained from documents 224, 64, and 218.

3.1. Center papers of the clusters

Cluster 1: This center paper (224) employed UAV-based aerial imagery as a flood detection method, utilizing a Convolutional Neural Network (CNN) to extract flood-related features from the images of the disaster zone. The study area was situated in a flood-prone region of the Indus River in Pakistan, and UAVs were employed to capture images of the area both before and after the disaster. 2150 image replacements were generated during the

training phase by resizing and cropping the source images. To validate the model, it was tested against both pre- and post-disaster images. The model has a 91% accuracy rate for affirmative flood detection results (Munawar et al., 2021).

Cluster 2: This center paper (64) proposed a joint data aggregation and computational outsourcing (JDACO) scheme for UAV-enabled IoT systems in post-disaster scenarios. The primary goal of JDACO is to reduce the overall energy consumption and latency in the aggregation and computation processes. It accomplishes this by utilizing UAVs as mobile edge computing servers and deploying numerous UAVs (Raivi and Moh, 2024).

Cluster 3: This center paper (218) examined a cognitive satellite-UAV network (CSUN), in which the satellite and UAVs are administered in a coordinated manner and opportunistically share spectrum to alleviate the spectrum scarcity issue. In particular, the paper proposed the UAV swarm to reduce the interference between satellites and UAVs. The proposed algorithm's superiority can be seen in the simulation results, which suggest that it may be a viable solution for enhancing the coverage performance of terrestrial 4G/5G networks (Liu et al., 2020).

These center papers collectively illustrate the diverse applications of UAV technology in disaster management and communication networks, highlighting innovative approaches to improve efficiency and effectiveness.

The 1st cluster contains 246 documents, the 2nd cluster contains 102 documents, and the 3rd cluster contains 85 documents. We identified the five critical topics in each cluster using LDA. Table 2 illustrates the significant topics of cluster 1 along with their probabilities.

Table 2. Important topics of cluster 1

| Cluster 1 | | | | |
|---------------------------|---------------------------|-------------------------|--------------------------|------------------------|
| Topic 1 | Topic 2 | Topic 3 | Topic 4 | Topic 5 |
| Word, Probability | Word, Probability | Word, Probability | Word, Probability | Word,Probability |
| "damage" 0.036289 | "network" 0.016966 | "rescue" 0.025189 | "remote" 0.01757 | "data" 0.01952 |
| "data" 0.022717 | "vehicle" 0.01523 | "emergency" 0.021701 | "sensing" 0.016471 | "accuracy" 0.018097 |
| "images" 0.022275 | "operations" 0.011567 | "relief" 0.014532 | "management" 0.016288 | "response" 0.017893 |
| "assessment" 0.019914 | "performance" 0.010796 | "vehicles" 0.0091068 | "technology" 0.011896 | "area" 0.01708 |
| "information" 0.017849 | "compared" 0.0096395 | "delivery" 0.008913 | "field" 0.010981 | "learning" 0.01342 |

Table 2 presents a cluster analysis with five topics, each containing words and their corresponding probabilities. The words with higher probabilities within each topic are considered more representative of that topic. Each topic contains keywords related to a specific subject, indicated by their probabilities. Higher probability words are more central to the topic. For example, in Topic 1, "damage" is the most significant word with a probability of 0.036289, followed by "data" and "images". Figure 3 shows the word cloud of cluster 1.

Ethics Permissions

This paper does not require ethics committee approval.

Author Contributions

Zeynep Yüksel conducted research and contributed to the drafting of the manuscript. Nazmiye Eligüznel created the original draft and complete the methodology and analysis. Süleyman Mete provided review, editing and verification.

Conflict of Interest

Authors declare that there is no conflict of interest for this paper.

References

- Bezdek, J. C., Ehrlich, R., and Full, W. (1984). FCM: The fuzzy c-means clustering algorithm. *Computers and Geosciences*, 10(2–3), 191–203. [https://doi.org/10.1016/0098-3004\(84\)90020-7](https://doi.org/10.1016/0098-3004(84)90020-7)
- Blei, D., Jordan, M., and Ng, A. Y. (2003). Latent Dirichlet allocation. *Journal of Machine Learning Research*, 3, 993–1022. <https://doi.org/10.1162/jmlr.2003.3.4-5.993>
- Calamoneri, T., Corò, F., and Mancini, S. (2024). Management of a post-disaster emergency scenario through unmanned aerial vehicles: Multi-depot multi-trip vehicle routing with total completion time minimization. *Expert Systems with Applications*, 251(February), 123766. <https://doi.org/10.1016/j.eswa.2024.123766>
- Faiz, T. I., Vogiatzis, C., and Noor-E-Alam, M. (2024). Computational approaches for solving two-echelon vehicle and UAV routing problems for post-disaster humanitarian operations. *Expert Systems with Applications*, 237(PB), 121473. <https://doi.org/10.1016/j.eswa.2023.121473>
- Freeman, M. R., Kashani, M. M., and Vardanega, P. J. (2021). Aerial robotic technologies for civil engineering: Established and emerging practice. *Journal of Unmanned Vehicle Systems*, 9(2), 75–91. <https://doi.org/10.1139/juvs-2020-0019>
- Garnica-Peña, R. J., and Alcántara-Ayala, I. (2021). The use of UAVs for landslide disaster risk research and disaster risk management: a literature review. *Journal of Mountain Science*, 18(2), 482–498. <https://doi.org/10.1007/s11629-020-6467-7>
- Ishiwatari, M. (2024). Leveraging drones for effective disaster management: A comprehensive analysis of the 2024 Noto Peninsula earthquake case in Japan. *Progress in Disaster Science*, 23(July), 100348. <https://doi.org/10.1016/j.pdisas.2024.100348>
- Lei, J., Zhang, T., Mu, X., and Liu, Y. (2024). NOMA for STAR-RIS assisted UAV networks. *IEEE Transactions on Communications*, 72(3), 1732–1745. <https://doi.org/10.1109/TCOMM.2023.3333880>
- Liu, C., Feng, W., Chen, Y., Wang, C. X., Li, X., and Ge, N. (2020). Process-oriented optimization for beyond 5G cognitive satellite-UAV networks (Invited Paper). 2020 29th Wireless and Optical Communications Conference, WOCC 2020. <https://doi.org/10.1109/WOCC48579.2020.9114919>
- Lozano, J. M., and Tien, I. (2023). Data collection tools for post-disaster damage assessment of building and lifeline infrastructure systems. *International Journal of Disaster Risk Reduction*, 94, 103819. <https://doi.org/10.1016/j.ijdr.2023.103819>
- Mao, W., and Xu, K. (2024). Enhancement of the classification performance of fuzzy c-means through uncertainty reduction with cloud model interpolation. *Mathematics*, 12(7), 975. <https://doi.org/10.3390/math12070975>
- Mohd Daud, S. M. S., Mohd Yusof, M. Y. P., Heo, C. C., Khoo, L. S., Chainchel Singh, M. K., Mahmood, M. S., and Nawawi, H. (2022). Applications of drone in disaster management: A scoping review. *Science and Justice*, 62(1), 30–42. <https://doi.org/10.1016/j.scijus.2021.11.002>
- Munawar, H. S., Ullah, F., Qayyum, S., Khan, S. I., and Mojtahedi, M. (2021). Uavs in disaster management: Application of integrated aerial imagery and convolutional neural network for flood detection. *Sustainability*, 13(14), 7547. <https://doi.org/10.3390/su13147547>
- Phadke, A., and Medrano, F. A. (2023). Examining application-specific resiliency implementations in UAV swarm scenarios. *Intelligence and Robotics*, 3(3), 453–478. <https://doi.org/10.20517/ir.2023.27>
- Qadir, Z., Le, K., Bao, V. N. Q., and Tam, V. W. Y. (2024). Deep learning-based intelligent post-bushfire detection using UAVs. *IEEE Geoscience and Remote Sensing Letters*, 21, 1–5. <https://doi.org/10.1109/LGRS.2023.3329509>
- Raivi, A. M., and Moh, S. (2024). JDACO: Joint data aggregation and computation offloading in UAV-enabled internet of things for post-disaster scenarios. *IEEE Internet of Things Journal*, 11(9), 16529–16544. <https://doi.org/10.1109/JIOT.2024.3354950>
- Wu, J., Chen, Q., Jiang, H., Wang, H., Xie, Y., Xu, W., Zhou, P., Xu, Z., Chen, L., Li, B., Wang, X., and Wu, D. O. (2024). Joint

power and coverage control of massive UAVs in post-disaster emergency networks: An aggregative game-theoretic learning approach. *IEEE Transactions on Network Science and Engineering*, 11(4), 3782–3799. <https://doi.org/10.1109/TNSE.2024.3385797>

Zhang, J., Zhu, Y., Li, X., Ming, M., Wang, W., and Wang, T. (2022). Multi-trip time-dependent vehicle routing problem with split delivery. *Mathematics*, 10(19), 3527. <https://doi.org/10.3390/math10193527>

Zhang, R., Dou, L., Xin, B., Chen, C., Deng, F., and Chen, J. (2024). A review on the truck and drone cooperative delivery problem. *Unmanned Systems*, 12(5), 823-847. <https://doi.org/10.1142/S2301385024300014>

Zou, R., Liu, J., Pan, H., Tang, D., and Zhou, R. (2024). An improved instance segmentation method for fast assessment of damaged buildings based on post-earthquake uav images. *Sensors*, 24(13), 4371. <https://doi.org/10.3390/s24134371>

Sensitive Microwave Sensor for Adulteration Detection in Olive Oil

Hüseyin KORKMAZ^{1*}, Uğur Cem HASAR¹

Keywords

*Microwave sensing,
Dielectric constant,
Quality factor,
Figure of merit,
Low cost*

Abstract – A novel reflection-based microwave sensor that is reproducible, feasible, and sensitive to changes in dielectric parameters has been specifically developed, fabricated, and analyzed to detect sunflower oil mixed with olive oil. The proposed sensor is built on an FR-4 dielectric substrate and shows a magnitude of -47.19 dB at a resonance frequency of 9.48 GHz. An electric field distribution analysis of the sensor was performed, and it was determined that the electric field was significantly concentrated in the upper regions of the resonator. Olive oil was mixed with sunflower oil at the rates of 10%, 20% and 30%. The prepared samples were placed directly on the sensor and the performance of the sensor in simulation and experimental environments was tested. Based on the measured dielectric constants, the results of the experiments and simulations were observed to be consistent. The proposed sensor demonstrated superior performance compared to other sensors proposed in the literature in experimental measurements with a Q-factor of 4635, normalized sensitivity value of 3.62%, a Figure of Merit of 6581, and resonance frequency shift of 62 MHz occurred between the pure olive oil and the 10% sunflower oil adulterated olive oil sample. The proposed sensor can be preferred in industrial and liquid chemical detection applications due to its high sensitivity, high-quality factor, low cost, and small amount of sample required.


1. Introduction

Food quality and composition are key parameters of critical importance in all processes of the food manufacturing industry. However, some manufacturers increase the adulteration of foods for profit maximization purposes (Göğüş et al., 2009). It is emphasized that olive oils are richer in composition and quality than other oils in daily use. However, due to differences in the production processes of these oils, the price range may vary from low-quality to high-quality oils. This can cause complexities in the marketing process when low-quality oils are mixed with high-quality oils (Osman et al., 2014). Extra virgin olive oil and other valuable oils are often mixed with more economical oils such as sunflower, corn, palm, and cottonseed (Gunstone, 2011). Such adulterations may utilize methods to conceal changes that make them difficult to detect by normal human senses or basic tools (Meenu et al., 2019). Infrared combined with traditional methods such as gas chromatography (GC) (Hashempour et al., 2024) and High-Performance Liquid Chromatography (HPLC) (Menegoz and Moret, 2024) as well as modern spectroscopic techniques such as thin layer chromatography (TLC) (Khursheed et al., 2024) and differential scanning calorimetry (DSC) (Islam et al., 2022a). Methods such as (IR) (Yılmaz-Düzyaman et al., 2024), ultraviolet (UV) (Musa, 2024) and fluorescence spectroscopy (Rueda et al., 2024) are also used in the analysis of oil samples. Although these analysis techniques are often criticized for being time-consuming, complex, and requiring high-cost facilities. Metamaterials (MMs) are defined as human-created materials with extraordinary exotic properties. One of the properties of metamaterials (MM) is that they can control and direct electromagnetic waves (Wu et al., 2024). Following experimental verification of the structures of metamaterials, significant research has been conducted in this field. One of the most striking features of this structure is the concept known as the "Invisibility Cloak", which is quite interesting (Ergin et al., 2010). Additionally, this structure allows energy absorption in wide band gaps (Krödel et al., 2015). Advances in absorber applications

^{1*}**Corresponding Author.** Gaziantep University, Graduate School of Natural and Applied Sciences, Department of Electrical and Electronics Engineering,

27310 Gaziantep, Türkiye. E-mail: muh.huseyinkorkmaz@gmail.com  OrcID: 0000-0002-3518-1943

²Gaziantep University, Faculty of Engineering, Department of Electrical and Electronics Engineering, 27310 Gaziantep, Türkiye. E-mail: uchasar@gantep.edu.tr

 OrcID: 0000-0002-6098-7762

Citation: Korkmaz, H., and Hasar, U. C. (2024). Sensitive microwave sensor for adulteration detection in olive oil. *Natural Sciences and Engineering Bulletin*, 1(2), 27-37.

have created opportunities for various studies on energy harvesting (Korkmaz and Hasar, 2021; Korkmaz et al., 2023; Obaidullah et al., 2021). Every year, new types of sensors are developed thanks to advances in micro and nanotechnology and electronics, photonics, and materials science (Hasar et al., 2024b; Shi et al., 2020). Recent research has focused on the development of sensors with high accuracy, compact size, and high sensitivity (Alahnomi et al., 2021). Microwave (MW) sensors use the electromagnetic field for sensing and generally have operating frequencies in the range of 300 MHz to terahertz (Mehrotra et al., 2019). The advantages of MW sensors compared to other options include features such as low cost, compact structure, high accuracy, easy production, and testability. Due to these obvious advantages, MW sensors play an important role in various fields of life, such as healthcare (Korostynska et al., 2014), the food industry (Hasar et al., 2024a), the defence sector (Hudec et al., 2009), and industry (Nyfors, 2000). MW sensors can generally be classified into two basic types: Broadband sensors and resonance-based sensors. Resonance-based sensors typically function with high sensitivity over a narrow frequency range and generally use a limited and intense electric field for sensing. The resonance frequency is extremely sensitive to dielectric loading in this region, and any instantaneous change can lead to a significant shift in the resonance frequency (Bhatti et al., 2022). In recent years, researchers have conducted a series of studies to detect adulteration with MW sensors. The use of MTM sensors in detecting various oils is demonstrated by (Bakır et al., 2019). For example, while the resonance frequency is 70 MHz in dirty and clean transformer oils, this value is reduced to 50 MHz in olive and corn oils. A high-efficiency portable sensor is mentioned to detect branded and unbranded fuel samples (Tümkiye et al., 2018). While the resonance frequency shift for branded and unbranded diesel was determined as 72 MHz, this frequency shifted by 12 MHz for branded and unbranded gasoline. A transmission line-based MTM sensor has been introduced to identify original and adulterated gasoline samples (Tamer et al., 2018). This sensor can discriminate between original and adulterated diesel samples with a frequency shift of 50 MHz. Reviews of the literature reveal that metamaterial-based sensors can be used over a wide frequency range (Bakır et al., 2019; Tümkiye et al., 2018; Tamer et al., 2018; Lee et al., 2017) and for a variety of materials from solid dielectrics to liquids, gases, and biomolecules (Vélez et al., 2017; Mohd Bahar et al., 2019; Lee and Yook, 2008). A sensitive MTM sensor has been introduced to discriminate between original and adulterated fuel samples (Tümkiye et al., 2017). The resonance frequency is shifted to 100 MHz. Rhombus MTM sensor was considered for flow sensing (Tümkiye et al., 2019), but the sensitivity and quality factors were low in this study. Another study proposed that a curved line metamaterial-based sensor used for polypropylene detection exhibited moderate performance (Islam et al., 2021). A sensor inspired by the MTM absorber has been proposed to detect liquid chemicals with changing electrical properties (Abdulkarim et al., 2019). The quality factor and sensitivity of the sensor were found to be inadequate. An omega-shaped sensor has been introduced for industrial applications (Altıntaş et al., 2020). The sensor operates in the 8–12 GHz frequency range and is designed with a 70 MHz frequency shift for clean and waste transformer oils. Additionally, another MTM sensor has been introduced to detect liquid chemicals (Abdulkarim et al., 2020c). In the study, quality factors and sensitivity are average. As a result of our literature research, it was determined that the sensitivity, quality factor (Q-factor), and Figure of Merit (FoM) of the proposed sensors are important performance parameters and that these parameters are potential limitations and disadvantages for the sensors proposed in the literature (Khalil et al., 2023). As a solution to the mentioned limitations and disadvantages, this study proposes a microwave (MW) sensor that is repeatable, feasible, and sensitive to changes in dielectric parameters to detect adulterations in olive oil. The proposed sensor is capable of successfully detecting adulteration in sunflower oil mixed with olive oil at 10%. The proposed sensor exhibits superior performance compared to other sensors reported in the literature. The proposed sensor operates at a frequency of 9.481 GHz with a maximum sensitivity of 3.62%, a quality factor value of 4635, and a FoM value of 6581. In addition, the proposed sensor or system is considered an important candidate for sensing applications. It has advantages such as high sensitivity, compact design, low manufacturing and measurement costs, small size, easy use, low sample consumption, and low cost. The rest of the manuscript is as follows. The design of the proposed sensor, analysis, and preparation of samples are presented in detail in the Materials and Methods section. In the next section, dielectric constant measurement and adulteration processes of sunflower oil mixed with olive oil were examined in detail. Additionally, the proposed sensor's Q-factor, FoM, and sensitivity analyses are presented in detail in the Results and Discussion section. In the last section, the conclusions obtained from the study are given.

2. Materials and Methods

2.1. Design and analysis

In this section, the proposed MW sensor developed and examined within the scope of this study will be explained in detail. The optimal design was obtained by meticulously adjusting the proposed dimensions, and its final version for the detection of liquid foods (especially oils) using MW techniques is shown in Figure 1a. The proposed design is presented in Figure 1a, and simulations were carried out using the finite integration technique (FIT)-based Computer Simulation Technology MW Studio (CST) program. The designed sensor consists of a resonator at the top, an FR-4 dielectric layer in the middle, and a copper grounding layer at the bottom. In the proposed design, the loss tangent value of FR-4 was determined to be 0.025, its relative permeability was 4.3, and its thickness was 1 mm. Considering the durability, cost analysis, market availability, and reproducibility of the study, FR-4 material can be considered as a more suitable material for this study. The total size of the sensor is 22.86x10.16 mm² (compatible with X-band waveguide) and is designed to operate in the 8-12 GHz frequency range. The $|S_{11}|_{dB}$ value of the reflection-based sensor (without sample) designed in the CST program is seen as -47.19 dB around 9.481 GHz in the graph in Figure 2b. To demonstrate the accuracy and repeatability of the designed sensor, the proposed sensor was fabricated in compliance with the X-band waveguide, and the $|S_{11}|_{dB}$ (reflectance) parameter was measured (without samples) as shown in Figure 1b. As shown in Figure 2b, as a result of the measurement using the VNA device, when there is no sample on the proposed reflection resonance sensor, the $|S_{11}|_{dB}$ value of the sensor is approximately -42.35 dB at the frequency of 9.467 GHz. In addition, effect of four strips that forming resonator of the proposed sensor to response of the $|S_{11}|_{dB}$ value shown in Figure 2b. The $|S_{11}|_{dB}$ value of the sensor is approximately -29.96 dB at the frequency of 9.493 GHz in the case without using the four strips in the design. It is evident that the four strips surrounding the main resonator induce a deeper reflection response and increase the response's quality.

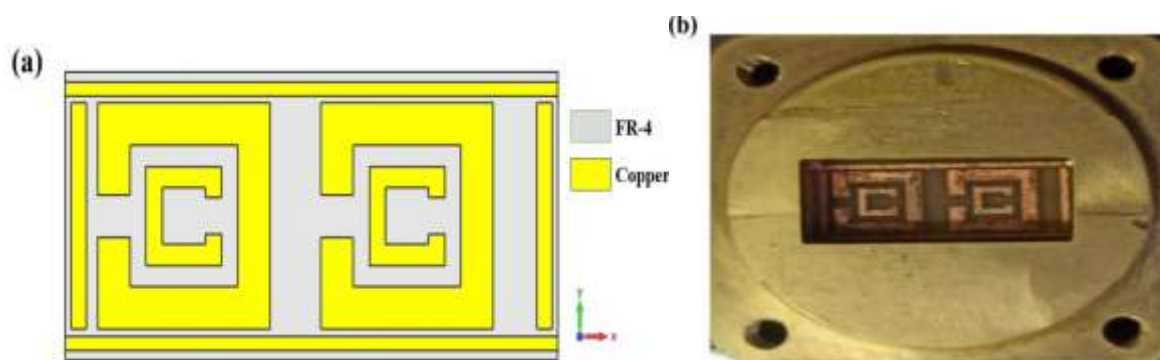


Figure 1. Proposed MW sensor (a) main structure in CST (b) front view of the fabricated sensor

Electric field distributions were examined to understand the working principle of the proposed sensor. Changes in the electric field provide information about the amount of energy the sensor can store (Islam et al., 2022b). The electric field distributions of the proposed sensor were simulated without samples at the resonance frequency of 9.48 GHz. As seen in Figure 2c, the electric field intensity is higher in the components that make up the resonator. Figure 2d represents the surface current distribution of the proposed sensor at the resonance frequency. Surface current distribution is observed to be concentrated on and around the elements forming the resonator. As a result, the proposed structure is capable of detecting even the smallest changes in the electrical properties of the sample. The proposed sensor has a design where the input port is provided at 1, the output port is measured at 2, and a two-port network is used to power the sensor, as the setup is shown in Figure 2a. When the electromagnetic wave was transmitted through port 1, most of the energy was stored in the sensing section during resonance. This energy then interacted with the dielectric properties of the tested oil sample, which were different from those of air, changing the resonance frequency. The resonance frequency was determined with the reflection coefficient $|S_{11}|_{dB}$. As a result of our market and literature research, we determined that sunflower oil is one of the oil types most commonly mixed with olive oil. Based on this observation, pure sunflower and olive oil purchased from the supermarket were adulterated at different rates. Maintaining the properties of all the oils we supply is important for the accuracy of the study. Therefore, all samples were stored in the refrigerator, protected from sunlight, in closed, dark glass bottles at approximately 5°C. Some samples were prepared to determine whether the designed MW sensor could detect oils or

determine minimum adulteration rate capacity. These samples consist of pure olive oil, pure sunflower oil, and pure sunflower oil (mixed with olive oil at 10%, 20%, and 30% rates).

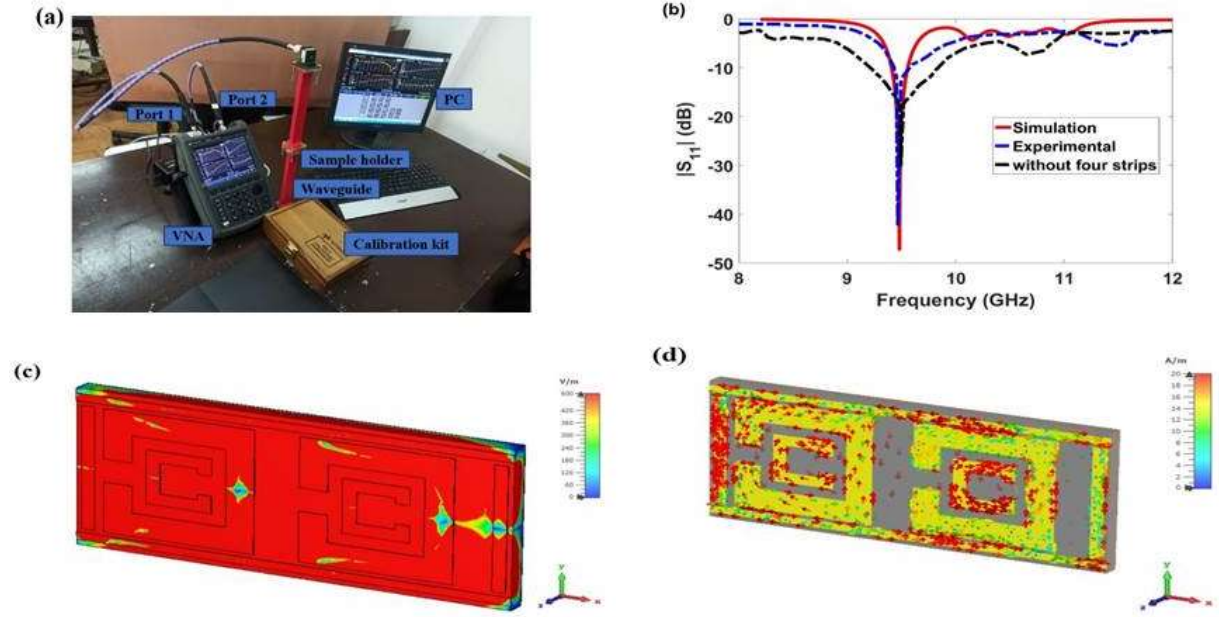


Figure 2. (a) Experimental setup for sample measurements with proposed sensor (b) experimental and simulated scattering parameter $|S_{11}|_{dB}$ of the proposed sensor in the air and $|S_{11}|_{dB}$ response without four strips (c) E-field and (d) surface current distribution of the proposed sensor at 9.481 GHz

3. Results and Discussion

The dielectric properties of all samples should be determined to simulate the response of the proposed sensor to samples prepared at different percentages and compared with experimental studies. For this purpose, the dielectric constants of the samples were determined in the 8-12 GHz frequency range using the dielectric probe measurement setup shown in Figure 3a. Dielectric constants of the prepared samples were determined using Keysight Technologies' open-ended coaxial dielectric probe kit (Model number: N1501A) with calibration steps such as short, clear, and distilled water and a calibrated VNA. The complex dielectric coefficient of the samples can be calculated using the formula given in (1).

$$\epsilon = \epsilon' - j\epsilon'' \quad (1)$$

Here ϵ' represents the real component of permittivity, and ϵ'' represents the imaginary component of the permittivity. Figure 3b shows the graph of the real dielectric constants of pure olive oil, pure sunflower oil, and olive oil-sunflower oil mixture samples at different ratios. It can be seen from Figure 3b that the real dielectric constant value of sunflower oil is greater than that of olive oil. Additionally, the real dielectric constant of the samples shows a linear decrease between 8 GHz and 12 GHz. The real dielectric constants measured at the resonance frequency of the samples for pure olive oil, sunflower oil mixed with 10%, 20%, and 30% olive oil, and pure sunflower oil are 2.53, 2.68, 2.73, 2.77, and 2.89, respectively.

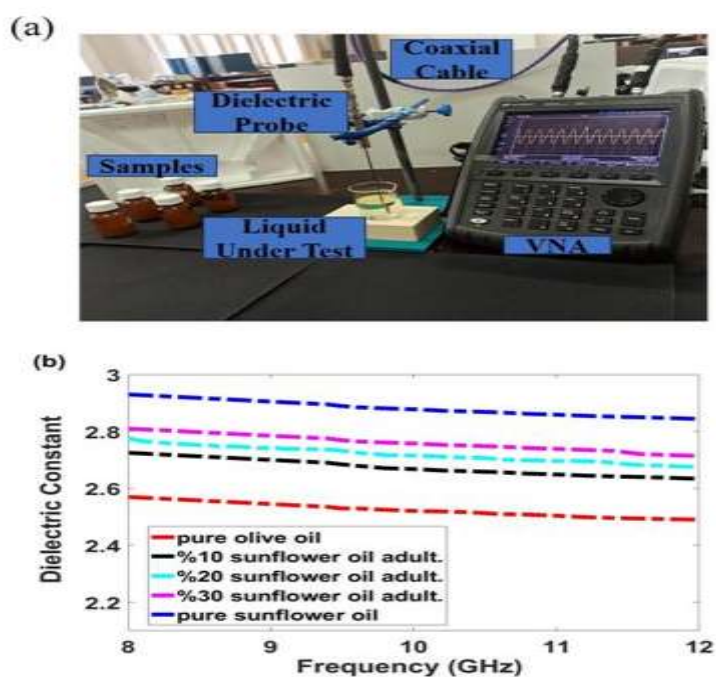


Figure 3. (a) Measurement set up for determining the dielectric constant of different samples using N1501A dielectric probe kit (b) dielectric constant curves for pure olive oil-sunflower oil adulteration

We stated that the dielectric properties of all prepared samples should be determined to simulate the response of the designed MW sensor to samples prepared at different percentages and compare it with experimental studies. The dielectric properties of the samples were determined using the dielectric probe assembly shown in Figure 3a, and the results are shown in Figure 3b. The measured dielectric constants were transferred to the CST simulation program and added to the CST library. All samples whose dielectric properties were determined and whose data were transferred to the CST library were simulated by placing them on the resonator. In this context, the response of the proposed sensor to samples prepared at different percentages was evaluated in a simulation environment.

3.1. Adulteration and analysis of olive oil with sunflower oil

In this section, the process of the proposed MW reflection resonance sensor to analyze the adulteration of olive oil and sunflower oil at different rates with simulation and experimental setups is examined. The proposed sensor was modeled in a simulation environment in the frequency range of 8 GHz to 12 GHz, using the dielectric property data of pure olive oil, pure sunflower oil, and 10%, 20%, and 30% sunflower oil-olive oil mixtures. Pure olive oil and pure sunflower oil samples were added to the CST library. The simulation results of adulteration of sunflower oil and olive oil are shown in Figure 4a. As observed in Figure 4a, the proposed reflection resonance sensor responds to different resonance frequencies and changing reflection magnitudes with the change of the sunflower oil ratio added to the olive oil. For the proposed sensor, the observed resonance frequency in the simulation environment (without samples) was found to be approximately 9.481 GHz and the $|S_{11}|_{dB}$ value was -47.19 dB. When pure olive oil is placed at the top of the resonator, the observed resonance frequency is approximately 9.274 GHz and the $|S_{11}|_{dB}$ magnitude is -35.23 dB, under conditions where all simulation parameters are kept same. In this case, changes were observed in the resonance frequency and $|S_{11}|_{dB}$ value of the proposed sensor when there was no sample in the simulation environment and pure olive oil was placed as a sample. In the simulation for the proposed sensor, according to the result obtained using pure sunflower oil dielectric constant data, the resonance frequency was observed to be approximately 8.824 GHz, and the $|S_{11}|_{dB}$ value was observed to be -23.13 dB. Simulation results (resonance frequency and magnitude) of 10% sunflower oil and pure olive oil mixture, 20% sunflower oil and pure olive oil mixture, and 30% sunflower oil and pure olive oil mixture were obtained as (-32.13 dB and 9.112 GHz), (-30.03 dB and 9.050 GHz), and (-28.83 dB and 8.980 GHz), respectively. The experimental results of adulteration of olive oil and sunflower oil

are presented in Figure 4b. When Figure 4b is examined, it is observed that the $|S_{11}|_{dB}$ values of the proposed reflection resonance sensor vary at different resonance frequencies, and in various samples.

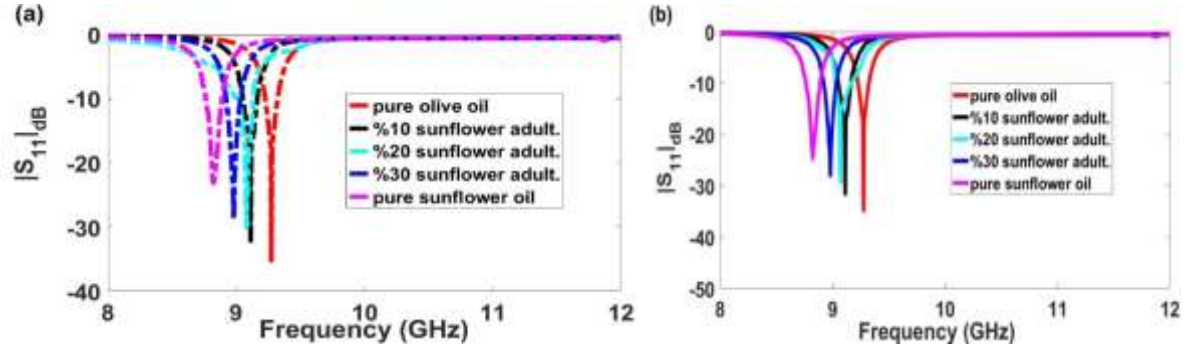


Figure 4. $|S_{11}|_{dB}$ graph for pure olive oil, pure sunflower oil, and pure olive oil- sunflower oil adulteration in different percentages (a) simulated result and (b) measured result

It has been observed that the experimental measurement results (magnitude and resonance frequency) for pure olive oil, 10% sunflower oil olive oil mixture, 20% sunflower oil olive oil mixture, 30% sunflower oil olive oil mixture, and pure sunflower oil samples are (-34.76 dB and 9.263 GHz), -31.57 dB and 9.101 GHz, (-29.17 dB and 9.042 GHz), (-27.97 dB and 8.971 GHz), (-22.73 dB and 8.811 GHz), respectively. Experimentally observed changes in the resonance frequency of the sensor were recorded as the ratio of sunflower oil mixed with olive oil increased. Figure 5a and Figure 5b show the resonance frequencies obtained from olive oil and sunflower oil mixtures in experimental and simulation setups and how these frequencies change compared to pure olive oil. According to the experimental measurement results, the resonance frequencies of pure olive oil, pure sunflower oil, and adulterated samples were determined. As a result of experimental measurements, the resonance frequency shifts of the samples compared to pure olive oil were determined as 0 MHz, 62 MHz, 221 MHz, 292 MHz, and 452 MHz, respectively. Additionally, in the simulation results, the resonance frequency shifts of the samples compared to pure olive oil were observed as 0 MHz, 62 MHz, 224 MHz, 294 MHz, and 450 MHz, respectively. According to the experimental and simulation results presented above, as the amount of sunflower oil added to pure olive oil increases, the resonance frequency decreases, and resonance frequency shifts increase. Table 1 shows the experimental and simulation results of olive oil-sunflower oil adulteration, including the resonance frequencies of the samples, $|S_{11}|_{dB}$, ϵ' values, and the resonance frequency shifts of the samples compared to pure olive oil.

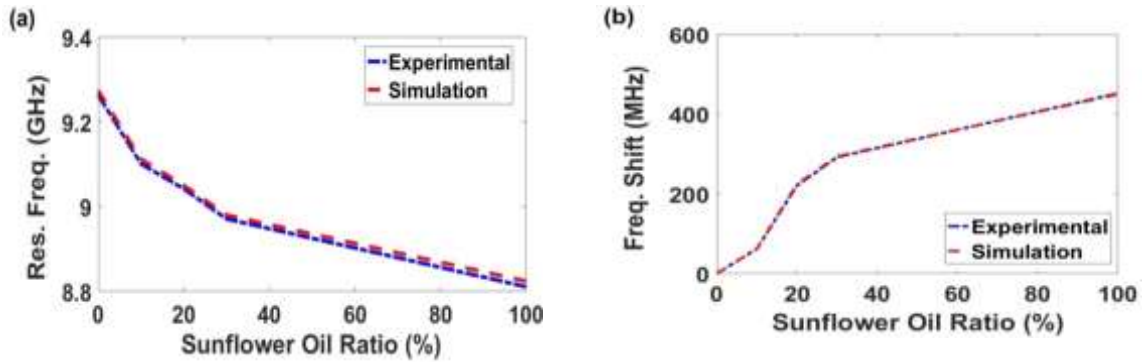


Figure 5. (a) Measured and simulated linearity plot of the resonant frequency versus sunflower oil concentration, (b) Measured and simulated linearity plot of the frequency shift versus sunflower oil concentration

When Table 1 is examined, the following inferences can be made regarding Figure 4a, Figure 4b, Figure 5a and Figure 5b. When the real dielectric constant values of the samples were listed from smallest to largest, an order was observed as pure olive oil, olive oil mixture containing 10% sunflower oil, olive oil mixture containing 20% sunflower oil, olive oil mixture containing 30% sunflower oil, and pure sunflower oil. In both simulation and experimental measurements, it is observed that the resonance frequency decreases as the ratio of sunflower oil mixed with pure olive oil increases. However, it is observed that as the sunflower oil ratio increases, the

resonance frequency shifts of the samples increase compared to pure olive oil. Additionally, when Figure 5a and Figure 5b are examined, it is observed that an almost linear graph is obtained. When Figure 5a and Figure 5b are examined, it is possible to estimate the resonance frequency of the olive oil sample to which a certain amount of sunflower oil is added and the frequency shift compared to pure olive oil. When we look at the $|S_{11}|_{dB}$ values according to the experimental and simulation results of olive oil-sunflower oil adulteration, it is observed that $|S_{11}|_{dB}$ values decrease as the amount of sunflower oil added to pure olive oil increases in both cases. Finally, when the resonance frequency and $|S_{11}|_{dB}$ values for olive oil and sunflower oil adulteration are examined, it is understood that the experimental and simulation results are compatible and are ranked according to the dielectric constant values.

Table 1. Resonance frequency, $|S_{11}|_{dB}$ value, ϵ' values, and resonance frequency shifts compared to pure olive oil for samples of olive oil-sunflower oil adulteration

| Samples | Res. Freq. (sim) | Res. Freq. (exp) | $ S_{11} _{dB}$ (sim) | $ S_{11} _{dB}$ (exp) | ϵ' | Freq. Shift (sim) | Freq. Shift (exp) |
|--------------------------------|------------------|------------------|-----------------------|-----------------------|-------------|-------------------|-------------------|
| Pure olive oil | 9.274 GHz | 9.263 GHz | -35.23 dB | -34.76 dB | 2.53 | 0 MHz | 0 MHz |
| 10% sunflower oil adulteration | 9.112 GHz | 9.101 GHz | -32.13 dB | -31.57 dB | 2.68 | 62 MHz | 62 MHz |
| 20% sunflower oil adulteration | 9.050 GHz | 9.042 GHz | 30.03 dB | 29.17 dB | 2.73 | 224 MHz | 221 MHz |
| 30% sunflower oil adulteration | 8.980 GHz | 8.971 GHz | -28.83 dB | -27.97 dB | 2.77 | 294 MHz | 292 MHz |
| Pure sunflower oil | 8.824 GHz | 8.811 GHz | -23.13 dB | -22.73 dB | 2.89 | 450 MHz | 452 MHz |

3.2. Sensitivity, quality factor, and figure of merit analysis

The performance of the sensor is generally determined by dimensionless sensor parameters such as sensitivity, quality factor, and FoM. The expressions in (2) and (3) were used to calculate the quality factor (Q-factor) and bandwidth frequency of the proposed sensor. Here f_c , f_b , f_h , and f_l represent center resonance frequency, bandwidth frequency, and higher and lower frequencies within -3 dB of the center frequency, respectively. As can be understood from (2), the bandwidth frequency has a critical effect on the Q-factor value.

$$Q = \frac{f_c}{f_b} \quad (2)$$

$$f_b = f_h - f_l \quad (3)$$

When the proposed sensor is tested in the region where the electric field is strongest by loading the sample, the resonance frequency changes depending entirely on the permeability of the tested material. This relationship shows that any change in relative permittivity ($\Delta\epsilon_r$) causes a linear change in resonance frequency (Δf_r). Therefore, sensitivity (S), an important parameter of the proposed sensor, can be determined by using (4).

$$S = \frac{\Delta f_r}{\Delta\epsilon_r} = \frac{f_{empty} - f_{\epsilon_r}}{\epsilon_r - 1} \quad (4)$$

Here, ϵ_r represents the dielectric constant of the sample, f_{empty} is the empty state resonance frequency of the proposed sensor, f_{ϵ_r} is the resonance frequency of the sensor in the state where the sample is placed. $S(\%)$ is the normalized sensitivity of the proposed sensor (Alahnomi et al., 2021). The normalized sensitivity of the proposed sensor can be determined by using expression (5).

$$S(\%) = \frac{f_{empty} - f_{\epsilon_r}}{f_{empty}(\epsilon_r - 1)} \times 100 \quad (5)$$

Within the scope of this study, the Q-factor and sensitivity values of olive oil and sunflower oil samples tested on the proposed sensor were calculated. The Q-factors of olive oil and sunflower oil are 4635 and 465, the sensitivity values are 1.42% and 3.62%, respectively. Additionally, the FoM value of the proposed sensor can be determined by using expression (6).

$$FoM = S \times Q - factor \quad (6)$$

Based on expression (6), the FoM values of olive oil and sunflower oil were calculated as 6581 and 1683, respectively. Olive oil, with a Q-factor value of 4635, and sunflower oil, with a normalized sensitivity value of 3.62%, have the highest values. The proposed sensor was evaluated based on the Q-factor, material detection, operating frequency, resonance frequency shift, and FoM criteria presented in Table 2 for comparison with other proposed sensors in the literature. When Table 2 is examined, it is seen that the proposed sensor in this study has the highest values with a Q-factor value of 4635 and FoM of 6581.

When we examine (2), it is understood that the bandwidth frequency is inversely proportional to the Q-factor value. The bandwidth of the proposed design at the ringing frequency is quite low compared to other studies in the literature. Therefore, the Q-factor value is expected to be higher. In addition, since the FoM value is directly proportional to the Q-factor (6), it is clear that the FoM value of the proposed sensor is higher compared to other studies in the literature. Our proposed sensor offers higher sensitivity, better quality factor, and higher FoM value compared to other studies published in the literature. Therefore, these results indicate that the proposed sensor is a suitable choice for practical applications.

Table 2. Comparison of the proposed sensor with other sensors available in the literature

| References | Material Sensing | Operating Frequency (GHz) | Resonance Frequency Shift (MHz) | Q-factor | FoM |
|----------------------------|---------------------------------|---------------------------|---------------------------------|-------------|-------------|
| (Altıntaş et al., 2019) | Transformer oil | 2-6 | 40 | 60 | 34 |
| (Abdulkarim et al., 2020b) | Oil | 1-8 | 63 | 90 | 32 |
| (Tamer et al., 2020) | Diesel | 8-12 | 60 | 110 | 37 |
| (Abdulkarim et al., 2020a) | Diesel | 8-12 | 120 | 105 | 41 |
| (Bakır et al., 2019) | Transformer oil | 8-12 | 70 | 100 | 48 |
| (Tümkiye et al., 2018) | Diesel | 10-12 | 72 | 90 | 52 |
| (Tamer et al., 2018) | Diesel | 8-12 | 100 | 95 | 38 |
| (Tümkiye et al., 2019) | Diesel | 8-12 | 92 | 105 | 43 |
| (Islam et al., 2022b) | Olive and corn oils | 8-12 | 100 | 135 | 76 |
| This work | Olive and sunflower oils | 8-12 | 450 | 4635 | 6581 |

4. Conclusion

Olive oil is a highly preferred food due to its healthy ingredients. Olive oil may be exposed to impurities during the production process due to high costs. This study proposes an MW sensor that is reproducible, feasible, and sensitive to changes in dielectric parameters to detect sunflower oil adulterated with olive oil. Simulation and experimental measurement results of the proposed reflection-based MW sensor were determined as -47.19 dB at 9.481 GHz frequency and -42.35 dB at 9.467 GHz frequency, respectively. When the simulation and experimental results are examined, it is observed that both measurements of the proposed sensor are consistent. In addition, the electric field and surface current distribution analyses of the proposed sensor were performed, and it was observed that the electric field was more intense in the parts forming the resonator. On the other hand, the dielectric constants of olive oil and sunflower oil were measured and analyzed using a dielectric measurement probe setup. Although the dielectric constants for olive oil and sunflower oil are close to each other, a resonance frequency shift of 62 MHz occurred between the pure olive oil and the 10% sunflower oil adulterated olive oil sample. The dielectric constants of the determined oils were significantly effective in frequency shift and magnitude interpretations in the simulation

environment and experimental measurements. Olive oil and sunflower oil were mixed in certain proportions, and the response of the samples prepared using the proposed reflection-based sensor was examined in both simulation and experimental environments. Finally, the performance of the proposed sensor is analyzed. Accordingly, the Q-factor, sensitivity, and FoM values of the proposed sensor were calculated. It has been observed that the proposed sensor performs better than other sensors published in the literature, with a Q-factor value of 4635, a normalized sensitivity value of 3.62%, and a FoM value of 6581. In conclusion, based on simulation, experimental data, and performance analysis, it was observed that the proposed MW sensor could detect sunflower oils added to olive oil at rates of 10% and above by using the frequency shift properties. For these reasons, the proposed sensor or system can be preferred in various applications, such as industrial and liquid chemical detection, with advantages such as high sensitivity, high-quality factors, superior performance, low cost, and little sample consumption.

Acknowledgment

The author Hüseyin Korkmaz acknowledges the Scientific and Technological Research Council of Turkey (TÜBİTAK) BİDEB 2211/C and Council of Higher Education (YÖK) 100/2000 Doctoral Scholarship program for supporting his studies.

Ethics Permissions

This paper does not require ethics committee approval.

Author Contributions

Hüseyin Korkmaz and Uğur Cem Hasar conducted the simulations and experiments; Hüseyin Korkmaz and Uğur Cem Hasar performed conceptualization analysis; Hüseyin Korkmaz and Uğur Cem Hasar prepared illustrations (visualization); Hüseyin Korkmaz and Uğur Cem Hasar analyzed the results; and Uğur Cem Hasar supervised the study.

Conflict of Interest

The authors declare that they have no known competing financial interests or personal relationships that could have appeared to influence the work reported in this paper.

References

- Abdulkarim, Y. I., Deng, L., Karaaslan, M., and Unal, E. (2019). Determination of the liquid chemicals depending on the electrical characteristics by using metamaterial absorber based sensor. *Chemical Physics Letters*, 732, 136655.
- Abdulkarim, Y. I., Deng, L., Karaaslan, M., Dalgaç, Ş., Mahmud, R. H., Ozkan Alkurt, F., Muhammadsharif, F. F., Awl, H. N., Huang, S., and Luo, H. (2020a). The detection of chemical materials with a metamaterial-based sensor incorporating oval wing resonators. *Electronics*, 9(5), 825.
- Abdulkarim, Y. I., Deng, L., Karaaslan, M., Altıntaş, O., Awl, H. N., Muhammadsharif, F. F., Liao, C., Unal, E., and Luo, H. (2020b). Novel metamaterials-based hypersensitized liquid sensor integrating omega-shaped resonator with microstrip transmission line. *Sensors*, 20(3), 943.
- Abdulkarim, Y. I., Deng, L., Luo, H., Huang, S., Karaaslan, M., Altıntaş, O., Bakır, M., Muhammadsharif, F. F., Awl, H. N., Sabah, C., and Al-badri, K. S. L. (2020c). Design and study of a metamaterial based sensor for the application of liquid chemicals detection. *Journal of Materials Research and Technology*, 9(5), 10291-10304.
- Alahnomi, R. A., Zakaria, Z., Yussof, Z. M., Althwayb, A. A., Alhegazi, A., Alsariera, H., and Rahman, N. A. (2021). Review of recent microwave planar resonator-based sensors: Techniques of complex permittivity extraction, applications, open challenges and future research directions. *Sensors*, 21(7), 2267.
- Altıntaş, O., Aksoy, M., Ünal, E., and Karaaslan, M. (2019). Chemical liquid and transformer oil condition sensor based on metamaterial-inspired labyrinth resonator. *Journal of the Electrochemical Society*, 166(6), B482.
- Altıntaş, O., Aksoy, M., and Ünal, E. (2020). Design of a metamaterial inspired omega shaped resonator based sensor for industrial implementations. *Physica E: Low-dimensional Systems and Nanostructures*, 116, 113734.
- Bakır, M., Karaaslan, M., Karadag, F., Dalgac, S., Ünal, E., and Akgöl, O. (2019). Metamaterial sensor for transformer oil, and microfluidics. *The Applied Computational Electromagnetics Society Journal (ACES)*, 799-806.
- Bhatti, M. H., Jabbar, M. A., Khan, M. A., and Massoud, Y. (2022). Low-cost microwave sensor for characterization and

adulteration detection in edible oil. *Applied Sciences*, 12(17), 8665.

Ergin, T., Stenger, N., Brenner, P., Pendry, J. B., and Wegener, M. (2010). Three-dimensional invisibility cloak at optical wavelengths. *Science*, 328(5976), 337-339.

Göğüş, F., Özkaya, M. T., and Ötleş, S. (2009). *Zeytinyağı*. Ankara: Eflatun Yayınevi.

Gunstone, F. D. (2011). Production and trade of vegetable oils. *Vegetable oils in food technology: Composition, properties and uses*, 2, 1-24.

Hasar, U. C., Hasar, H., Ozturk, H., Korkmaz, H., Kaya, Y., Ozkaya, M. A., Ebrahimi, A., Barroso, J. J., Nayyeri, V., and Ramahi, O. M. (2024a). Simple and inexpensive microwave setup for industrial based applications: Quantification of flower honey adulteration as a case study. *Scientific Reports*, 14(1), 8847.

Hasar, U. C., Ozturk, H., Korkmaz, H., Nayyeri, V., and Ramahi, O. M. (2024b). De-embedding method for a sensing area characterization of planar microstrip sensors without evaluating error networks. *Scientific Reports*, 14(1), 10062.

Hashempour-baltork, F., Zade, S. V., Mazaheri, Y., Alizadeh, A. M., Rastegar, H., Abdian, Z., Torbati, M., and Damirchi, S. A. (2024). Recent methods in detection of olive oil adulteration: State-of-the-Art. *Journal of Agriculture and Food Research*, 16, 101123.

Hudec, P., Raboch, J., Randus, M., Hoffmann, K., Holub, A., Svanda, M., and Polivka, M. (2009, September). Microwave radar sensors for active defense systems. In *2009 European Radar Conference (EuRAD)* (pp. 581-584). IEEE.

Islam, M. T., Islam, M. R., Islam, M. T., Hoque, A., and Samsuzzaman, M. (2021). Linear regression of sensitivity for meander line parasitic resonator based on ENG metamaterial in the application of sensing. *Journal of Materials Research and Technology*, 10, 1103-1121.

Islam, M., Bełkowska, L., Konieczny, P., Fornal, E., and Tomaszewska-Gras, J. (2022a). Differential scanning calorimetry for authentication of edible fats and oils—What can we learn from the past to face the current challenges?. *Journal of Food and Drug Analysis*, 30(2), 185.

Islam, M. R., Islam, M. T., Bais, B., Almalki, S. H., Alsaif, H., and Islam, M. S. (2022b). Metamaterial sensor based on rectangular enclosed adjacent triple circle split ring resonator with good quality factor for microwave sensing application. *Scientific reports*, 12(1), 6792.

Khalil, M. A., Yong, W. H., Islam, M. T., Hoque, A., Islam, M. S., Leei, C. C., and Soliman, M. S. (2023). Double-negative metamaterial square enclosed QSSR for microwave sensing application in S-band with high sensitivity and Q-factor. *Scientific Reports*, 13(1), 7373.

Khursheed, M., Ahmad, A., Noor, S. E., García del Moral, L. F., and Martos Núñez, V. (2024). Chromatographic Techniques for the Detection and Identification of Olive Oil Adulteration.

Korkmaz, H., and Hasar, U. (2021). Wide band metamaterial absorber with lumped element. *The International Journal of Materials and Engineering Technology*, 4(1), 61-66.

Korkmaz, H., Hasar, U. C., and Ramahi, O. M. (2023). Thin-film MXene-based metamaterial absorber design for solar cell applications. *Optical and Quantum Electronics*, 55(6), 530.

Korostynska, O., Mason, A., and Al-Shamma'a, A. (2014). Microwave sensors for the non-invasive monitoring of industrial and medical applications. *Sensor Review*, 34(2), 182-191.

Krödel, S., Thomé, N., and Daraio, C. (2015). Wide band-gap seismic metastructures. *Extreme Mechanics Letters*, 4, 111-117.

Lee, H. J., and Yook, J. G. (2008). Biosensing using split-ring resonators at microwave regime. *Applied Physics Letters*, 92(25).

Lee, Y., Kim, S. J., Park, H., and Lee, B. (2017). Metamaterials and metasurfaces for sensor applications. *Sensors*, 17(8), 1726.

Meenu, M., Cai, Q., and Xu, B. (2019). A critical review on analytical techniques to detect adulteration of extra virgin olive oil. *Trends in Food Science & Technology*, 91, 391-408.

Menegoz Ursol, L., and Moret, S. (2024). Evaluation of the impact of olive milling on the mineral oil contamination of extra-virgin olive oils. *European Journal of Lipid Science and Technology*, 126(3), 2300123.

Mehrotra, P., Chatterjee, B., and Sen, S. (2019). EM-wave biosensors: A review of RF, microwave, mm-wave and optical sensing. *Sensors*, 19(5), 1013.

Mohd Bahar, A. A., Zakaria, Z., Md. Arshad, M. K., Isa, A. A. M., Dasril, Y., and Alahnomi, R. A. (2019). Real time microwave biochemical sensor based on circular SIW approach for aqueous dielectric detection. *Scientific Reports*, 9(1), 5467.

- Musa, I. (2024). Investigation the optical properties of Palestinian olive oils for different geographical regions by optical spectroscopy technique. *Food Chemistry Advances*, 4, 100584.
- Nyfors, E. (2000). Industrial microwave sensors—A review. *Subsurface Sensing Technologies and Applications*, 1(1), 23-43.
- Osman, S. B., Korostynka, O., Mason, A., Cullen, J. D., and Al-Shamma'a, A. I. (2014). Application of microwave spectroscopy analysis on determining quality of vegetable oil. *International Journal on Smart Sensing and Intelligent Systems*, 7(5), 1-4.
- Obaidullah, M., Esat, V., and Sabah, C. (2021). Multi-band (9, 4) chiral single-walled carbon nanotube based metamaterial absorber for solar cells. *Optics & Laser Technology*, 134, 106623.
- Rueda, M. P., Domínguez-Vidal, A., Llorent-Martínez, E. J., Aranda, V., and Ayora-Cañada, M. J. (2024). Monitoring organic matter transformation of olive oil production residues in a full-scale composting plant by fluorescence spectroscopy. *Environmental Technology & Innovation*, 103695.
- Shi, Q., Dong, B., He, T., Sun, Z., Zhu, J., Zhang, Z., and Lee, C. (2020). Progress in wearable electronics/photronics-moving toward the era of artificial intelligence and internet of things. *InfoMat*, 2(6), 1131-1162.
- Tamer, A., Alkurt, F. O., Altintas, O., Karaaslan, M., Unal, E., Akgol, O., Karadag, F., and Sabah, C. (2018). Transmission line integrated metamaterial based liquid sensor. *Journal of the Electrochemical Society*, 165(7), B251.
- Tamer, A., Karadağ, F., Ünal, E., Abdulkarim, Y. I., Deng, L., Altintas, O., Bakır, M., and Karaaslan, M. (2020). Metamaterial based sensor integrating transmission line for detection of branded and unbranded diesel fuel. *Chemical Physics Letters*, 742, 137169.
- Tümkaya, M. A., Dinçer, F., Karaaslan, M., and Sabah, C. (2017). Sensitive metamaterial sensor for distinction of authentic and inauthentic fuel samples. *Journal of Electronic Materials*, 46, 4955-4962.
- Tümkaya, M. A., Karaaslan, M., and Sabah, C. (2018). Metamaterial-based high efficiency portable sensor application for determining branded and unbranded fuel oil. *Bulletin of Materials Science*, 41, 1-8.
- Tümkaya, M. A., Ünal, E., and Sabah, C. (2019). Metamaterial-based fuel sensor application with three rhombus slots. *International Journal of Modern Physics B*, 33(24), 1950276.
- Vélez, P., Su, L., Grenier, K., Mata-Contreras, J., Dubuc, D., and Martín, F. (2017). Microwave microfluidic sensor based on a microstrip splitter/combiner configuration and split ring resonators (SRRs) for dielectric characterization of liquids. *IEEE Sensors Journal*, 17(20), 6589-6598.
- Wu, B., Jiang, W., Jiang, J., Zhao, Z., Tang, Y., Zhou, W., and Chen, W. (2024). Wave manipulation in intelligent metamaterials: recent progress and prospects. *Advanced Functional Materials*, 2316745.
- Yılmaz-Düzyaman, H., de la Rosa, R., Velasco, L., Núñez-Sánchez, N., and León, L. (2024). Oil quality prediction in olive oil by near-infrared spectroscopy: Applications in olive breeding. *Agriculture*, 14(5), 721.

Understanding Consumer Preferences in Kahramanmaraş for Bulgur and Bulgur Products

Reyyan ŞİMŞEK¹, Sevim KAYA^{2*}

Keywords

*Bulgur,
Fine bulgur,
Kahramanmaraş,
Packaging,
Consumer preference*


Abstract – Bulgur and bulgur products may be sold and stored in bags composed of cloth or polymer, which exhibit disparate permeability and physical characteristics that could potentially impact the product. The products can be sold in bulk without individual packaging, directly from sacks or specific bulk storage, in accordance with customer requirements. The aim of the study was to evaluate preferred storage-packaging systems for bulgur and bulgur products by consumers in Kahramanmaraş region. In the region, some consumers produce their own bulgur at home instead of buying it from the market. Accordingly, an investigation of bulgur and its derivatives has been undertaken to ascertain consumer preferences with regard to home production, direct purchases from sacks, bulk purchases, and purchases of those already packed. These factors are important for the purpose of revealing bulgur consumption habits. The recommendations that can be drawn from the results obtained in this study are expected to contribute to the consumption and marketing of the bulgur. In addition, awareness was created of the preference for bulgur, fine bulgur, firik, and very fine bulgur and their importance in terms of health, packaging systems, and storage in Kahramanmaraş province. This survey was applied to 350 households in order to interview face-to-face with households living in the urban area of Kahramanmaraş province. The statistical examination of the data revealed that consumers lack sufficient information regarding the nutritional value of the products in question. Furthermore, it was evaluated that the effect of the packaging materials used for bulgur and bulgur products on the product properties, including shelf life, is not widely understood by consumers.

1. Introduction

Throughout human history, bulgur has been of great importance as a basic food source and different foods have been developed by processing with various methods. Studies on the processing of bulgur since the Stone Age show that bulgur may be one of the first processed foods in human history (Bayram, 2007; Bilgiçli and Soyulu, 2016). In the Kahramanmaraş region, bulgur production is both a commercial and household practice, reflecting the area's deep-rooted agricultural traditions. Approximately 40% of the population still produces their own bulgur at home, while a significant portion opts for bulk purchases or pre-packaged bulgur, highlighting diverse consumption patterns in the region. This duality in production and consumption presents unique challenges and opportunities for manufacturers. For instance, local producers must balance between traditional bulk sales and modern packaging techniques that extend the products' shelf life, preserve their nutritional value, and meet consumer demand for convenience. Recent studies in the region have identified the need for innovation in bulgur packaging (Kasar et al., 2021; Kayaoğlu and Gülmez, 2022; Özbay et al., 2016). Most consumers prefer packaged bulgur due to its hygienic advantages and extended shelf life (Gupta et al., 2023; Sumiahadi et al., 2020).

¹ Gaziantep University, Graduate School of Natural and Applied Sciences, Gaziantep, Türkiye. E-mail: reyyansimsek1997@gmail.com  ORCID: 0009-0009-1291-767X

^{2*}Corresponding Author. Gaziantep University, Faculty of Engineering, Department of Food Engineering, Gaziantep, Türkiye. E-mail: skaya@gantep.edu.tr

 ORCID: 0000-0003-4790-7630

Citation: Şimşek, R. and Kaya, S. (2024). Understanding consumer preferences in Kahramanmaraş for bulgur and bulgur products. *Natural Sciences and Engineering Bulletin*, 1(2), 38-56.

However, some of the consumers prefer buying the products in bulk, even some of them producing their bulgur and its derivatives by themselves. The increasing awareness of health and nutritional benefits linked to bulgur consumption also suggests that there is a rising demand for improved packaging solutions that better cater to consumer health-consciousness. Bulgur is a highly nutritious cereal product rich in several key nutrients. It contains a high amount of fiber, which supports digestive health, and is an excellent source of complex carbohydrates that provide sustained energy (Dönmez et al., 2004). Additionally, bulgur is rich in B vitamins (especially B1 and folate), which are important for energy metabolism and nervous system health (Özbay et al., 2016). It also contains essential minerals like magnesium, iron, potassium, and phosphorus, which contribute to bone health, blood pressure regulation, and muscle function (Michel and Bayram, 2024). Its general composition includes 9-13% water, 10-16% protein, 1.2-1.5% fat, 76-78% carbohydrate, 1.2-1.4% ash and 1.1-1.3% fiber. In addition, it has higher values in terms of nutrients such as protein, calcium, iron, vitamin B1 and niacin compared to other cereal products such as bread and pasta (Saad et al., 2018). Bulgur is a product produced by cleaning, cooking, drying and grinding bulgur to certain sizes and has the ability to be stored for a long time due to the inactivation of enzymes during the cooking process (Belibağlı et al., 2009). Bulgur is known as a staple food widely used especially in Middle Eastern and Mediterranean cuisines. Fine bulgur is smaller in size than bulgur and represents the smallest size of the yellow bulgur varieties except very fine bulgur, but very fine bulgur is also not cooked during production. Fine bulgur is rich in fiber, vegetable protein, minerals and vitamins (Michel and Bayram, 2024). Firik is a traditional product obtained by roasting wheat in the milk stage with fire and has a green brown color and a sooty aroma, these characteristics are considered as quality parameters of firik (Yılmaz and Yıldırım, 2020). Figure 1 shows main wheat derivatives, bulgur, fine bulgur, dövme and firik. Effective packaging is essential to preserve the quality and extend the shelf life of bulgur products. Packaging needs and storage conditions of bulgur and bulgur products are given in Table 1. The sensitivity of these products to moisture, oxygen and light requires the selection of appropriate packaging materials (Sumiahadi et al., 2020; Xie, 2017). Inappropriate storage conditions can lead to mold, oxidation, and loss of nutritional value. This study aims to assess the level of knowledge of local people about the packaging and storage conditions of bulgur and fine bulgur in Kahramanmaraş region, to examine the effects of the materials used in the packaging of these products on product quality and to analyze data on consumer preferences. The objective of this study is to ascertain the extent of knowledge held by the local population in the Kahramanmaraş region with regard to the packaging and storage of bulgur and related products. Furthermore, this study seeks to identify consumer preferences for purchasing these products with or without packaging, as well as to determine which types of packaging options are preferred. Furthermore, the relationship between consumer characteristics, including age, gender, education level, income level, and demographic and socioeconomic status, and consumption of bulgur and bulgur products was examined. The study also investigated which traditional foods are most commonly prepared with bulgur and its derivatives.

Table 1. Summary table of bulgur and fine bulgur packaging and storage conditions.

| Product | Packaging Material | Storage Conditions* | Labeling Details |
|-------------|---|--|---|
| Bulgur | Food-grade plastic/paper bags or containers | Cool, dry place (15-25°C), low humidity ^{*1} , protect from direct sunlight ^{*2} | Product name, packaging date, expiration date, storage instructions |
| Fine bulgur | Food-grade plastic/paper bags or containers | Cool, dry place (15-25°C), low humidity ^{*1} , protect from direct sunlight ^{*2} | Product name, packaging date, expiration date, storage instructions |

^{*1}from a label of a related product pack, ^{*2}Sumiahadi, et al., 2020



Figure 1. Visual presentation of some wheat derivatives

2. Methodology

This study was conducted in order to determine the consumption habits of bulgur and bulgur products of consumers residing in the urban area of Kahramanmaraş. In addition to the local people living in the Kahramanmaraş region, workers working in various factories in the Organized Industrial Zone (OIZ) were also included in the research. Data collection was conducted through face-to-face surveys between March 2024 and April 2024. The study consists of a total of 350 people living in the urban area of Kahramanmaraş province. In the selection of the respondents, the location of Kahramanmaraş province in the Mediterranean region was taken into account, ensuring a general representativeness in terms of income and educational status of the region. In the questionnaire form, questions were included to determine the consumption levels of these products of the participants and their level of knowledge about the packaging methods of them. In addition, demographic information such as gender, age, education level, occupation, number of people in the household, and income level was also collected. The reason for choosing this method is to determine the level of knowledge of local people about the packaging and storage of bulgur and bulgur products in the most accurate way, to understand the reasons for the preference of these products and to analyze the demographic and socioeconomic factors behind these preferences in detail. Face-to-face interviews increase the reliability of the results by providing a better understanding of the survey questions and enabling respondents to provide more reliable data. In the study, the confidentiality and anonymity of the participants were protected during data collection and analysis. The participants were informed that the information they provided would only be used for academic purposes and that their personal information would be kept confidential. In addition, the participants were voluntarily included in the study and no pressure or coercion was applied. During data collection, all procedures were carried out in accordance with the rules of academic ethics and the rights of the participants were respected. The data obtained were analyzed using statistical evaluation methods. These analyses include detailed evaluations of the reasons for the preference for bulgur and fine bulgur, factors affecting consumption, nutritional content, packaging, and storage. In line with the results of the research, deficiencies in the level of public knowledge on bulgur and fine bulgur packaging and storage were identified and it was aimed to raise awareness on this issue.

In this study, a 44-question survey was used to assess the knowledge of consumers living in the urban area of Kahramanmaraş on the packaging and storage of bulgur and fine bulgur, as well as to gather data on their preferences, consumption factors, and nutritional awareness, providing a quick and economical method to evaluate attitudes, behaviors, and opinions on these topics.

2.1. Survey structure

The survey questions were structured with classification and ranking scales. Closed-ended questions were used to ensure that respondents provided their answers within predetermined categories. These categories were organized as simple binary options (e.g. 'yes' or 'no', 'male' or 'female') or more complex lists of alternatives from which respondents could choose. Closed-ended questions provided nominal and ordinal data, allowing the data to be analyzed systematically (Gökkaya Erdem et al., 2023).

2.2. Sampling and data collection process

The study sample consisted of individuals living in the urban area of Kahramanmaraş province who agreed to participate in the research. Sample selection was randomized, and data were collected through face-to-face surveys at the OIZ. The inclusion criteria included individuals residing in the Kahramanmaraş region who

accepted the survey, while the exclusion criteria included factors such as not consuming cereal products, general health status, and age.

2.3. Data analysis

The collected data were analyzed using the free trial version of SPSS (Statistical Package for Social Sciences) for Windows 25.0 software. Descriptive statistical methods (number, percentage) were used to evaluate the data. The relationships between variables were analyzed by the Chi-square test. The chi-square test has been chosen because it is more appropriate for analyzing categorical data, does not assume a normal distribution, and is more flexible regarding the assumptions about the data, making it suitable for scenarios where parametric tests may not be applicable. Statistical analyses were performed at a 95% confidence interval, and the significance level was accepted as 0.05. This methodology allowed the analysis of consumer preferences and knowledge levels on bulgur and fine bulgur consumption, packaging, and storage in accordance with the objectives of the study.

3. Results and Discussion

3.1. Demographic characteristics of consumers

The study surveyed 350 households in the urban area of Kahramanmaraş to understand their consumption habits of bulgur and bulgur products. The survey sample of 350 respondents may not be fully representative of the entire Kahramanmaraş region. However, it provides meaningful insights into consumer preferences in urban areas. Future studies could focus on more specific areas, such as industrial zones or universities, to obtain results that are more representative of these particular communities. Table 2 summarizes the demographic characteristics of the participants. The majority of the respondents were young to middle-aged adults, with 54.3% being female and 51.7 % being married. In terms of education, 35.7% of respondents held undergraduate degrees, while 31.7% were high school graduates. Most of the participants were employed (50.6%), while 18% were students. In terms of household size, 67.7% of the participants lived in families with 3-5 members, and 17.1% lived in households with 6-7 members. Family income distribution varied, with 33.4% of households earning between 17,000 TL and 30,000 TL per month and 23.7% earning below 17,000 TL. For future readers to accurately assess the monetary amounts mentioned in this section, it is important to provide context regarding the minimum wage at the time of writing. As of 2024, the minimum wage in Turkey was 17,002 TL per month. This wage serves as a benchmark for understanding income brackets within the study. For instance, households earning below 17,000 TL per month are likely earning close to or slightly above the minimum wage, whereas those in higher income brackets (above 30,000 TL) represent the middle and upper-income segments. This context helps assess the economic standing of participants in relation to their consumption behaviors and purchasing power. The data on income levels in this region directly influences consumer preferences, especially in terms of the types of bulgur products they purchase. Higher-income consumers tend to prefer packaged products for their convenience and perceived hygiene, while lower-income households are more likely to purchase in bulk or produce bulgur at home. Bulgur and fine bulgur hold a significant place in the diets of many urban populations in Turkey, including Kahramanmaraş, where these products are a staple due to their affordability, ease of preparation, and versatility (Dönmez et al., 2004). Studies show that demographic factors such as income, education, and household size influence the consumption patterns of bulgur. For example, households with lower income and larger family sizes tend to consume bulgur more frequently due to its cost-effectiveness and high nutritional value (Kayaoğlu and Gülmez, 2022). Bulgur, particularly fine bulgur, is commonly used in dishes like *kısır* (a bulgur-based salad) and *raw köfte*, where its light texture and fast preparation are appreciated. It can be soaked rather than cooked, making it an accessible and convenient ingredient for many. Moreover, bulgur's high fiber content and lower glycemic index compared to rice and pasta make it a popular choice among health-conscious consumers (Tekin-Çakmak et al., 2024). For companies aiming to develop marketing strategies around bulgur, understanding these consumption patterns and demographic factors provides essential insights. Marketing efforts could emphasize its health benefits, convenience, and versatility to appeal to a broad range of consumers across various socioeconomic segments (Kayaoğlu and Gülmez, 2022).

Table 2. Participants' descriptive information

| | | Number | % |
|--|---------------------------------|--------|------|
| Age | 25 and below | 118 | 33.7 |
| | 26-35 | 110 | 31.4 |
| | 36-45 | 65 | 18.6 |
| | 46+ | 57 | 16.3 |
| Gender | Male | 160 | 45.7 |
| | Female | 190 | 54.3 |
| Marital Status | Single | 169 | 48.3 |
| | Married | 181 | 51.7 |
| Education Status | Primary school | 53 | 15.1 |
| | High school | 111 | 31.7 |
| | Associate Degree | 39 | 11.1 |
| | License | 125 | 35.7 |
| | Master Degree/PhD | 22 | 6.3 |
| Employment Status | Employed | 177 | 50.6 |
| | Not employed | 59 | 16.9 |
| | Stay-at-home parent | 46 | 13.1 |
| | Student | 63 | 18.0 |
| | Other | 5 | 1.4 |
| Number of family members | 1-2 | 39 | 11.1 |
| | 3-5 | 237 | 67.7 |
| | 6-7 | 60 | 17.1 |
| | 8-10 | 11 | 3.1 |
| | 10+ | 3 | 0.9 |
| Monthly family income (as of 2024, min wage is 17,002 TL) | < 17.000TL | 83 | 23.7 |
| | 17,000 TL- 30,000TL | 117 | 33.4 |
| | 30,000 TL- 45,000 TL | 70 | 20.0 |
| | 45,000 TL- 60,000 TL | 36 | 10.3 |
| | > 60,000 TL | 44 | 12.6 |
| Consumption Frequency | I consume every day | 73 | 20.9 |
| | I consume one day a week | 186 | 53.1 |
| | I consume it every fifteen days | 53 | 15.1 |
| | I consume it once a month | 38 | 10.9 |

3.2. Consumption methods of consumers for wheat derivatives

Table 3 shows the consumption preferences of consumers living in the urban area of Kahramanmaraş province for wheat derivatives, especially bulgur and fine bulgur, and the dishes made from these products. The data reveals that bulgur is the most preferred wheat derivative among consumers in the region. While 78.6% of the respondents stated that they consume bulgur the most, 21.4% stated that they prefer fine bulgur. It was observed that bulgur is a widely consumed food in Kahramanmaraş and is frequently used in traditional dishes, especially in rural areas. Among the participants who preferred bulgur, the most popular dish was infertile, with a rate of 50.9%. This was followed by stuffed (içli) köfte at 28.0%, bulgur soup at 13.8%, and plain bulgur pilaf at 13.1%. Among the participants who preferred fine bulgur, the most consumed food was raw köfte with 42.6%, followed by fine bulgur köfte with 41.3%. These results show that fine bulgur is mostly used in local and special dishes. Participants who preferred pounded bulgur preferred traditional dishes such as plain pounded pilaf (20.2%) and aşure (4.1%). This shows that pounded bulgur is used especially in certain types of dishes and has an important place in traditional cuisine. Among the respondents who preferred firik, the most popular dish was firik pilaf (78.5%). Firik is also used in making tarhana (49.4%) and soup (15.2%). Firik is not known like other wheat derivatives, but it stands out as a food with high nutritional value. In conclusion, wheat derivatives are widely consumed in the urban area of Kahramanmaraş province, especially bulgur, which is used in various dishes. These findings show that bulgur and fine bulgur have an important place in the local cuisine and that the consumption habits of these products are closely related to the nutritional culture of the people of the region.

Table 3. Distribution of participants' consumption preference for wheat derivatives

| | | Number | % |
|---|------------------------------|---------------|----------|
| Which of the wheat derivatives, bulgur, and its products, do you consume the most? | Fine bulgur | 75 | 21.4 |
| | Bulgur | 275 | 78.6 |
| Apart from bulgur and its products, do you consume the most? | Very fine bulgur | 28 | 8.0 |
| | Dövme | 243 | 69.4 |
| | Firik | 79 | 22.6 |
| Please examine the listed dishes (including mainly bulgur) and indicate your preference (n=275) | Plain bulgur pilaf | 36 | 13.1 |
| | Bulgur pilaf with vegetables | 28 | 10.2 |
| | Pilaf with meat | 9 | 3.3 |
| | Soup | 38 | 13.8 |
| | Analı kızılı köfte | 11 | 4.0 |
| | Köfte with sour | 20 | 7.2 |
| | Sömelek köfte | 21 | 7.6 |
| | Yağlama | 2 | 0.7 |
| | Kısır | 140 | 50.9 |
| | Sarma/Dolma | 11 | 4.0 |
| | Mumbar | 3 | 1.1 |
| | Stuffed(İçli) köfte | 77 | 28.0 |
| Please examine the listed dishes (including mainly fine bulgur) and indicate your preference (n=75) | Fine bulgur köfte | 31 | 41.3 |
| | Lentil köfte | 19 | 25.3 |
| | Fellah köfte | 9 | 12.0 |
| | Batırık köfte | 1 | 1.3 |
| | Raw köfte | 32 | 42.6 |
| Please examine the listed dishes (including mainly dövme) and indicate your preference (n=243) | Plain dövme rice | 49 | 20.2 |
| | Dövme rice with vegetables | 3 | 1.2 |
| | Soup | 9 | 3.7 |
| | Dövme soup with yogurt | 8 | 3.3 |
| | Dövme aşı | 3 | 1.2 |
| | Aşure | 10 | 4.1 |
| Please examine the listed dishes (including mainly firik) and indicate your preference (n=79) | Pilaf | 62 | 78.5 |
| | Tarhana | 39 | 49.4 |
| | Soup | 12 | 15.2 |
| Please examine the listed dishes (including mainly very fine bulgur) and indicate your preference (n=28) | Fine bulgur köfte | 28 | 100.0 |

3.3. Consumption preferences of consumers

This study examined the reasons why consumers living in urban areas of Kahramanmaraş province prefer bulgur derivatives such as bulgur and fine bulgur. The data obtained show that the majority of the participants (82.6%) prefer these products because they find them nutritious and satisfying. In addition, 84.6% of the participants stated that they consume dishes made from bulgur derivatives because they find them delicious. Furthermore, 75.1% of the participants reported that they prefer these products because they can be stored for a long time without spoiling. This is consistent with previous findings that highlight bulgur's long shelf life and minimal need for preservatives, making it a durable food choice for households. Moreover, 80.6% emphasized that they prefer these products for their health benefits, a sentiment echoed by studies showing that bulgur is rich in fiber, protein, and essential nutrients. A previous study by Bayram (2007) found that Turkish consumers' preference for bulgur is also driven by its versatile use in both daily meals and traditional dishes. These findings, which align with our results, confirm that bulgur holds a significant place in Turkish cuisine, particularly in

Kahramanmaraş, where both traditional and modern consumption patterns coexist. In conclusion, our findings reaffirm that bulgur and similar products are widely preferred in Kahramanmaraş due to their nutritional value, durability, and health benefits. These preferences are consistent with broader trends observed in Turkish bulgur consumption studies. The strong cultural and practical reasons for the preference for these products make them integral to the local diet, highlighting the potential for further studies to explore how modern packaging methods could enhance their appeal and marketability. Recent research in Turkey highlights the increasing consumer demand for health-conscious and sustainably packaged products. For example, a study by Kayaoğlu and Gülmez (2022) indicates that Turkish consumers are becoming more mindful of packaging materials and their impact on product quality and safety. This aligns with the findings of this study, which underscores the growing importance of packaging in influencing consumer choices, particularly for staple foods like bulgur. Another similar study was conducted by Özbay et al. (2016); they examined the consumption of bulgur in Karaman province, with a particular focus on the factors that influence purchasing decisions and consumer knowledge about its effects on human health. The majority of consumers are farmers and civil servants with varying levels of education. The study finds that factors such as expiration date, brand, and price significantly impact consumers' purchasing decisions, with flavor also being an important criterion. In contrast, packaging and cooking time are less significant factors. It is generally observed that men are responsible for purchasing decisions. Additionally, most consumers lack sufficient information about the health effects of bulgur, although highly educated consumers tend to have better knowledge about its nutritional benefits, and this knowledge increases with their level of education. The study also revealed that bulgur is mostly consumed as pilaf, with the least frequent consumption being once a month.

3.4. Main factors in consumers' preference

In this part, the reasons why consumers living in the urban area of Kahramanmaraş prefer bulgur and similar bulgur derivatives and the factors behind these preferences have been investigated (Tables 4-5). 63.1% of the participants stated that they prefer these products due to the high production rate in their region. This shows the impact of local production on consumer preferences. In addition, 86.6% of the participants stated that bulgur and similar products are frequently consumed by their families and circles, indicating that cultural and social factors play an important role in the preference for bulgur derivatives. However, 44.3% of the respondents indicated that they were interested in learning about the benefits of bulgur from social media, radio, and/or television programs. However, this rate indicates that interest in information is limited and that more awareness-raising activities are needed.

Table 4. Evaluation of participants' reasons for preference

| | Yes | | No | |
|---|--------|------|--------|------|
| | Number | % | Number | % |
| I prefer it because it is nutritious and satisfying. | 289 | 82.6 | 61 | 17.4 |
| I prefer it because it cooks quickly. | 218 | 62.3 | 132 | 37.7 |
| I prefer it because it has a long shelf life | 263 | 75.1 | 87 | 24.9 |
| I enjoy consuming dishes made from this product because of its taste. | 296 | 84.6 | 54 | 15.4 |
| I prefer it because it's well-loved and enjoyed by my family. | 279 | 79.7 | 71 | 20.3 |
| I select it because it promotes good health. | 282 | 80.6 | 68 | 19.4 |

Table 5. Evaluation of participants' reasons for preference

| | Yes | | No | |
|---|--------|------|--------|------|
| | Number | % | Number | % |
| I prefer it because of the high production rate in the region where I live. | 221 | 63.1 | 129 | 36.9 |
| It is consumed a lot in my family and circle. | 303 | 86.6 | 47 | 13.4 |
| I am interested in information about the benefits of bulgur on social media, radio, and/or TV programs. | 155 | 44.3 | 195 | 55.7 |

In conclusion, local production, family, and environmental impacts play an important role in the preference for bulgur and similar products in Kahramanmaraş province. However, more information about the benefits of bulgur through the media may increase consumers' interest in these products. These findings emphasize that local production and social environment are determining factors in food preferences.

3.5. Importance of nutrition and health

The nutritional value of a human diet is important for being healthy. This part was conducted to assess participants' views on nutrient content (Table 6). According to the data obtained, it was found that the majority of the participants (66%) had information about different types of bulgur and paid attention to this when shopping. The proportion of participants who prefer organic production is as high as 81.4%. In addition, 63.4% of the participants stated that they prefer organic foods because they are rich in fiber, vitamin B1, and folic acid. 62.9% of the participants stated that they prefer foods because they do not contain cholesterol and unsaturated fats. 57.4% of the participants stated that they were informed that it contains gluten and that people with gluten sensitivity should use it with caution. Finally, 55.1% of the participants stated that they preferred the foods because of the low glycemic index. These results show the participants' awareness and preferences regarding nutrient content. In particular, a high level of awareness was observed regarding organic production and the potential effects of nutrients on health. These data provide valuable information for research on dietary habits and health awareness.

Table 6. Evaluation of participants' views on nutrient content

| | Yes | | No | |
|--|--------|------|--------|------|
| | Number | % | Number | % |
| I know there are different types of bulgur, and I pay attention to that when I buy. | 231 | 66.0 | 119 | 34.0 |
| I prefer organic production. | 285 | 81.4 | 65 | 18.6 |
| I prefer it because it is rich in pulses/fiber, vitamin B1, and folic acid. | 222 | 63.4 | 128 | 36.6 |
| I prefer it because it is free of cholesterol and unsaturated fat. | 220 | 62.9 | 130 | 37.1 |
| I have information that it contains gluten and that people who are sensitive to gluten should use it with caution. | 201 | 57.4 | 149 | 42.6 |
| I prefer it because it has a low glycemic index. | 193 | 55.1 | 157 | 44.9 |

3.6. Evaluation of participants' preference for packaging and storage

This study was conducted to assess the opinions of the participants about packaged products and products sold in the open. Consumer preferences regarding the packaging needs for bulgur and bulgur products are shown in Table 7. According to the data obtained, 91.1% of the participants prefer products that do not contain foreign substances (stones, soil, etc.). 54.6% of the participants stated that they make their own products from bulgur at home. While 40.9% of the respondents buy products sold in the open, 73.7% prefer packaged products, 67.7% of respondents have knowledge about the packaging materials used in the market, and 66.6% know the differences between these materials and their effects on the product. 90.3% of respondents think that packaging should have a label indicating product content, optimal use, and storage conditions. 89.1% of the respondents think that the packaging design should best represent the product and be easy to use, and 71.1% of the participants stated that they place the packaged product in the cupboard when they bring it home.

The rate of those who pay attention to the production and expiration date on the packaging of the product is 92.6%. 95.7% of the participants stopped consuming when they noticed any change in the smell, color, or taste of the product. 76.3% of the respondents stopped consumption when they noticed that the product was insect-infested during storage. 43.4% of respondents think that the characteristics of packaged products and products sold in the open are the same. Finally, 58.9% of respondents know that the storage temperature should not be above 18°C and humidity should not be above 65%. These results shed light on respondents' awareness and

preferences regarding packaged and openly sold products. A high level of awareness of the importance of packaging on product quality and safety was observed.

Table 7. Evaluation of participants' packaging and storage preferences

| Items | Yes | | No | |
|---|--------|------|--------|------|
| | Number | % | Number | % |
| I prefer no foreign matter (stones, soil, etc.). | 319 | 91.1 | 31 | 8.9 |
| At home, we make our own from bulgur. | 191 | 54.6 | 159 | 45.4 |
| I buy products sold in the open. | 143 | 40.9 | 207 | 59.1 |
| I buy the packaged product. | 258 | 73.7 | 92 | 26.3 |
| I know the packaging materials used in the market. (Example: polyethylene, cellophane, polypropylene, paper, cloth or sack) | 237 | 67.7 | 113 | 32.3 |
| I know the differences between the packaging materials used and their impact on the product. | 233 | 66.6 | 117 | 33.4 |
| The packaging must have a label indicating the contents, optimal use, and storage conditions of the product. | 316 | 90.3 | 34 | 9.7 |
| The packaging design should best represent the product and be easy to use. | 312 | 89.1 | 38 | 10.9 |
| When I buy a packaged product and bring it home, I put it packaged in the cupboard. | 249 | 71.1 | 101 | 28.9 |
| When buying, I pay attention to the production and expiration date on the packaging. | 324 | 92.6 | 26 | 7.4 |
| If I notice any change in the smell, color, or taste of the product, I stop consuming it. | 335 | 95.7 | 15 | 4.3 |
| If I see that the product is infested during storage, I stop consuming it. | 267 | 76.3 | 83 | 23.7 |
| The characteristics of packaged products and products sold in the open are the same. | 152 | 43.4 | 198 | 56.6 |
| I know that the storage temperature should be 18°C, and the humidity should not be above 65%. | 206 | 58.9 | 144 | 41.1 |

3.7. Determination of the factors affecting the packaging and storage preferences of consumers

This study aimed to analyze the relationship between consumers' packaging and storage preferences and age. According to the data obtained, consumers showed different packaging and storage preferences according to age groups.

Preference for products without foreign substances: 91.1% of the participants preferred products without foreign substances, while there was no statistically significant difference between age groups ($p=0.090$).

Making your own products from bulgur at home: A significant difference was found between age groups in the proportion of those who made their own products at home ($p=0.014$). Participants in the 26-35 age group (30.4%) stand out as the group with the highest rate of this habit.

Purchasing openly sold products: The preference for buying products sold in the open did not show a significant difference between age groups ($p=0.203$).

Buying packaged products: The preference for buying packaged products did not show a significant difference between age groups ($p=0.056$).

Knowledge about packaging materials: Participants' knowledge about packaging materials did not show a significant difference between age groups ($p=0.155$).

Knowing the differences between packaging materials: The rates of knowing the differences between packaging materials did not show a significant difference between age groups ($p=0.649$).

Packaging should have a label: The proportion of respondents who thought that packaging should have a label indicating the contents, optimal use, and storage conditions showed a significant difference between age groups ($p=0.013$). Respondents in the 26-35 age group adopted these views the most.

Packaging design represents the product in the best way: The view that packaging design should represent the product in the best way possible showed a significant difference between age groups ($p=0.023$). Participants in the 26-35 age group adopted this view the most.

Putting the packaged product in the cupboard when you bring it home: The habit of putting the packaged product in the cupboard when brought home did not show a significant difference between age groups ($p=0.090$).

Paying attention to the production and expiration dates on the packaging: The rates of paying attention to the production and expiration dates did not show a significant difference between age groups ($p=0.698$).

Stopping consumption if they notice changes in the smell, color, or taste of the product: The proportion of those who noticed changes in the smell, color, or taste of the product did not show a significant difference between age groups ($p=0.616$).

Stopping consumption if the product is insect-infested: There was no significant difference between age groups in the rates of stopping consumption if the product was insect-infested ($p=0.742$).

Thinking that the characteristics of packaged products and openly sold products are the same: This opinion showed a significant difference between age groups ($p=0.048$). Respondents aged 25 and under were more likely to hold this view.

Having information about storage temperature and humidity: Knowledge about storage temperature and humidity did not show a significant difference between age groups ($p=0.409$).

These results show that consumers have different awareness and habits about packaging and storage preferences according to age groups. In particular, participants in the 26-35 age groups are more conscious and careful about packaging and storage. These data provide important information for future studies on consumer habits and packaging strategies.

3.7.1. Analyzing the relationship between consumers' packaging and storage preferences and age

The effect of consumers' age and education level on packaging types and storage needs of bulgur and products were tabulated in Tables 8-9.

3.7.2. Analyzing the relationship between consumers' packaging and storage preferences and education level

This study aimed to analyze the relationship between respondents' packaging and storage preferences and their level of education (Table 9). According to the data obtained, participants showed different packaging and storage preferences according to their level of education.

Preference for products without foreign substances: 91.1% of the participants preferred products without foreign substances, while there was no statistically significant difference between the levels of education ($p=0.476$).

Making your own products from bulgur at home: No significant difference was found between education levels in the proportion of those who make their own products at home ($p=0.476$).

Purchasing openly sold products: The preference for buying openly sold products showed a significant difference between education levels ($p=0.019$). Secondary education graduates stand out as the group with this habit the most.

Buying packaged products: The preference for buying packaged products did not show a significant difference between education levels ($p=0.155$).

Knowledge about packaging materials: Participants' knowledge about packaging materials did not show a significant difference between education levels ($p=0.776$).

Table 8. The relationship between participants' packaging and storage preferences and age

| | | 25 and below | | 26-35 | | 36-45 | | 46+ | | X ² | P |
|---|-----|--------------|------|--------|------|--------|------|--------|------|----------------|--------|
| | | Number | % | Number | % | Number | % | Number | % | | |
| I prefer no foreign matter (stones, soil, etc.). | Yes | 103 | 32.3 | 99 | 31.0 | 61 | 19.1 | 56 | 17.6 | 6.501 | 0.090 |
| | No | 15 | 48.4 | 11 | 35.5 | 4 | 12.9 | 1 | 3.2 | | |
| At home, we make our own from bulgur. | Yes | 57 | 29.8 | 58 | 30.4 | 34 | 17.8 | 42 | 22.0 | 10.553 | 0.014* |
| | No | 61 | 38.4 | 52 | 32.7 | 31 | 19.5 | 15 | 9.4 | | |
| I buy products sold in bulk. | Yes | 44 | 30.8 | 41 | 28.7 | 28 | 19.6 | 30 | 21.0 | 4.610 | 0.203 |
| | No | 74 | 35.7 | 69 | 33.3 | 37 | 17.9 | 27 | 13.0 | | |
| I buy the packed product. | Yes | 95 | 36.8 | 79 | 30.6 | 49 | 19.0 | 35 | 13.6 | 7.567 | 0.056 |
| | No | 23 | 25.0 | 31 | 33.7 | 16 | 17.4 | 22 | 23.9 | | |
| I know the packaging materials used in the market. (e.g. polyethylene, cellophane, pp, paper, cloth or sack). | Yes | 72 | 30.4 | 77 | 32.5 | 50 | 21.1 | 38 | 16.0 | 5.234 | 0.155 |
| | No | 46 | 40.7 | 33 | 29.2 | 15 | 13.3 | 19 | 16.8 | | |
| I know the differences between the packaging materials used and their impact on the product. | Yes | 74 | 31.8 | 77 | 33.0 | 45 | 19.3 | 37 | 15.9 | 1.648 | 0.649 |
| | No | 44 | 37.6 | 33 | 28.2 | 20 | 17.1 | 20 | 17.1 | | |
| The packaging must have a label indicating the contents, optimal use, and storage conditions of the product. | Yes | 98 | 31.0 | 104 | 32.9 | 61 | 19.3 | 53 | 16.8 | 10.730 | 0.013* |
| | No | 20 | 58.8 | 6 | 17.6 | 4 | 11.8 | 4 | 11.8 | | |
| The packaging design should best represent the product and be easy to use. | Yes | 97 | 31.1 | 101 | 32.4 | 62 | 19.9 | 52 | 16.7 | 9.557 | 0.023* |
| | No | 21 | 55.3 | 9 | 23.7 | 3 | 7.9 | 5 | 13.2 | | |
| When I buy a packaged product and bring it home, I put it packaged in the cupboard. | Yes | 78 | 31.3 | 74 | 29.7 | 51 | 20.5 | 46 | 18.5 | 6.496 | 0.090 |
| | No | 40 | 39.6 | 36 | 35.6 | 14 | 13.9 | 11 | 10.9 | | |
| When buying, I pay attention to the | Yes | 109 | 33.6 | 104 | 32.1 | 60 | 18.5 | 51 | 15.7 | 1.432 | 0.698 |

| | | | | | | | | | | | |
|--|-----|-----|------|-----|------|----|------|----|------|-------|--------|
| production and expiration date on the packaging. | No | 9 | 34.6 | 6 | 23.1 | 5 | 19.2 | 6 | 23.1 | | |
| If I notice any change in the smell, color, or taste of the product, I stop consuming it. | Yes | 111 | 33.1 | 107 | 31.9 | 63 | 18.8 | 54 | 16.1 | 1.795 | 0.616 |
| | No | 7 | 46.7 | 3 | 20.0 | 2 | 13.3 | 3 | 20.0 | | |
| If I see that the product is infested during storage, I stop consuming it. | Yes | 89 | 33.3 | 82 | 30.7 | 53 | 19.9 | 43 | 16.1 | 1.247 | 0.742 |
| | No | 29 | 34.9 | 28 | 33.7 | 12 | 14.5 | 14 | 16.9 | | |
| The characteristics of packaged products and products sold in the open are the same. | Yes | 47 | 30.9 | 40 | 26.3 | 36 | 23.7 | 29 | 19.1 | 7.926 | 0.048* |
| | No | 71 | 35.9 | 70 | 35.4 | 29 | 14.6 | 28 | 14.1 | | |
| I know that the storage temperature should be 18 °C, and the humidity should not be above 65%. | Yes | 66 | 32.0 | 72 | 35.0 | 36 | 17.5 | 32 | 15.5 | 2.891 | 0.409 |
| | No | 52 | 36.1 | 38 | 26.4 | 29 | 20.1 | 25 | 17.4 | | |

Knowing the differences between packaging materials: The rate of knowing the differences between packaging materials did not show a significant difference between educational levels ($p=0,784$).

Packaging should have a label: The proportion of respondents who thought that packaging should have a label indicating the contents, optimal use, and storage conditions did not show a significant difference between education levels ($p=0.511$).

The packaging design should represent the product in the best way: The opinion that the packaging design should represent the product in the best possible way did not show a significant difference between educational levels ($p=0.257$).

Putting the packaged product in the cupboard when you bring it home: The habit of putting the packaged product in the cupboard after bringing it home showed a significant difference between educational levels ($p=0.022$). Secondary education graduates had this habit the most.

Paying attention to the production and expiry dates on the packaging: The rates of paying attention to the production and expiry dates did not show a significant difference between educational levels ($p=0.313$).

Stopping consumption if they notice changes in the smell, color, or taste of the product: The rates of those who noticed changes in the smell, color, or taste of the product did not show a significant difference between education levels ($p=0.368$).

Stopping consumption in the event of insect infestation: The rates of stopping consumption if the product was insect-infested showed a significant difference between educational levels ($p=0.002$). Secondary education graduates stand out as the group with the highest level of awareness on this issue.

Thinking that the characteristics of packaged products and openly sold products are the same: This opinion showed a significant difference between education levels ($p=0.000$). Secondary education graduates were the group that adopted those views the most.

Having information about storage temperature and humidity: Knowledge about storage temperature and humidity did not show a significant difference between educational levels ($p=0.797$).

These results show that consumers have different awareness and habits about packaging and storage preferences according to their educational levels. Secondary education graduates are more careful and conscious about packaged products and storage of products.

Table 9. The relationship between participants' preference for packaging and storage and education level

| | | Primary school | | High school | | Associate degree | | License | | Master's Degree/ PhD | | X ² | P |
|--|-----|----------------|------|-------------|------|------------------|------|---------|------|-------------------------|-----|----------------|--------|
| | | Number | % | Number | % | Number | % | Number | % | Number | % | | |
| I prefer no foreign matter (stones, soil, etc.). | Yes | 51 | 16.0 | 100 | 31.3 | 37 | 11.6 | 112 | 35.1 | 19 | 6.0 | 3.512 | 0.476 |
| | No | 2 | 6.5 | 11 | 35.5 | 2 | 6.5 | 13 | 41.9 | 3 | 9.7 | | |
| At home, we make our own from bulgur. | Yes | 40 | 20.9 | 65 | 34.0 | 21 | 11.0 | 55 | 28.8 | 10 | 5.2 | 16.431 | 0.476 |
| | No | 13 | 8.2 | 46 | 28.9 | 18 | 11.3 | 70 | 44.0 | 12 | 7.5 | | |
| I buy products sold in the open. | Yes | 26 | 18.2 | 56 | 39.2 | 14 | 9.8 | 38 | 26.6 | 9 | 6.3 | 11.756 | 0.019* |
| | No | 27 | 13.0 | 55 | 26.6 | 25 | 12.1 | 87 | 42.0 | 13 | 6.3 | | |
| I buy the packaged product. | Yes | 35 | 13.6 | 82 | 31.8 | 28 | 10.9 | 100 | 38.8 | 13 | 5.0 | 6.664 | 0.155 |
| | No | 18 | 19.6 | 29 | 31.5 | 11 | 12.0 | 25 | 27.2 | 9 | 9.8 | | |
| I know the packaging materials used in the market. (Example: polyethylene, cellophane, pp, paper, cloth or sack). | Yes | 39 | 16.5 | 73 | 30.8 | 24 | 10.1 | 86 | 36.3 | 15 | 6.3 | 1.778 | 0.776 |
| | No | 14 | 12.4 | 38 | 33.6 | 15 | 13.3 | 39 | 34.5 | 7 | 6.2 | | |
| I know the differences between the packaging materials used and their impact on the product. | Yes | 37 | 15.9 | 75 | 32.2 | 23 | 9.9 | 82 | 35.2 | 16 | 6.9 | 1.739 | 0.784 |
| | No | 16 | 13.7 | 36 | 30.8 | 16 | 13.7 | 43 | 36.8 | 6 | 5.1 | | |
| The packaging must have a label indicating the contents, optimal use, and storage conditions of the product. | Yes | 49 | 15.5 | 102 | 32.3 | 37 | 11.7 | 109 | 34.5 | 19 | 6.0 | 3.288 | 0.511 |
| | No | 4 | 11.8 | 9 | 26.5 | 2 | 5.9 | 16 | 47.1 | 3 | 8.8 | | |

| | | | | | | | | | | | | | |
|---|-----|----|------|-----|------|----|------|-----|------|----|------|--------|--------|
| The packaging design should best represent the product and be easy to use. | Yes | 50 | 16.0 | 99 | 31.7 | 37 | 11.9 | 106 | 34.0 | 20 | 6.4 | 5.309 | 0.257 |
| | No | 3 | 7.9 | 12 | 31.6 | 2 | 5.3 | 19 | 50.0 | 2 | 5.3 | | |
| When I buy a packaged product and bring it home, I put it packaged in the cupboard. | Yes | 45 | 18.1 | 84 | 33.7 | 27 | 10.8 | 81 | 32.5 | 12 | 4.8 | 11.472 | 0.022* |
| | No | 8 | 7.9 | 27 | 26.7 | 12 | 11.9 | 44 | 43.6 | 10 | 9.9 | | |
| When buying, I pay attention to the production and expiration date on the packaging. | Yes | 48 | 14.8 | 102 | 31.5 | 39 | 12.0 | 116 | 35.8 | 19 | 5.9 | 4.756 | 0.313 |
| | No | 5 | 19.2 | 9 | 34.6 | 0 | 0.0 | 9 | 34.6 | 3 | 11.5 | | |
| If I notice any change in the smell, color, or taste of the product, I stop consuming it. | Yes | 53 | 15.8 | 105 | 31.3 | 37 | 11.0 | 118 | 35.2 | 22 | 6.6 | 4.291 | 0.368 |
| | No | 0 | 0.0 | 6 | 40.0 | 2 | 13.3 | 7 | 46.7 | 0 | 0.0 | | |
| If I see that the product is infested during storage, I stop consuming it. | Yes | 46 | 17.2 | 90 | 33.7 | 29 | 10.9 | 92 | 34.5 | 10 | 3.7 | 16.783 | 0.002* |
| | No | 7 | 8.4 | 21 | 25.3 | 10 | 12.0 | 33 | 39.8 | 12 | 14.5 | | |
| The characteristics of packaged products and products sold in the open are the same. | Yes | 34 | 22.4 | 57 | 37.5 | 15 | 9.9 | 41 | 27.0 | 5 | 3.3 | 22.076 | 0.000* |
| | No | 19 | 9.6 | 54 | 27.3 | 24 | 12.1 | 84 | 42.4 | 17 | 8.6 | | |
| I know that the storage temperature should be 18°C, and the humidity should not be above 65%. | Yes | 30 | 14.6 | 68 | 33.0 | 20 | 9.7 | 76 | 36.9 | 12 | 5.8 | 1.664 | 0.797 |
| | No | 23 | 16.0 | 43 | 29.9 | 19 | 13.2 | 49 | 34.0 | 10 | 6.9 | | |

3.7.3. Analyzing the relationship between consumers' packaging and storage preferences and monthly income

The data revealed were listed in Tables 10-11.

Table 10. The relationship between participants' packaging and storage preferences and monthly income

| | | <17.000 TL | | 17.000-30.000TL | | 30.000 – 45.000 TL | | 45.000-60.000 TL | | > 60.000 TL | | X ² | p |
|---|-----|------------|------|-----------------|------|--------------------|------|------------------|------|-------------|------|----------------|--------|
| | | Number | % | Number | % | Number | % | Number | % | Number | % | | |
| I prefer no foreign matter (stones. soil. etc.). | Yes | 75 | 23.5 | 109 | 34.2 | 62 | 19.4 | 36 | 11.3 | 37 | 11.6 | 7.436 | 0.115 |
| | No | 8 | 25.8 | 8 | 25.8 | 8 | 25.8 | 0 | 0.0 | 7 | 22.6 | | |
| At home. We make our own from bulgur. | Yes | 57 | 29.8 | 67 | 35.1 | 36 | 18.8 | 13 | 6.8 | 18 | 9.4 | 15.542 | 0.004* |
| | No | 26 | 16.4 | 50 | 31.4 | 34 | 21.4 | 23 | 14.5 | 26 | 16.4 | | |
| I buy products sold in the open. | Yes | 38 | 26.6 | 45 | 31.5 | 24 | 16.8 | 14 | 9.8 | 22 | 15.4 | 3.942 | 0.414 |
| | No | 45 | 21.7 | 72 | 34.8 | 46 | 22.2 | 22 | 10.6 | 22 | 10.6 | | |
| I buy the packaged product. | Yes | 54 | 20.9 | 84 | 32.6 | 55 | 21.3 | 33 | 12.8 | 32 | 12.4 | 10.293 | 0.036* |
| | No | 29 | 31.5 | 33 | 35.9 | 15 | 16.3 | 3 | 3.3 | 12 | 13.0 | | |
| I know the packaging materials used in the market. (Example: Polyethylene, cellophane, pp. paper, cloth or sack). | Yes | 57 | 24.1 | 85 | 35.9 | 45 | 19.0 | 26 | 11.0 | 24 | 10.1 | 5.540 | 0.236 |
| | No | 26 | 23.0 | 32 | 28.3 | 25 | 22.1 | 10 | 8.8 | 20 | 17.7 | | |
| I know the differences between the packaging materials used and their impact on the product. | Yes | 58 | 24.9 | 80 | 34.3 | 49 | 21.0 | 23 | 9.9 | 23 | 9.9 | 5.108 | 0.276 |
| | No | 25 | 21.4 | 37 | 31.6 | 21 | 17.9 | 13 | 11.1 | 21 | 17.9 | | |
| The packaging must have a | Yes | 74 | 23.4 | 108 | 34.2 | 67 | 21.2 | 31 | 9.8 | 36 | 11.4 | 7.330 | 0.119 |

| | | | | | | | | | | | | | |
|---|-----|----|------|-----|------|----|------|----|------|----|------|-------|-------|
| label indicating the contents. Optimal use and storage conditions of the product. | No | 9 | 26.5 | 9 | 26.5 | 3 | 8.8 | 5 | 14.7 | 8 | 23.5 | | |
| The packaging design should best represent the product and be easy to use. | Yes | 73 | 23.4 | 106 | 34.0 | 62 | 19.9 | 32 | 10.3 | 39 | 12.5 | 0.415 | 0.981 |
| | No | 10 | 26.3 | 11 | 28.9 | 8 | 21.1 | 4 | 10.5 | 5 | 13.2 | | |
| When I buy a packaged product and bring it home. I put it packaged in the cupboard. | Yes | 62 | 24.9 | 88 | 35.3 | 49 | 19.7 | 23 | 9.2 | 27 | 10.8 | 4.473 | 0.346 |
| | No | 21 | 20.8 | 29 | 28.7 | 21 | 20.8 | 13 | 12.9 | 17 | 16.8 | | |
| When buying. I pay attention to the production and expiration date on the packaging. | Yes | 74 | 22.8 | 107 | 33.0 | 69 | 21.3 | 33 | 10.2 | 41 | 12.7 | 5.351 | 0.253 |
| | No | 9 | 34.6 | 10 | 38.5 | 1 | 3.8 | 3 | 11.5 | 3 | 11.5 | | |
| If I notice any change in the smell, color, or taste of the product. I stop consuming it. | Yes | 78 | 23.3 | 113 | 33.7 | 69 | 20.6 | 35 | 10.4 | 40 | 11.9 | 4.895 | 0.298 |
| | No | 5 | 33.3 | 4 | 26.7 | 1 | 6.7 | 1 | 6.7 | 4 | 26.7 | | |
| If I see that the product is infested during storage. I stop consuming it. | Yes | 62 | 23.2 | 94 | 35.2 | 53 | 19.9 | 26 | 9.7 | 32 | 12.0 | 1.829 | 0.767 |
| | No | 21 | 25.3 | 23 | 27.7 | 17 | 20.5 | 10 | 12.0 | 12 | 14.5 | | |
| The characteristics of packaged products and products sold in the open are the same. | Yes | 40 | 26.3 | 54 | 35.5 | 29 | 19.1 | 14 | 9.2 | 15 | 9.9 | 3.098 | 0.542 |
| | No | 43 | 21.7 | 63 | 31.8 | 41 | 20.7 | 22 | 11.1 | 29 | 14.6 | | |
| I know that the storage temperature should be 18°C, and the humidity should not be above 65%. | Yes | 56 | 27.2 | 66 | 32.0 | 34 | 16.5 | 25 | 12.1 | 25 | 12.1 | 7.632 | 0.106 |
| | No | 27 | 18.8 | 51 | 35.4 | 36 | 25.0 | 11 | 7.6 | 19 | 13.2 | | |

* $p \leq 0.05$

Table 11. The relationship between participants' packaging and storage preferences and the frequency of consumption of the preferred product

| | | Daily (%) | | Weekly (%) | | Biweekly (%) | | Monthly (%) | | X ² | p |
|--|-----|-----------|------|------------|------|--------------|------|-------------|------|----------------|--------|
| Prefer no foreign matter in bulgur and its derivatives (stones, soil, etc.). | Yes | 70 | 21.9 | 168 | 52.7 | 48 | 15.0 | 33 | 10.3 | 3.086 | 0.379 |
| | No | 3 | 9.7 | 18 | 58.1 | 5 | 16.1 | 5 | 16.1 | | |
| Producing own bulgur and its derivatives from bulgur at home. | Yes | 48 | 25.1 | 95 | 49.7 | 25 | 13.1 | 23 | 12.0 | 6.314 | 0.097 |
| | No | 25 | 15.7 | 91 | 57.2 | 28 | 17.6 | 15 | 9.4 | | |
| Buying bulgur and its derivatives in bulk | Yes | 41 | 28.7 | 65 | 45.5 | 25 | 17.5 | 12 | 8.4 | 11.996 | 0.007* |
| | No | 32 | 15.5 | 121 | 58.5 | 28 | 13.5 | 26 | 12.6 | | |
| Buying bulgur and its derivatives packed | Yes | 63 | 24.4 | 132 | 51.2 | 36 | 14.0 | 27 | 10.5 | 7.749 | 0.051 |
| | No | 10 | 10.9 | 54 | 58.7 | 17 | 18.5 | 11 | 12.0 | | |
| Knowing packaging materials used (cellophane, pp, paper, cloth, or sack). | Yes | 57 | 24.1 | 135 | 57.0 | 30 | 12.7 | 15 | 6.3 | 22.459 | 0.000* |
| | No | 16 | 14.2 | 51 | 45.1 | 23 | 20.4 | 23 | 20.4 | | |
| Knowing the differences between packaging materials | Yes | 52 | 22.3 | 135 | 57.9 | 28 | 12.0 | 18 | 7.7 | 14.525 | 0.002* |
| | No | 21 | 17.9 | 51 | 43.6 | 25 | 21.4 | 20 | 17.1 | | |
| Putting packaged products in the cupboard | Yes | 61 | 24.5 | 125 | 50.2 | 34 | 13.7 | 29 | 11.6 | 8.647 | 0.034* |
| | No | 12 | 11.9 | 61 | 60.4 | 19 | 18.8 | 9 | 8.9 | | |
| Paying attention to production/expiration dates | Yes | 73 | 21.8 | 175 | 52.2 | 53 | 15.8 | 34 | 10.1 | 10.452 | 0.015* |
| | No | 0 | 0.0 | 11 | 73.3 | 0 | 0.0 | 4 | 26.7 | | |
| Believing packaged and sold in bulk products are the same | Yes | 53 | 25.7 | 114 | 55.3 | 21 | 10.2 | 18 | 8.7 | 16.319 | 0.001* |
| | No | 20 | 13.9 | 72 | 50.0 | 32 | 22.2 | 20 | 13.9 | | |

*p≤"0.05

Thinking that the properties of packaged products and openly sold products are the same: The rates of thinking that the properties of packaged products and openly sold products are the same showed a significant difference according to the frequency of consumption (p=0.001). The rate of those who hold this view is higher among those who consume once a week.

There was no significant difference between the rates of knowledge of other items and income levels. These results show that consumers have different awareness and habits about packaging and storage preferences according to their consumption frequency. Those who consume every day are especially careful and conscious about packaging and storage. These data provide important information for future studies on consumer habits and packaging strategies.

4. Conclusion

The data obtained in this study demonstrate that Turkish consumers exhibit a strong preference for packaged products and demonstrate a high level of attention to the information presented on the packaging, particularly with regard to production and expiration dates. While these findings suggest an increase in consumer awareness, no concrete data were identified to assess the direct impact of technological innovations and product diversity on this awareness. Nevertheless, consumer behavior regarding packaging and storage preferences offers some insight into the potential impact of technological developments and increased product variety. The fact that the majority of consumers prefer packaged products and are aware of the information about these products indicates

a growing awareness among consumers in general. However, to reach a more definitive conclusion on this issue, further research is needed that directly examines the effects of technological innovations and product variety on conscious consumption. In the Kahramanmaraş region, bulgur and bulgur products are still manufactured using the traditional home production technique, which has been in use for centuries. The products were ready for sale in sacks or in bulk, in cloth bags, or in polymer packages with various features. The purchased products are then stored in tin cans, glass jars, cloth bags, or in the polymer packages in which they were purchased. The survey results show that consumers prefer to store bulgur and bulgur products in the same package in which they bought them. These items should be stored in a cool and dry place. However, consumers lack sufficient information about the nutritional and health benefits of these products. Providing this information should be the responsibility of authorized individuals. Additionally, consumers should not be aware of the impact of the packaging materials used on the product features. The findings of the thesis study indicate that bulgur and fine bulgur are widely consumed products, with a preference for the latter in urban areas of the Kahramanmaraş province. In the course of the research, 350 households were surveyed in person, and the consumption habits, packaging preferences, and storage conditions of the participants were examined. The results of the statistical analysis indicated that 75% of the participants consume bulgur at least once a week, with 60% of them including it in their families' daily diet. Furthermore, 40% of respondents typically consume bulgur openly or as it is produced in their own homes, while 35% prefer products packaged in polymer bags. These findings indicate that bulgur is a significant food item in Kahramanmaraş province, with consumption habits largely based on traditional methods. However, it was revealed that consumers lack sufficient knowledge about the effects of packaging materials on shelf life, underscoring the need for increased awareness of this issue. It is recommended that after consumers become aware of this, incentive policies and practices should be developed to determine their preferences, and they can develop new packaging systems to eliminate deterioration of the products by insects, light, etc.

Based on the identified gaps in consumer knowledge, the following policy recommendations might be proposed:

- A.** For companies: Develop marketing campaigns that emphasize the nutritional benefits of bulgur, such as its high fiber and vitamin content. Introducing innovative packaging designs that highlight these health benefits could attract more health-conscious consumers.
- B.** For government institutions: Launch public awareness programs to educate consumers about the health benefits of bulgur and other traditional foods. Nutrition labeling requirements could also be enforced to improve consumer understanding.
- C.** For non-governmental organizations: Work with local communities to organize workshops on traditional bulgur production methods and their nutritional value. These initiatives can help bridge the knowledge gap, especially among younger generations.

The key findings of this study could be summarized as follows:

- A.** A significant portion of consumers prefer packaged bulgur due to its hygiene and longer shelf life.
- B.** Many consumers are unaware of the nutritional value of bulgur, suggesting a need for better consumer education.
- C.** Bulk purchases and home production remain common, particularly among older generations, indicating a cultural element in bulgur consumption patterns.

Ethics Permissions

The appropriate protocols were utilized to protect the rights and privacy of all participants during the execution of the research and were approved by the Science and Engineering Ethics Committee of Gaziantep University (Protocol no: 006, 26/02/2024). In this study, participation was not mandatory, and the research requirements and risks were fully disclosed. All participants provided verbal consent and had the option to withdraw from the study at any time.

Author Contributions

Reyyan Şimşek: Writing- Original draft preparation, Formal analysis, Investigation, Statistical Analysis. Validation.

Sevim Kaya (Corresponding author): Project administration, Conceptualization, Writing-Reviewing and Editing.

Conflict of Interest

The authors declare that they have no known competing financial interests or personal relationships that could have appeared to influence the work reported in this paper.

References

- Bayram, M., 2007. Application of bulgur technology to food aid programs. *Cereal Foods World*, 52(5), 249-256.
- Belibağlı, K. B., Vardin, H. and Dalğıç, A.Ç. (2009). Bulgur işlemede gıda güvenliği ve kalite yönetim sistemlerinin uygulanması. *Italian Journal of Food Science/Rivista Italiana di Scienza degli Alimenti*, 21(4), 509-516.
- Bilgiçli, N. and Soylu, S. (2016). Buğday ve un kalitesinin sektörel açıdan değerlendirilmesi. *Bahri Dağdaş Bitkisel Araştırma Dergisi*, 5(2), 58-67.
- Dönmez, E., Salantur, A., Yazar, S., Akar, T. and Yıldırım Y., (2004). Situation of bulgur in Turkey and cultivar development for bulgur. *Tarla Bitkileri Merkez Araştırma Enstitüsü Dergisi*, 13(1-2).
- Gupta, O. P., Kumar, S., Pandey, A., Khan, M. K., Singh, S. K., and Singh, G. P. (Eds.). (2023). Wheat science: Nutritional and anti-nutritional properties, processing, storage, bioactivity, and product development. *CRC Press*.
- Gökkaya Erdem, B., Masri, B., and Kaya, S. (2023). Determining the factors affecting drinking milk consumption habits in Turkey: The example of Gaziantep province. *Harran Üniversitesi Mühendislik Dergisi*, 8(3), 198-216. <https://doi.org/10.46578/humder.1367836>.
- Kayaoğlu, A., and Gülmez, Y. S. (2022). Determination of factors affecting consumers' bulgur consumption preferences. *Anemon Muş Alparslan Üniversitesi Sosyal Bilimler Dergisi*, 10(2), 869-885.
- Kasar, H., Gokmen, S. and Çağlar, A. (2021). Farklı pişirme tekniklerinin bazı geleneksel fırın ürünlerinin duyu kalitelerini geliştirmede ve besin kayıplarını azaltmada kullanılabilirlikleri üzerine bir araştırma. *Avrupa Bilim ve Teknoloji Dergisi*, (28), 70-74.
- Michel, S., and Bayram, M. (2024). Influence of cooking water hardness on the chemical, color and textural characteristics of bulgur at different processing stages. *Journal of Cereal Science*, 115, 103826
- Özbay, M., Karataş, M. and Asim, M. A. (2016). Determination of different demographic, socio-economic factors on bulgur consumption in Karaman. *Journal of Applied Biological Sciences*, 10(3), 53-60.
- Saad, I. Y., Bayram, M., and Kesen, S. (2018). Characterization of volatile compounds of bulgur (Antep type) produced from durum wheat. *Hindawi Journal of Food Quality*, 2018(1), 8564086. <https://doi.org/10.1155/2018/8564086>.
- Sumiahadi, A., Mülayim, M., Acar, R., and Dağdaş, B. (2020). Tahılların depolanmasında genel prensipler ve çeltiğin depolanması. *Bitkisel Araştırma Dergisi Journal of Bahri Dagdas Crop Research*, 9(1), 102-112.
- Tekin-Cakmak, Z. H., Ozer, C., Ozkan, K., Yildirim, H., Sestili, F., Jilal, A., Sagdic, O., Ozgolet, M., and Koksel, H. (2024). High-beta-glucan and low-glycemic index functional bulgur produced from high-beta-glucan barley. *Journal of Functional Foods*, 112, 105939. <https://doi.org/10.1016/j.jff.2023.105939>.
- Xie, Y. (2017). *Research on grains packaging design and consumer preferences*. Conference: In 2017 7th International Conference on Mechatronics, Computer and Education Informationization (MCEI 2017) (pp.225-336). Atlantis Press. 10.2991/mcei-17.2017.73.
- Yılmaz, M. S., and Yıldırım, A. (2020). Firik üretim teknikleri ve fonksiyonel özellikleri. *Harran Üniversitesi Mühendislik Dergisi*, 5(2), 109-121.

A Hybrid Plant-Soil Electrical Analogy and Control Engineering Framework for Dynamically Modeling Cancer Cell Growth in an Elastic Environment

Bayram Arda KUŞ^{1*}, Mustafa GÜRBÜZ²

Keywords

Cancer cell growth modeling, Plant-soil analogy, Control engineering, Dynamic mathematical models, Tumor growth simulations, Therapeutic conditions, Nonlinear simulation models

Abstract – This research introduces a novel approach to cancer cell growth modeling by integrating principles from the plant-soil analogy and control engineering. The proposed model offers a flexible alternative to traditional dynamic mathematical models, enabling simulations of tumor growth under therapeutic conditions. The simulator, operational on an annual basis, considers diverse patient characteristics and treatment approaches. Nonlinear simulation models provide a comprehensive comparison, showcasing trajectory and precision improvements relative to conventional time-dependent dynamic mathematical models. The study further proposes an elastic cancer modeling mechanism, exploring optimal drug dosage concentrations and patient resistance to cancer drugs. A dynamic model is introduced to identify optimal dosages and frequencies for cancer drugs, demonstrating enhanced operational flexibility through computer simulations. The proposed elastic modeling mechanism is validated through existing mathematical growth models, revealing its practical value within ethical constraints. This research offers a promising path for developing effective therapeutic strategies in cancer tumor growth.


1. Introduction

In the realm of biomedical research, classical cell lines and animal models have played a pivotal role, significantly advancing our understanding of cellular signaling pathways, drug target identification, and the design of therapeutics for diseases like cancer and infectious diseases during the late 20th and early 21st centuries (Bähr and Wolf, 2012; Brodaczewska et al., 2016; Gurumurthy and Kent Lloyd, 2019; Lee et al., 2018). However, challenges arise in translating findings from model systems to humans, with recent studies emphasizing the importance of human-specific biological processes (Fischer, 2008). In response to these challenges, human in vitro 3D cell culture approaches, particularly organoids, have attracted attention as promising tools to overcome limitations associated with traditional models (Bernard et al., 2012; LaBarbera et al., 2012).

While prior attempts, such as 2D cell cultures, bio-printing, and microfluidic devices, have shown potential in drug screening and disease research, organoids stand out due to their self-organizing 3D structure that closely resembles human organs (Hrynevich et al., 2023; Ma et al., 2018; Mi et al., 2018). Generated from pluripotent or adult stem cells, organoids replicate human development or regeneration, providing valuable insights into these processes, as well as serving as effective models for studying diseases (Hrynevich et al., 2023; Verfaillie, 2002; Young and Black, 2004).

Concurrently, understanding and predicting the growth patterns of solid tumors remain paramount in cancer research (Gerlee, 2013). Despite numerous theories, achieving consensus on these growth patterns has proven elusive. Accurate tumor growth models are essential for evaluating screening methods, optimizing radiation treatment protocols, and making informed decisions about patient treatment (Friberg and Mattson, 1997; Michaelson et al., 1999; Sachs et al., 2001).

^{1*}Corresponding Author. İlbank Gaziantep Regional Directorate, Gaziantep, Turkey. E-mail: akus@ilbank.gov.tr  OrcID: 0000-0002-0921-9418

²Adana City Training and Research Hospital, Adana, Turkey. E-mail: drgurubuz123@gmail.com  OrcID: 0000-0001-7680-4142

Citation: Kuş, B. A. and Gürbüz, M. (2024). A hybrid plant-soil electrical analogy and control engineering framework for dynamically modeling cancer cell growth in an elastic environment. *Natural Sciences and Engineering Bulletin*, 1(2), 57-77.

Observing the growth of solid tumors effectively, especially prior to therapeutic interventions, requires volumes exceeding 1mm^3 , representing a critical step in carcinogenesis (Sachs et al., 2001). The expansion to neoplasm size, driven by the upregulation of cell division in malignant cells, is a fundamental observation in cancer studies (Hanahan and Weinberg, 2011).

The multicellular tumor spheroids (MTS) culture technique emerges as a valuable experimental paradigm, providing insights into the prevascular phase of tumor growth without the confounding effects of tumor-host interactions (Sutherland, 1988). This technique facilitates the exploration of three-dimensional cell-cell interactions that regulate tumor growth. Spheroids, by providing oxygen and nutrients through their surface, result in the formation of necrotic cells at the tumor's core (Sutherland, 1988).

The Machine Conception of the Cell (MCC), adopting an analogical approach for cell discussions based on various analogies between machines and organisms, has been instrumental in understanding cellular dynamics (Nicholson, 2019). Mathematical cancer modeling, spanning over five decades, has explored continuous, discrete, or hybrid combinations based on a physical representation of key biological components (Al-Tuwairqi et al., 2020; Altrock et al., 2015; Cunningham et al., 2018; Dhoruri et al., 2020; Hartung et al., 2014; He et al., 2020; Jarrett et al., 2018; Lo et al., 2013; Marušić, 1996; Piantadosi et al., 1983; Rivaz et al., 2019; Vallverdú et al., 2018; West and Newton, 2019).

The highly nonlinear and multimodal nature of cancer tumor growth and treatment poses significant challenges, particularly in therapeutic conditions (Friberg and Mattson, 1997). Identifying optimal or sub-optimal solutions in the same system becomes complex due to multiple constraints and competing objectives (Guocheng et al., 2011; Yang et al., 2021)

Despite extensive efforts, accurately simulating tumor progression remains a formidable challenge (Buosi et al., 2024; Das et al., 2024; Hussein et al., 2024; Zhang et al., 2024). Various growth functions have been proposed in ecological and epidemiological research (Sethanan et al., 2023), yet a comprehensive model for cancer cell growth through computer simulations is still elusive (Hanahan and Weinberg, 2011).

This study endeavors to address this complexity by considering personal and therapeutic variables, employing an electrical simulation across a broad spectrum. The proposed three-layered electrical model, analogous to cancer cell growth in the MTS culture technique, symbolizes cancer cell growth as an electrical circuit comprising resistors, capacitors, and inductors. Inspired by the soil-plant model, the electrical analogy provides an effective means to convert non-electrical systems into electrical systems for accurate and efficient solutions (Anayochukwu, 2013; Hunt et al., 1991; Jakubaszek and Stadnik, 2019; Molz and Remson, 1970; Ruggiero et al., 1999; Stirzaker and Passioura, 1996; van Bavel, 1996)

This article is structured as follows: Section 2 presents the problem formulation, materials and methods, including discussions on mathematical derivations of cancer cell growth models based on electrical analogies, electrical model structure, and similarities with the plant-soil method, and advancements in cancer cell growth. Section 3 graphically represents simulation results and discusses simulator performance. Section 4 delves into the model's results and potential advantages in depth, and Section 5 provides concluding observations and recommendations for future research.

This comprehensive exploration integrates diverse aspects of biomedical research, ranging from advanced cell culture techniques and tumor growth dynamics to mathematical modeling and electrical analogies, aiming to contribute to our understanding of cancer and pave the way for improved treatment strategies.

2. Problem Formulation and Methodology

The understanding of mathematical concepts governing complex systems, despite their pivotal role in comprehending natural phenomena, remains incompletely deciphered. Drawing inspiration from Newton's principles, the application of mathematical models encompassing physical, chemical, and biological aspects is deemed essential for a comprehensive understanding of any system (Ducheyne, 2005). Real-world challenges, particularly in biological processes, exhibit intricate complexity. Diverse mathematical models, varying in complexity from basic to highly elaborate, have been formulated to accurately represent these processes, guided by the dynamics of the system and specific modeling requirements (Rivaz et al., 2019).

Initiating the mathematical modeling process involves defining functional specifications, including the purpose, accuracy, boundaries, and time scaling, essential for constructing an effective model. While achieving an exact replication of "actual" behavior through mathematical models is often unfeasible, establishing modeling objectives aids in understanding the requirements and determining the necessary degree of precision (Piantadosi et al., 1983; Stare et al., 2006; West and Newton, 2019). Subsequently, computer simulations are employed to observe the behavior of these models.

2.1. Classical mathematical models

In the realm of tumor growth analysis, classical mathematical models focus on changes in tumor volume over time, employing first-order ordinary differential equations based on initial assumptions. This section presents commonly referenced tumor growth models found in the literature.

2.1.1. Exponential and Malthusian model

One such model is the exponential growth model shown in Figure 1, which approximates tumor growth for small time values. Equations incorporating intrinsic growth rates, such as the widely used Malthusian model, represent the simplest form of a differential equation describing tumor growth.

$$\frac{dV}{dt} = rV \quad (1)$$

$$V(t) = V_0 e^{rt} \quad (2)$$

The solution for $V(t) = V_0 e^{rt}$, where V_0 is the volume at time 0.

The Malthusian model, initially introduced by Collins (Collins et al., 1956) and extensively applied in various systems, was subsequently employed in the context of cancer cell growth. The utilization of tumor doubling time ($DT = (\ln 2)/r$) served as a quantification of growth rates in their study.

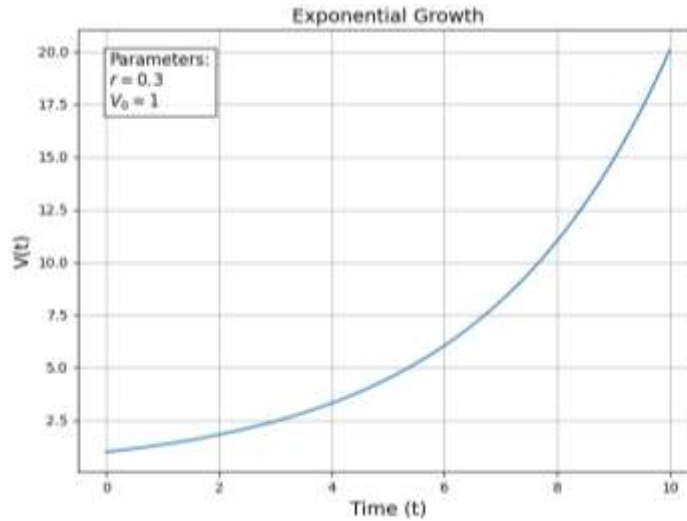


Figure 1. Exponential growth model

The exponential growth law has been found applicable in modeling leukemia, and an investigation involving over 300 untreated lung cancers similarly demonstrated the suitability of exponential growth modeling (Friberg and Mattson, 1997). Particularly advantageous for simulating early tumor growth, this model, however, lacks consideration for spatial limitations and constraints arising from dependencies on nutrients and oxygen (Talkington and Durrett, 2015).

2.1.2. The power law model

Proposed approximately five decades ago (Dethlefsen et al., 1968), the power law differential equation asserts that the rate of increase is proportionate to the volume raised to the power of α , shown in Figure 2.

$$\frac{dV}{dt} = rV(t)^\alpha \tag{3}$$

When α is equal to 1, this model transforms into an equivalent of the exponential growth model. However, for cases where α is less than 1, the equation takes on a different form.

$$V(t) = V_0^{1-\alpha} + ((1 - \alpha)rt)^{1/(1-\alpha)} \tag{4}$$

The power law with linear death formed as follows;

$$\frac{dV}{dt} = rV(t)^\alpha - r \frac{V(t)}{K^{1-\alpha}} = rV^\alpha \left(1 - \left(\frac{V}{K} \right)^{1-\alpha} \right) \tag{5}$$

Comprehending the assumptions and ramifications of these models is essential, as they frequently serve as the underpinning for more intricate tumor growth models (Forys and Marciniak-Czochra, 2003).

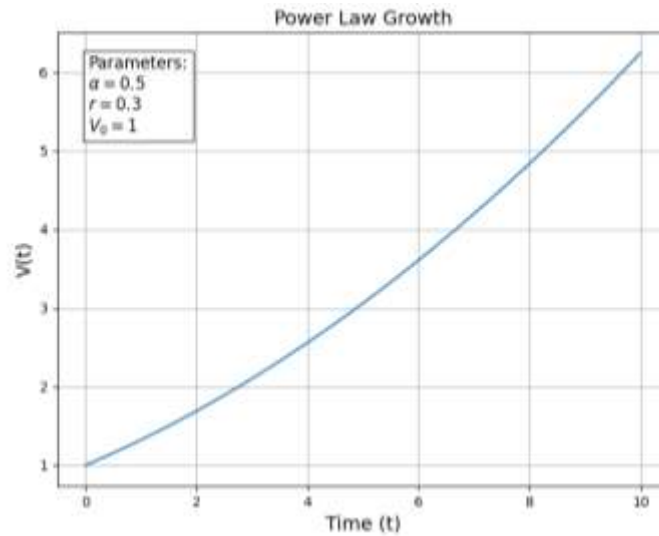


Figure 2. Power law growth model

2.1.3. The Gompertz model

Benjamin Gompertz's research primarily centered on mortality curves in humans, while Wright recognized the suitability of the Gompertz model for biological growth (Gompertz B., 1825) demonstrated in Figure 3. The Gompertz model, as proposed by Gompertz, gained prominence in cancer research, with Laird demonstrating its effectiveness. Wright expressed the alteration in tumor volume through the formulation of a differential equation.

$$\frac{dV}{dt} = \alpha(t)V(t) \text{ where } \frac{d\alpha}{dt} = -r\alpha(t) \tag{6}$$

This equation is solved as follows:

$$V(t) = V_0 \exp\left(\frac{\alpha_0}{r}(1 - e^{-rt})\right) \tag{7}$$

To derive the logistic growth, the first differential equation is

$$\frac{dV}{dt} = rV(t)\log(K/V(t)) \tag{8}$$

where $K = V_\infty = \lim_{t \rightarrow \infty} (V(t))$

The solution of this equation is:

$$V(t) = V_0 \exp(A(1 - e^{-rt})) \quad (9)$$

where $A = \log(V_\infty / V_0)$

$$A = \ln(10^{12}) = 27.631 \quad (10)$$

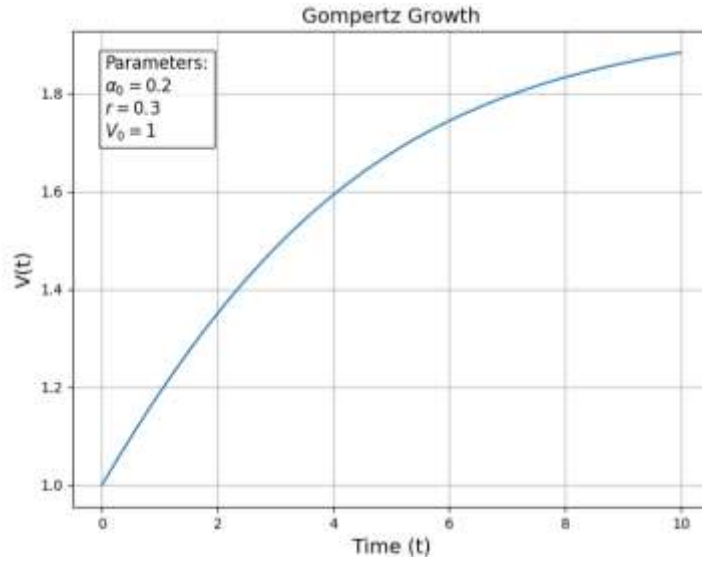


Figure 3. Gompertz growth model

2.1.4. The generalized logistic

The generalization of the logistic model is achieved through interpolating between the Gompertz and logistic models.

$$\frac{dV}{dt} = rV(t) (1 - V(t)/K)^\beta \quad (11)$$

The solution to this equation is:

$$V(t) = K(1 + Q \exp(-\beta rt))^{-1/\beta} \quad (12)$$

where $Q = [(K/V_0)^\beta - 1]$ and K is the carrying capacity, r is the growth rate and V_0 is the initial volume.

When $\beta = 1$, the generalized logistic model simplifies to the standard logistic model. The equation becomes:

$$V(t) = K(1 + Q \exp(-rt))^{-1} \quad (13)$$

with Q reducing to:

$$Q = [(K/V_0) - 1] \quad (14)$$

This paper illustrates diverse graphical representations of models sourced from the literature depicting the progression of tumor mass or volume over time. A spectrum of growth prediction models is accessible, spanning from the elementary single-parameter Exponential model to sophisticated ones such as the Gompertz and Generalized Logistics models (Forys and Marciniak-Czochra, 2003). Additionally, the Fractional Logistic Equation presents another model alternative (Varalta et al., 2014).

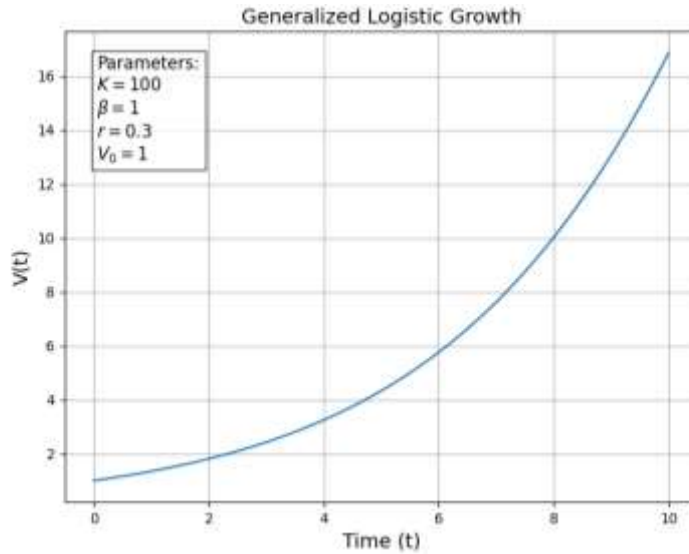


Figure 4. Logistic growth model

Researchers and practitioners often find the generalized logistic differential equation valuable due to its ability to capture more complex growth patterns compared to simpler models. Its application extends to fields such as ecology, where it is used to model population dynamics, and epidemiology, where it may describe the spread of diseases within a population. The generalized logistic differential equation serves as a powerful tool for modeling diverse growth processes, providing a balance between simplicity and flexibility as shown in Figure 4. Its parameters allow for fine-tuning the model to match specific scenarios, making it a valuable asset in the study of dynamic systems across various disciplines.

2.1.5. Bertalanffy growth model

The Bertalanffy Growth Model, proposed by Ludwig von Bertalanffy, is a mathematical representation designed to capture the growth patterns of organisms over time. Introduced as an alternative to simplistic linear or exponential growth models, Bertalanffy's model accounts for the biological principle that growth rates tend to decrease as an organism approaches maturity. This model has found applications in fields such as biology, ecology, fisheries science, and even in understanding the growth trajectories of individual organisms illustrated in Figure 5.

The Bertalanffy Growth Model is typically expressed as:

$$W(t) = W_{\infty} (1 - e^{-k(t-t_0)}) \tag{15}$$

This model is particularly useful when studying the growth of fish, where it has been extensively applied to estimate growth parameters and predict the size distribution of populations. The asymptotic maximum length L_{∞} provides insight into the potential size an organism could reach under optimal conditions, while the growth rate constant k determines how quickly an organism approaches this maximum length.

One notable feature of the Bertalanffy Growth Model is its ability to accommodate non-linear growth patterns, which is often observed in organisms that experience changing environmental conditions or resource availability. This makes it a valuable tool for researchers seeking a more realistic representation of growth dynamics in natural populations.

The Bertalanffy Growth Model has proven to be a versatile and widely applicable tool in the study of biological growth. Its consideration of the asymptotic limit and the decelerating growth rate aligns more closely with the biological realities of many organisms, making it a valuable asset in various scientific disciplines. Researchers continue to refine and adapt this model to address specific challenges and gain deeper insights into the complex dynamics of growth in living organisms.

The von Bertalanffy Growth Model, adapted for fisheries, stands as a cornerstone in fisheries biology, offering a robust framework to comprehend the growth dynamics of fish populations. This model has been tailored to the specific characteristics of fish growth, rendering it a vital tool in fisheries science. Its application extends to the estimation of critical parameters such as asymptotic weight, growth rate, and age at which growth commences

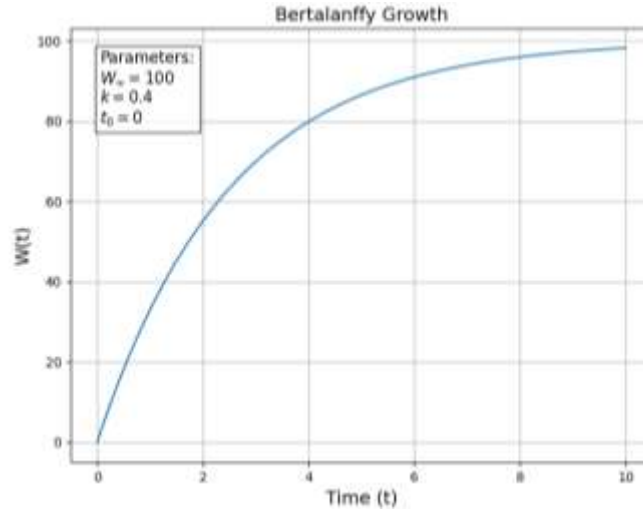


Figure 5. The von Bertalanffy Growth Model

This model plays a pivotal role in elucidating the growth patterns of fish populations over time. Through the estimation of its parameters from observed weight-at-age data, scientists gain valuable insights for fisheries management. The von Bertalanffy Growth Model enables the determination of sustainable harvest levels, evaluation of population structure, and prediction of future size distributions.

2.2. Reaction-diffusion models

Reaction-diffusion models represent a powerful class of mathematical frameworks widely employed to elucidate the spatiotemporal dynamics of various biological phenomena, including cancer tumor growth. These models integrate the effects of local interactions (reaction) and movement across space (diffusion) to capture the complex patterns emerging in biological systems. In this academic text, we delve into the fundamentals and applications of reaction-diffusion models, with a specific focus on their relevance to the understanding of cancer biology.

Reaction-diffusion models are partial differential equations (PDEs) that describe how the concentrations of interacting substances change over both time and space. In the context of cancer biology, these models prove invaluable in simulating the spread of tumor cells and capturing the emergent patterns arising from interactions with the microenvironment.

The general form of a one-dimensional reaction-diffusion equation is given by

$$\frac{\partial u}{\partial t} = D \frac{\partial^2 u}{\partial x^2} + f(u) \tag{16}$$

Here, $u(x, t)$ represents the concentration of a substance (e.g., tumor cells), D is the diffusion coefficient, and $f(u)$ describes the local reaction, often representing processes such as cell proliferation, death, or migration.

2.2.1. Fisher-KPP equation

The Fisher-KPP equation is a classic reaction-diffusion model frequently applied to describe the invasion of a new population into a spatial domain. In the context of tumor biology, this equation is particularly relevant for capturing the spread of cancer cells within tissues. The Fisher-KPP equation is given by:

$$\frac{\partial u}{\partial t} = D \frac{\partial^2 u}{\partial x^2} + ru \left(1 - \frac{u}{K}\right) \tag{17}$$

Here, r represents the net growth rate of the tumor cells, and K is the carrying capacity.

Reaction-diffusion models in cancer research offer a valuable tool for investigating the interplay between local cell behaviors and spatial constraints. These models aid in predicting tumor invasion patterns, understanding the impact of different microenvironmental factors, and evaluating potential therapeutic strategies.

Reaction-diffusion models stand as a valuable and versatile tool in the realm of cancer biology. Their ability to bridge the gap between molecular-level interactions and macroscopic patterns provides a nuanced understanding of tumor growth dynamics, paving the way for more informed strategies in cancer treatment and intervention. As research continues to advance, the refinement and application of reaction-diffusion models will undoubtedly contribute to unraveling the intricacies of cancer biology.

3. Soil-Plant model analogy for cancer cell growth electrical circuit model

The application of mathematical modeling, drawing inspiration from the electrical analogy of water flow through the soil-plant system, can help to gain profound insights into the complex dynamics of cancer tumor growth. By adapting the principles of fluid dynamics and electrical conductivity to the tumor microenvironment, we aim to provide a quantitative framework for understanding nutrient transport, resistance factors, and their impact on cancer cell proliferation.

The concept of plant water uptake was devised to enrich our comprehension of the water transport process from the soil to the leaf. This concept delineates a physiological cycle that unfolds under typical conditions. Various factors, including plant configuration, soil water potential, root circulation, and climatic variables, collectively contribute to the non-steady transient flow within this framework (Zhuang et al., 2014).

In the soil-plant system, the electrical analogy represents water flow through the soil as an electrical concept. Adapting this analogy to cancer biology, we equate nutrient transport within the tumor microenvironment to fluid dynamics, where the movement of nutrients is analogous to the flow of water. A comprehensive mechanistic delineation of transient water uptake is yet to be established. Consequently, a non-steady state biophysical model, rooted in the Electrical Circuit Analogous to Water Flow RLC circuit, has been formulated, as illustrated in Figure 6.

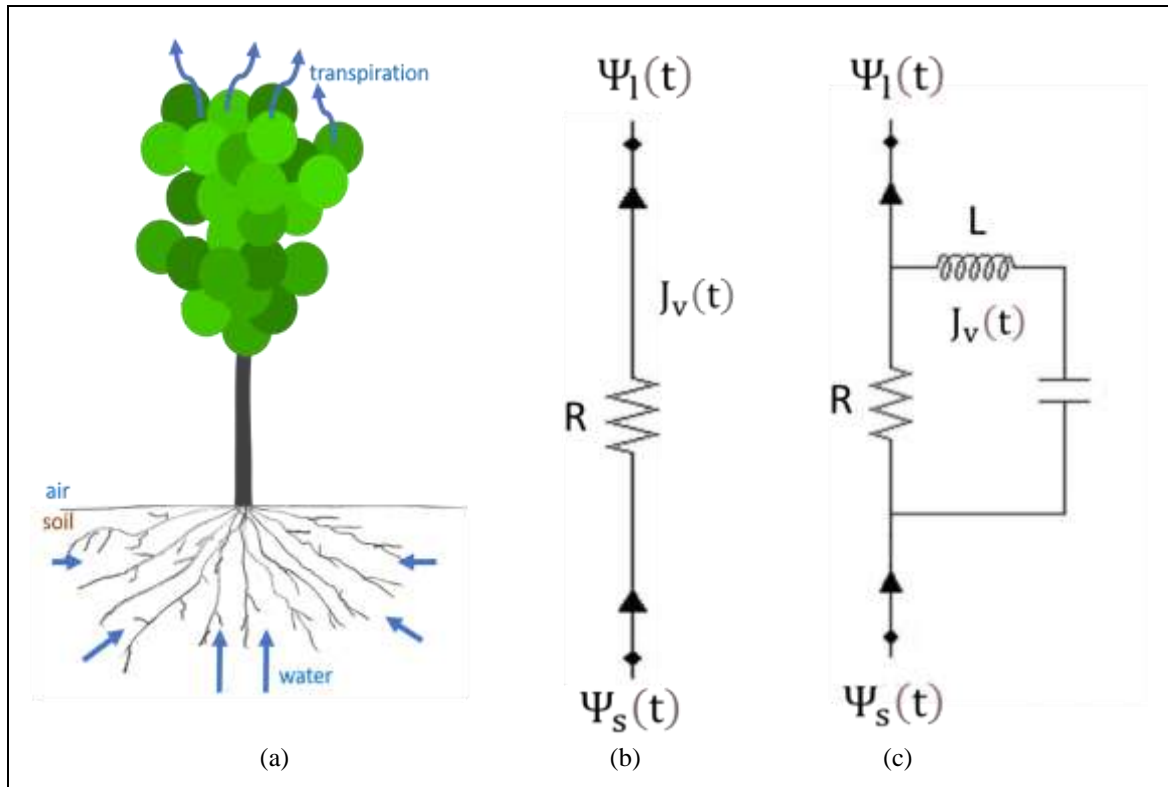


Figure 6. An electrical analogy of water flow through the soil-plant system: (a) soil-plant system, (b) traditional steady state model, and (c) non-steady state model.

Measuring the physiological properties of plants or trees, such as cell wall extensibility, hydraulic resistance, and hydraulic capacitance, poses considerable challenges. Models derived from the electrical analogy of the soil-plant hydraulic method incorporate variable capacitors, inductors, and resistors (Chapman et al., 2012; De Pauw et al., 2008; Hunt et al., 1991). Figure 6 illustrates the water potential difference (Ψ), depicting a positive correlation between soil and leaf water uptake. The observed hysteresis in plant water uptake indicates retardation. A mechanistic approach allows the analysis of changes in uptake rates in response to water stress. In the electrical analogy, resistances influence the flow of current. Similarly, in cancer biology, resistances to nutrient diffusion play a crucial role. These resistances can be mathematically represented as barriers impacting the movement of nutrients within the tumor microenvironment.

Similar to the soil-plant model, the Multicellular Tumor Spheroid (MTS) system, depicted in Figure 7, comprises three layers: the necrotic core (I), quiescent (non-proliferating) cells (II), and proliferating cells (III). The growth curves of tumor spheroids can be accurately determined through dense measurements and high precision (Freyei and Sutherland, 1986). In this study, these three layers are regarded as a combination of three distinct sets of electrical components, namely, A variable AC source, an RLC circuit transitioning to a purely resistive load, and another RLC circuit composed of resistance, capacitance, and inductance.

Employing mathematical models that incorporate nutrient transport, resistance factors, and the cellular response to nutrient availability allows us to simulate cancer cell proliferation dynamics. The simulation provides a quantitative representation of how nutrient availability influences tumor growth and potentially guides therapeutic interventions.

Analyzing the cases in these layers provides insights into the growth rate of cancer cells and assists in optimizing chemotherapy doses.

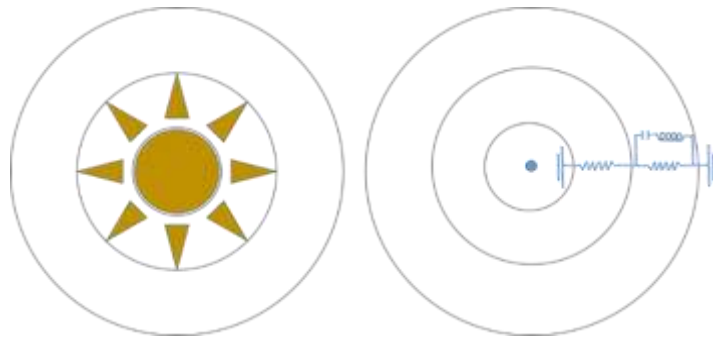


Figure 7. MTS system presentation as a simple electrical circuit (Growth Control in Tumor Dynamics: Bridging Electrical Control Systems and Cancer Intervention Strategies)

This study delves into the utilization of mathematical models to comprehend the mechanisms of infinite growth in tumor development and assess intervention strategies. By incorporating mathematical models that account for nutrient transport, resistance factors, and cellular responses to nutrient availability, we can simulate the dynamics of cancer cell proliferation. This simulation provides a quantitative representation of how nutrient availability influences tumor growth, offering valuable insights into optimizing chemotherapy doses and guiding therapeutic interventions.

In the context of electrical definitions, the treatment of tumor growth aligns with the concept of a closed-loop control system. After delineating the natural conditions of tumor growth within an electrical circuit, configuring it with a control mechanism becomes imperative. This approach allows us to draw analogies between the control of tumor growth and the principles of closed-loop control systems, shedding light on potential strategies for effective intervention and treatment modalities in the pathological condition of uncontrolled proliferation.

The incorporation of this concept not only enhances our understanding of tumor dynamics but also underscores the importance of adopting control strategies to manage and mitigate unregulated proliferation effectively. The analogy drawn between tumor growth and closed-loop control systems provides a conceptual framework that may inform innovative approaches to cancer intervention.

3.1. Model formulation

The following is a typical description of a mass flow of water in the soil-plant concept:

$$J_v(t) = \left(\frac{r^2}{8\eta} \right) \frac{\Delta\Psi(t)}{s} \quad (18)$$

$$J_v(t) = \frac{\Psi_s(t) - \Psi_l(t)}{R_{s-1}(t)} \quad (19)$$

In our examination of the steady-state van den Hornert model, we incorporated the impact of hysteresis by introducing hydraulic capacitance, a concept consistent with prior research. Analogously, in the context of patients undergoing chemotherapy, capacitance is conceptualized as the body's tolerance to the treatment.

$$J_v(t) = \frac{\Psi_s(t) - \Psi_l(t)}{R_{s-1}(t)} - C_h \frac{d\Psi_l(t)}{dt} \quad (20)$$

In the tree-soil concept, the fluctuations in instantaneous water flow rates across various segments of the tree induce an "inductance" effect. This effect has the potential to alter the average driving force of water flow within the plant, a phenomenon analogous to proliferation in the dynamics of cancer cells. As the root water potential declines more rapidly than the soil water potential, the presence of a biological contact potential, functioning akin to a "fuse" in an electrical circuit (Figure 8), is considered susceptible to environmental stress within the tree-soil concept (16) and (17) (Edwards et al., 1986; Ghimire et al., 2016; Jackson et al., 2000; Tuzet et al., 2003; Zweifel et al., 2007).

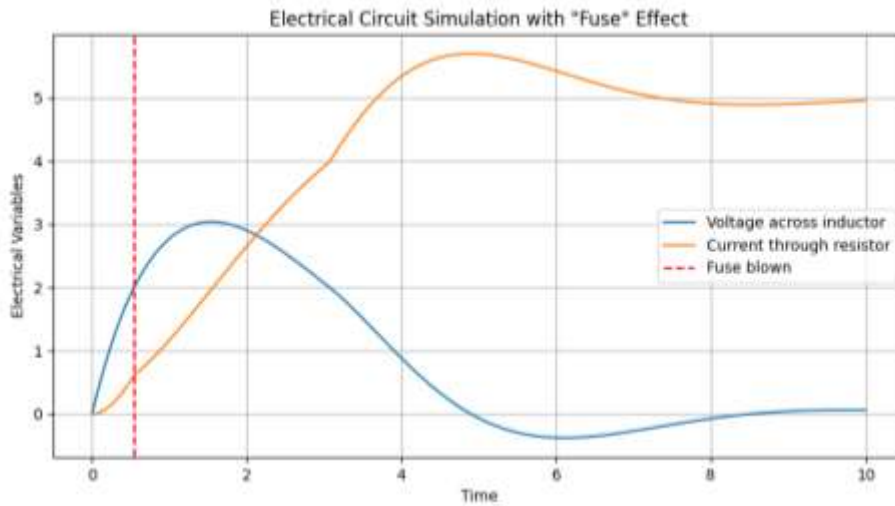


Figure 8. Modeling and Simulation of an Electrical Circuit Analogous to Water Flow in Tree-Soil Systems: Incorporating an Inductance Effect and Environmental Stress Response

$$J_v(t) = \frac{\Psi_s(t) - \Psi_l(t)}{R_{s-1}(t)} - \frac{L dJ_v(t)}{R_{s-1} dt} - C_h \frac{d\Psi_l(t)}{dt} - \frac{A}{R_{s-1}} \quad (21)$$

$$\Delta\Psi_c = - \frac{dJ_v(t)}{dt} \quad (22)$$

The term $\frac{A}{R_{s-1}}$ serves a crucial role in the water flow dynamics between the soil and leaf. Here, A represents a constant related to specific hydraulic properties of the system, reflecting an effective area for water movement. The biological contact potential (A in kg/m/s²) acts similarly to a "fuse" in an electrical circuit. This potential is particularly sensitive to environmental stresses, especially when root water potential decreases more rapidly than soil water potential.

To accurately represent these dynamics, we have integrated the principles of "inductance" and "fuse" into (19), resulting in the formulation of a non-steady state model based on the RCL circuit framework. This model facilitates a comprehensive understanding of the complex interactions between water potentials and flow rates, thereby enhancing our insight into the processes governing water movement within the plant system.

The resistance term R_{s-1} denotes the hydraulic resistance to water flow from the soil to the leaf, which can vary based on factors such as soil moisture content and plant physiology. The expression is similar to a fuse, regulating the flow dynamics by limiting the maximum flow rate that can occur under certain conditions.

Here, L represents the inductance arising from the diversity of leaf water potentials at various plant heights. The term $dJ_v(t)$ acts in opposition to the change in flow rate, signifying the resistance to alterations in flow rate.

$$R_0 = \sqrt{\frac{4L}{C}} \quad (23)$$

$$f = \frac{4L}{2\pi\sqrt{LC}} \quad (24)$$

$$\Psi_s(t) = \frac{\sum_i \lambda_{r,i}(t)\Psi_{s,i}(t)}{\sum_i \lambda_{r,i}(t)} \quad (25)$$

Cancer cell growth models exhibit notable similarities with the tree-soil paradigm, as both can be elucidated using fundamental principles related to electrically conductive materials and growth rates. The mathematical similarity and electrical analogies prevalent in soil-plant modeling literature are applied in this study to mechanistically represent cancer cell proliferation.

The tumor growth mechanism is depicted through the utilization of an RLC circuit. An elevation in the value of dh , attributed to cancer cell activity, indicates a rise in potential energy within the necrotic core. The duration required for treating cancer over a specified period is perceived as an inductive load on the system, depicted in a sample in Figure 9.

A pivotal aspect of the modeling process involves defining an appropriate model structure. This structure captures tumor dynamics by incorporating considerations of initial tumor volume, chemotherapy doses and frequencies, and tumor proliferation.

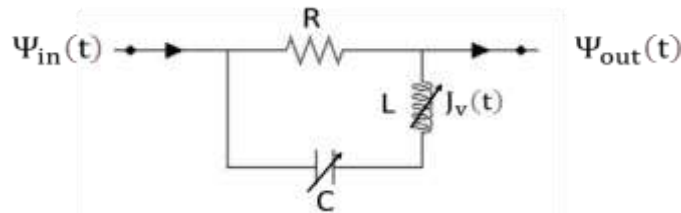


Figure 9. A simple electrical circuit for tumor proliferation modeling

The electrical analogy derived from the soil-tree concept is seamlessly applied to represent tumor growth in (21), and the simulator is depicted in Figure 10. (Zhuang et al., 2014)

$$J_v(t) = \frac{\Psi_{in}(t) - \Psi_{out}(t)}{R_{out-in}(t)} - \frac{LdJ_v(t)}{R_{out-in}dt} - C \frac{d\Psi_{in}(t)}{dt} - \frac{A}{R_{out-in}} \quad (26)$$

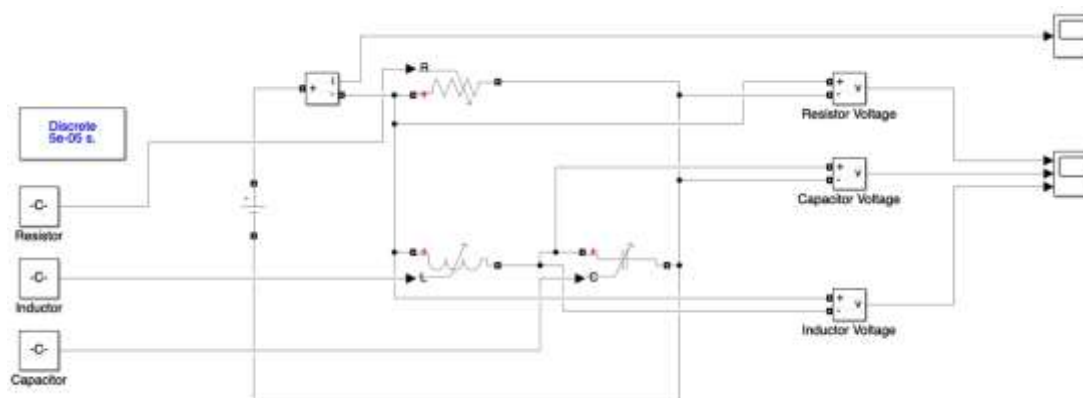


Figure 10. A tumor growth model computer simulator based on electrical analogy

A living cell can be analogized to a piece of machinery, although its intricacy sets it apart from artificially manufactured machines. Despite recent studies utilizing advanced experimental techniques capable of real-time tracking of individual molecules within cells, challenging the conventional engineering perspective of the cell, the machine conception of the cell continues to derive much of its success from the traditional methods employed in molecular biology (Nicholson, 2019).

The dynamics of the tumor system are inherently nonlinear, playing a pivotal role in determining the optimal chemotherapy dose and frequency crucial for effective treatment. Advanced optimal control algorithms have been introduced to investigate tumor treatment under random perturbation conditions. This involves formulating a model-based optimal control problem and integrating it with updated parameters to devise an optimal treatment strategy.

Frequent comparisons of simulation results with actual values allow for the assessment of accuracy, facilitating adjustments to the model to approach the optimal solution. Both system optimization and parameter estimation rely on this iterative approach. Despite variations in the model's reality, the iterative method effectively approximates the optimal solution to the initial optimal control problem.

4. Simulations and Test Results

An indispensable tool for initial design studies, a graphical simulator facilitates the enhancement of treatment strategies by illustrating treatment methodologies in relation to physical performance. At each stage, the evaluation of process block performance is contingent upon patient-specific characteristics. The capability to observe tumor growth simulations across diverse pathologies contributes to the formulation of innovative treatment approaches. The graphical simulator proves instrumental in crafting the most effective and optimized scenarios, guiding preliminary design research.

Moreover, the simulator serves the purposes of forecasting and long-term planning. During the Research and Development stages, therapeutic interventions are simulated through a user-friendly interface. The outcomes of a series of simulations can be extrapolated to similar patients, providing insights into tumor and patient characteristics. Graphs derived from these simulations play a pivotal role in assessing patient performance under therapeutic conditions.

4.1. Benchmark of existing mathematical models with an electrical analogy

The simulator undergoes monthly and annual operations for short-term and long-term tests, respectively. Monthly simulations facilitate the observation of various tumor growth scenarios and the assessment of system dynamics accuracy, while annual simulations offer insights into long-term conditions. The outcomes are then juxtaposed with data obtained from one year of observations based on existing mathematical models.

Current research findings from actual measurements can be treated as system output data based on a nonlinear model. These nonlinear measurements are compared to validate the process model employed in the simulation.

Figure 7 illustrates the Electrical Analogy (EA) method alongside a comparison with the existing exponential growth model, with the results scaled over an annual period. The EA method provides an accurate and observable modeling approach for different tumor growth parameters. However, it is crucial to acknowledge that this model is suitable for demonstrating tumor growth in an infinite space without considering treatment methods and natural conditions.

The notion of unbridled tumor growth proves impractical; the assumption of exponential tumor growth is encumbered by various constraints. Consequently, multiple models have been devised to incorporate saturation limits. Notable examples include the Gompertz and generalized logistic models, which have demonstrated satisfactory outcomes in the scientific literature. The nonlinear model based on the electrical analogy of tumor growth is simulated to achieve an efficient and adaptable treatment approach. This simulator elucidates the optimal configuration of a cancer cell growth model, taking into consideration treatment effects and natural conditions within the human body. The equivalent circuits for tumor growth are dynamically specified.

Within the simulator, the dynamic behavior of the tumor in the analogous electrical model is observed, allowing for the classification of tumor sizes and characteristics. The simulation results of the proposed alternative electrical analogies model are scrutinized and interpreted within the context of existing studies.

Different tumor types may require the utilization of varied models in various studies focused on simulating tumor growth. In Figure 11, the interface of the simulator developed within the scope of this study is presented, enabling a comparative evaluation of the system's exponential growth with the electrical analogy model.

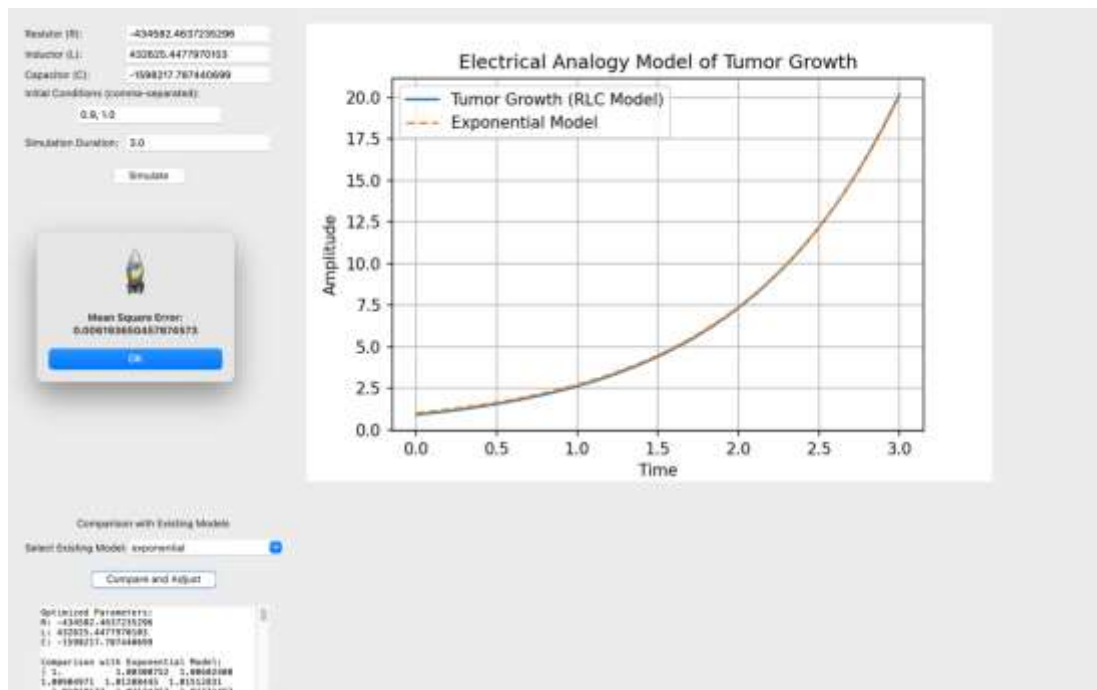


Figure 11. Exponential growth and EA growth performance

Figures 12-17 illustrate power-law and Gompertz models for comparative analysis, respectively. This approach allows for the examination of model effectiveness across different tumor types, contributing to a more comprehensive understanding of tumor growth dynamics in simulation studies.

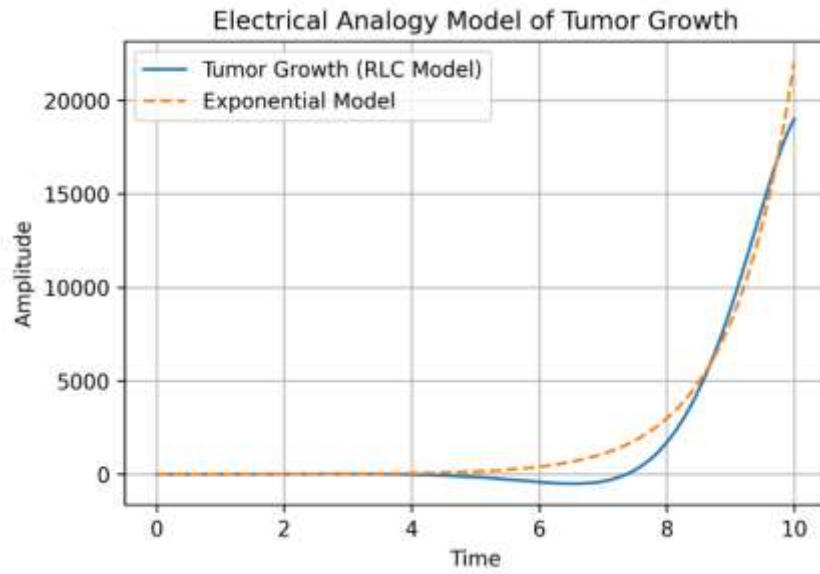


Figure 12. Exponential growth and EA growth performance

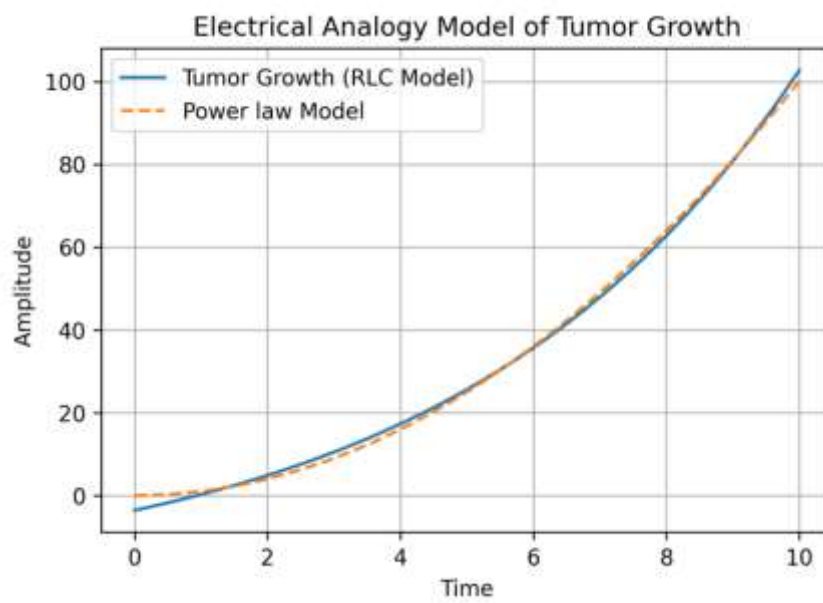


Figure 13. Power Law growth and EA growth performance

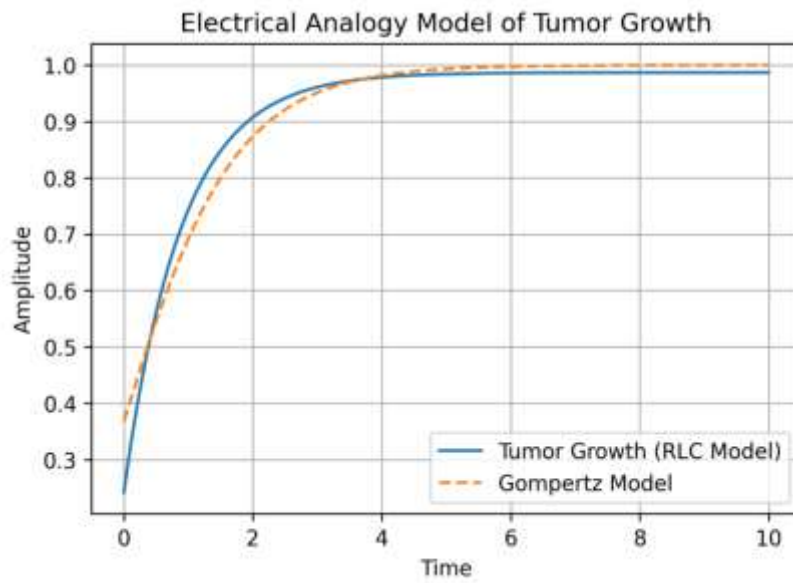


Figure 14. Gompertz growth and EA growth performance

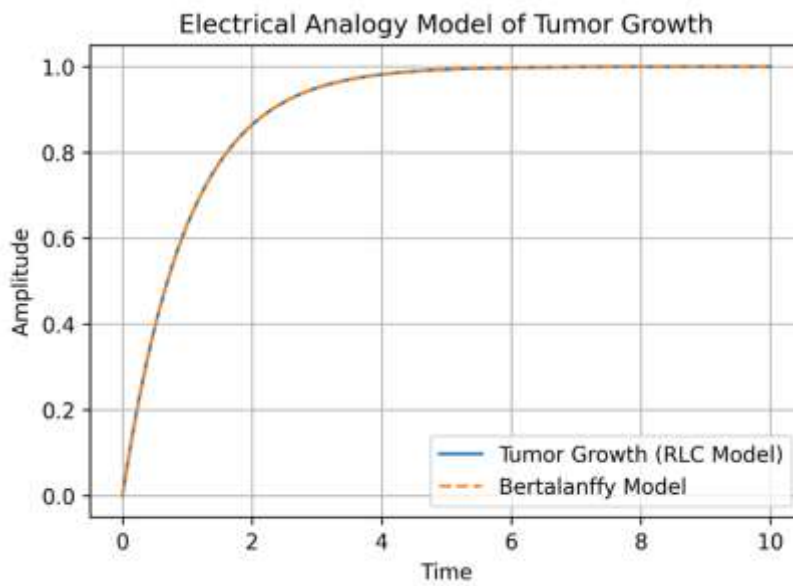


Figure 15. Bertalanffy growth and EA growth performance

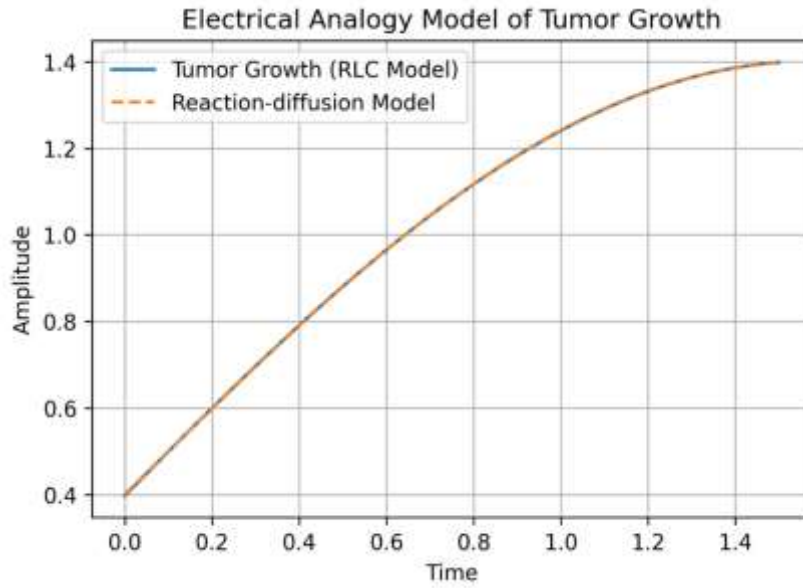


Figure 16. Reaction-diffusion growth and EA growth performance

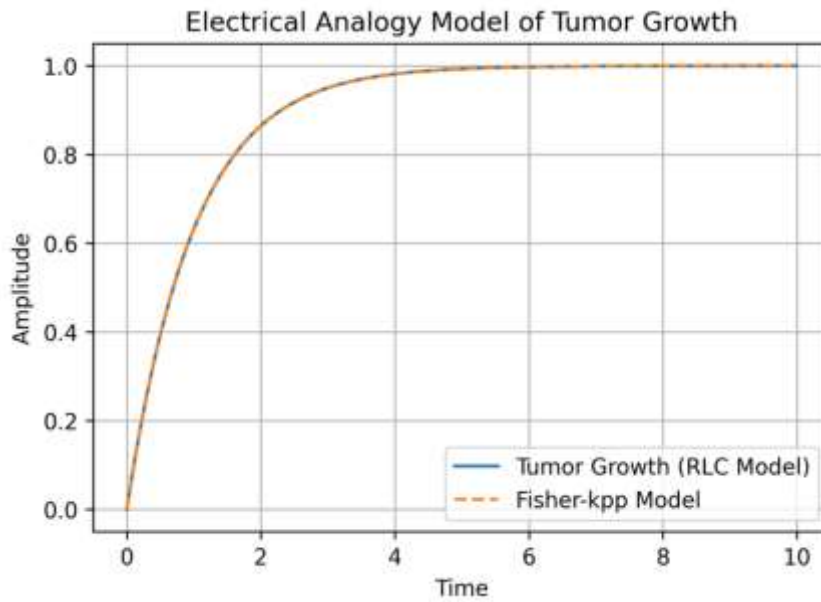


Figure 17. Fisher-KPP growth and EA growth performance

Consequently, Electrical Analogy (EA) emerges as a versatile alternative to create personalized models by incorporating pertinent control parameters into the control structure. Within this control framework, factors like cancer cell types and cell growth rates can be effectively modeled, especially in the presence of therapeutic or external disturbances. This approach is pivotal for formulating precise and dynamic treatment strategies within the framework of control engineering.

$$MSE = \frac{1}{n} \sum_{i=1}^n (y_i - \hat{y}_i)^2 \tag{27}$$

where n is the total number of observations, y_i is the observed value (actual data), \hat{y}_i is the predicted value (model output).

Table 1. Comparison of Tumor Growth Models: Mean Square Error Analysis

| Existing Tumor Growth Models | Mean Square Error |
|------------------------------|-------------------|
| Exponential | 0.0061 |
| Power Law | 0.0059 |
| Gompertz | 0.048 |
| Bertalanffy | 0.0093 |
| Reaction-Diffusion Models | 0.0057 |
| Fisher-KPP Equation | 0.0034 |

5. Conclusion and Future Works

The comprehensive integration of principles from the plant-soil analogy and control engineering into mathematical modeling for cancer research presents a novel and dynamic framework for understanding tumor growth. This interdisciplinary approach not only contributes to the theoretical foundation but also holds significant promise in guiding the development of targeted therapeutic strategies in the ongoing battle against cancer.

The research adopts an electrical analogy of water flow through the soil-plant system to construct a cancer cell growth model, providing a quantitative and dynamic representation of tumor development under various treatment methods. In contrast to traditional dynamic mathematical models, this model simulates tumor growth specifically under therapeutic conditions. The simulations consider a range of treatments and patient scenarios, offering insights into the advantages of different treatment strategies and optimal designs for the efficient eradication of cancer cells. The simulator operates annually, incorporating diverse patient characteristics and treatment approaches.

Utilizing nonlinear simulation models allows for a comparative analysis of results in terms of trajectory and precision, providing a valuable alternative to conventional time-dependent dynamic mathematical models. The introduction of a novel elastic cancer modeling mechanism further contributes to the identification of optimal drug dosages and frequencies for cancer treatment. Through computer simulations, the model demonstrates substantial improvements in operational flexibility, showcasing its effectiveness in cancer treatment.

The proposed elastic modeling mechanism is suggested as a case study, demonstrating the practical value of the approach within ethical boundaries. The empirical results highlight that the optimally designed tumor growth system outperforms existing models, emphasizing the pragmatic significance of the study. Consequently, the proposed approach offers a promising avenue for modeling and formulating therapeutic strategies in cancer tumor growth, with potential implications for advancing cancer treatment methodologies.

The current study presents a robust framework for comprehending tumor growth and optimizing therapeutic strategies. However, several promising pathways for future research and exploration warrant attention:

Integration of Multi-Omics Data: The incorporation of multi-omics data, encompassing genomics, transcriptomics, and proteomics, into the existing modeling framework can significantly enhance predictive precision. Future investigations may delve into methodologies to effectively integrate these complex datasets, providing a more nuanced portrayal of the molecular intricacies governing tumor behavior.

Personalized Treatment Approaches: Subsequent research efforts could focus on refining the model to facilitate personalized treatment approaches. This entails tailoring therapeutic strategies based on individual patient characteristics, including genetic profiles, with the objective of optimizing treatment efficacy while minimizing adverse effects.

Incorporation of Immunotherapy: Given the rising prominence of immunotherapy in cancer treatment, future models could benefit from incorporating immune system dynamics. Such an inclusion would allow for an assessment of the synergistic effects between traditional treatments and immunotherapies.

Validation and Clinical Trials: Rigorous validation of the proposed model through both retrospective analyses and prospective clinical trials is imperative. Collaborative efforts with clinical researchers and oncologists will be instrumental in translating theoretical insights into pragmatic applications, ensuring the model's relevance and reliability in real-world clinical scenarios.

Exploration of Drug Resistance Mechanisms: A deeper understanding of drug resistance mechanisms is pivotal for developing effective long-term treatment strategies. Future research could delve into the molecular intricacies underlying resistance and integrate this knowledge into the model for predicting and counteracting emerging resistance patterns.

Continuous Model Refinement: Embracing a dynamic approach, the model should undergo continual refinement to align with advancements in cancer research. This may involve the incorporation of real-time patient data, fine-tuning simulation parameters, and adapting the model to evolving therapeutic paradigms.

Ethical and Social Implications: The ethical dimensions of model development and implementation are paramount. Subsequent research endeavors should address ethical concerns related to patient privacy, consent, and the responsible utilization of predictive models in clinical decision-making.

Global Collaboration: Encouraging collaboration among researchers, clinicians, and institutions on a global scale holds promise for the amalgamation of diverse datasets and perspectives. Such collaborative efforts can lead to more comprehensive models that account for population-specific variations and global trends in cancer biology and treatment.

In summation, prospective research endeavors should strive to augment the precision, applicability, and ethical considerations of cancer growth models. By addressing these areas, researchers can make significant contributions to the evolving landscape of cancer research and facilitate the development of more effective and personalized cancer treatments.

Ethics Permissions

This paper does not require ethics committee approval.

Author Contribution

Bayram Arda Kuş conceptualized the study by identifying the research gap, designed and developed the cancer growth modeling framework, performed simulations, analyzed the outcomes, and drafted the manuscript. Mustafa Gürbüz critically reviewed the manuscript, provided scientific validation, and ensured the methodological rigor and accuracy of the findings. AI-based tools were employed for text revisions and editing.

Conflict of Interest

The authors declare that they have no known competing financial interests or personal relationships that could have appeared to influence the work reported in this paper.

References

- Al-Tuwairqi, S. M., Al-Johani, N. O., and Simbawa, E. A. (2020). Modeling dynamics of cancer radiotherapy. *Journal of Theoretical Biology*, 506, 110405. <https://doi.org/10.1016/j.jtbi.2020.110405>
- Altrock, P. M., Liu, L. L., and Michor, F. (2015). The mathematics of cancer: Integrating quantitative models. *Nature Reviews Cancer*, 15(12), 730–745. <https://doi.org/10.1038/nrc4029>
- Anayochukwu, A. V. (2013). Analogous electrical model of water processing plant as a tool to study “The Real Problem” of process control. *International Journal of Control Theory and Computer Modeling*, 3(1), 1–18. <https://doi.org/10.5121/ijctcm.2013.3101>
- Bähr, A., and Wolf, E. (2012). Domestic animal models for biomedical research. *Reproduction in Domestic Animals*, 47(SUPPL.4), 59–71. <https://doi.org/10.1111/j.1439-0531.2012.02056.x>
- Bernard, A., Kimko, H., Mital, D., and Poggesi, I. (2012). Mathematical modeling of tumor growth and tumor growth inhibition in oncology drug development. *Expert Opinion on Drug Metabolism and Toxicology*, 8(9), 1057–1069. <https://doi.org/10.1517/17425255.2012.693480>
- Brodaczewska, K. K., Szczylik, C., Fiedorowicz, M., Porta, C., and Czarnecka, A. M. (2016). Choosing the right cell line for renal cell cancer research. *Molecular Cancer*, 15:83. BioMed Central Ltd. <https://doi.org/10.1186/s12943-016-0565-8>

- Buosi, S., Timilsina, M., Janik, A., Costabello, L., Torrente, M., Provencio, M., Fey, D., and Nováček, V. (2024). Machine learning estimated probability of relapse in early-stage non-small-cell lung cancer patients with aneuploidy imputation scores and knowledge graph embeddings. *Expert Systems with Applications*, 235, 121127. <https://doi.org/10.1016/j.eswa.2023.121127>
- Chapman, N., Miller, A. J., Lindsey, K., and Whalley, W. R. (2012). Roots, water, and nutrient acquisition: Let's get physical. In *Trends in Plant Science* 17(12), 701–710. <https://doi.org/10.1016/j.tplants.2012.08.001>
- Collins, V. P., Loeffler, R. K., and Tivey, H. (1956). Observations on growth rates of human tumors. *The American Journal of Roentgenology, Radium Therapy, and Nuclear Medicine*, 76(5), 988–1000.
- Cunningham, J. J., Brown, J. S., Gatenby, R. A., and Staňková, K. (2018). Optimal control to develop therapeutic strategies for metastatic castrate resistant prostate cancer. *Journal of Theoretical Biology*, 459, 67–78. <https://doi.org/10.1016/j.jtbi.2018.09.022>
- Das, A. K., Biswas, S. K., Mandal, A., Bhattacharya, A., and Sanyal, S. (2024). Machine learning based intelligent system for breast cancer prediction (MLISBCP). *Expert Systems with Applications*, 242, 122673. <https://doi.org/10.1016/j.eswa.2023.122673>
- De Pauw, D. J. W., Steppe, K., and De Baets, B. (2008). Identifiability analysis and improvement of a tree water flow and storage model. *Mathematical Biosciences*, 211(2), 314–332. <https://doi.org/10.1016/j.mbs.2007.08.007>
- Dethlefsen, L. A., Prewitt, J. M. S., and Mendelsohn, M. L. (1968). Analysis of tumor growth curves. *JNCI: Journal of the National Cancer Institute*, 40(2), 389–405. <https://doi.org/10.1093/JNCI/40.2.389>
- Dhoruri, A., Ratna Sari, E., and Lestari, D. (2020). Mathematical model of tumor cell growth based on age structure. *International Journal of Modeling and Optimization*, 10(2), 57–60. <https://doi.org/10.7763/ijmo.2020.v10.747>
- Ducheyne, S. (2005). Mathematical models in Newton's Principia: A new view of the "Newtonian style." *International Studies in the Philosophy of Science*, 19(1), 1–19. <https://doi.org/10.1080/02698590500051035>
- Edwards, W. R. N., Jarvis, P. G., Landsberg, J. J., and Talbot, H. (1986). A dynamic model for studying flow of water in single trees. *Tree Physiology*, 1(3), 309–324. <https://doi.org/10.1093/treephys/1.3.309>
- Fischer, H. P. (2008). Mathematical modeling of complex biological systems: From parts lists to understanding systems behavior. *Alcohol Research and Health*, 31(1), 49–59. <http://teaching.anhb.uwa.edu.au/mb140/>
- Forys, U., and Marciniak-Czochra, A., (2003). Logistic equations in tumour growth modelling. *International Journal of Applied Mathematics and Computer Science*, 13(3), 317–325.
- Freyei, J. P., and Sutherland, R. M. (1986). Regulation of growth saturation and development of necrosis in emt6/r0 multicellular spheroids by the glucose and oxygen supply. *Cancer Research*, 46(7), 3504–3512.
- Friberg, S., and Mattson, S. (1997). On the growth rates of human malignant tumors: Implications for medical decision making. *Journal of Surgical Oncology*, 65(4), 284–297. [https://doi.org/10.1002/\(SICI\)1096-9098\(199708\)65:4<284::AID-JSO11>3.3.CO;2-2](https://doi.org/10.1002/(SICI)1096-9098(199708)65:4<284::AID-JSO11>3.3.CO;2-2)
- Gerlee, P. (2013). The model muddle: In search of tumor growth laws. *Cancer Research*, 73(8), 2407–2411. <https://doi.org/10.1158/0008-5472.CAN-12-4355>
- Gompertz B. (1825) On the nature of the function expressive of the law of human mortality, and on a new mode of determining the value of life contingencies. In a letter to Francis Baily, Esq. F. R. S. & C. *Philosophical Transactions of the Royal Society of London*, 115, 513–583. <https://doi.org/10.1098/rstl.1825.0026>
- Ghimire, B., Riley, W. J., Koven, C. D., Mu, M., and Randerson, J. T. (2016). Representing leaf and root physiological traits in CLM improves global carbon and nitrogen cycling predictions. *Journal of Advances in Modeling Earth Systems*, 8(2), 598–613. <https://doi.org/10.1002/2015MS000538>
- Guocheng, Z., Huaili, Z., Peng, Z., Shaojie, J., Jiangya, M., and Wenyan, C. (2011). Decision model for optimization of coagulation/flocculation process for wastewater treatment. *2011 Third International Conference on Measuring Technology and Mechatronics Automation*, 821–826. <https://doi.org/10.1109/ICMTMA.2011.207>
- Gurumurthy, C. B., and Kent Lloyd, K. C. (2019). Generating mouse models for biomedical research: Technological advances. *DMM Disease Models and Mechanisms*, 12(1). <https://doi.org/10.1242/dmm.029462>
- Hanahan, D., and Weinberg, R. A. (2011). Hallmarks of cancer: The next generation. *Cell*, 144(5), 646–674. <https://doi.org/10.1016/j.cell.2011.02.013>
- Hartung, N., Mollard, S., Barbolosi, D., Benabdallah, A., Chapuisat, G., Henry, G., Giacometti, S., Iliadis, A., Ciccolini, J., Faivre, C., and Hubert, F. (2014). Mathematical modeling of tumor growth and metastatic spreading: Validation in tumor-bearing mice. *Cancer Research*, 74(22), 6397–6407. <https://doi.org/10.1158/0008-5472.CAN-14-0721>
- He, W., Demas, D. M., Conde, I. P., Shajahan-Haq, A. N., and Baumann, W. T. (2020). Mathematical modelling of breast cancer cells in response to endocrine therapy and Cdk4/6 inhibition. *Journal of the Royal Society Interface*, 17(169). <https://doi.org/10.1098/rsif.2020.0339rsif20200339>

- Hrynevich, A., Li, Y., Cedillo-Servin, G., Malda, J., and Castilho M.,(2023). (Bio) fabrication of microfluidic devices and organs-on-a-chip. In Kalaskar, D.M., (Ed.) *3D Printing in Medicine* (2nd Ed. pp 273-336) Woodhead Publishing.
- Hunt, E. R., Running, S. W., and Federer, C. A. (1991). Extrapolating plant water flow resistances and capacitances to regional scales. *Agricultural and Forest Meteorology*, 54(2–4), 169–195. [https://doi.org/10.1016/0168-1923\(91\)90005-B](https://doi.org/10.1016/0168-1923(91)90005-B)
- Hussein, M., Elnahas, M., and Keshk, A. (2024). A framework for predicting breast cancer recurrence. *Expert Systems with Applications*, 240. <https://doi.org/10.1016/j.eswa.2023.122641>
- Jackson, R. B., Sperry, J. S., and Dawson, T. E. (2000). Root water uptake and transport: using physiological processes in global predictions. *Trends in Plant Science*, 5(11), 482–488. [https://doi.org/10.1016/S1360-1385\(00\)01766-0](https://doi.org/10.1016/S1360-1385(00)01766-0)
- Jakubaszek, A., and Stadnik, A. (2019). Efficiency of sewage treatment plants in the sequential batch reactor. *Civil and Environmental Engineering Reports*, 28(3), 121–131. <https://doi.org/10.2478/ceer-2018-0040>
- Jarrett, A. M., Lima, E. A. B. F., Hormuth, D. A., McKenna, M. T., Feng, X., Ekrut, D. A., Resende, A. C. M., Brock, A., and Yankeelov, T. E. (2018). Mathematical models of tumor cell proliferation: A review of the literature. *Expert Review of Anticancer Therapy*, 18(12), 1271–1286. <https://doi.org/10.1080/14737140.2018.1527689>
- LaBarbera, D. V., Reid, B. G., and Yoo, B. H. (2012). The multicellular tumor spheroid model for high-throughput cancer drug discovery. *Expert Opinion on Drug Discovery*, 7(9), 819–830. <https://doi.org/10.1517/17460441.2012.708334>
- Lee, N. P., Chan, C. M., Tung, L. N., Wang, H. K., and Law, S. (2018). Tumor xenograft animal models for esophageal squamous cell carcinoma. In *Journal of Biomedical Science* (Vol. 25, Issue 1). BioMed Central Ltd. <https://doi.org/10.1186/s12929-018-0468-7>
- Lo, W. C., Martin, E. W., Hitchcock, C. L., and Friedman, A. (2013). Mathematical model of colitis-associated colon cancer. *Journal of Theoretical Biology*, 317, 20–29. <https://doi.org/10.1016/j.jtbi.2012.09.025>
- Ma, J., Wang, Y., and Liu, J., (2018). Bioprinting of 3D tissues/organs combined with microfluidics. *RSC Advances*. 8, 21712-21727.
- Marušić, M. (1996). Mathematical models of tumor growth. *Mathematical Communications*, 1(2), 175–188.
- Mi, S., Du, Z., Xu, Y., and Sun, W. (2018). The crossing and integration between microfluidic technology and 3D printing for organ-on-chips. *Journal of Materials Chemistry B*. 6(39):6191-6206. doi: 10.1039/c8tb01661e.
- Michaelson, J. S., Halpern, E., and Kopans, D. B. (1999). Breast cancer: Computer simulation method for estimating optimal intervals for screening. *Radiology*, 212(2), 551–560. <https://doi.org/10.1148/radiology.212.2.r99au49551>
- Molz, F. J., and Remson, I. (1970). Extraction term models of soil moisture use by transpiring plants. *Water Resources Research*, 6(5), 1346-1356. <https://doi.org/10.1029/WR006i005p01346>
- Nicholson, D. J. (2019). Is the cell really a machine? *Journal of Theoretical Biology*, 477, 108–126. <https://doi.org/10.1016/j.jtbi.2019.06.002>
- Piantadosi, S., Hazelrig, J. B., and Turner, M. E. (1983). A model of tumor growth based on cell cycle kinetics. *Mathematical Biosciences*, 66(2), 283–306. [https://doi.org/10.1016/0025-5564\(83\)90094-9](https://doi.org/10.1016/0025-5564(83)90094-9)
- Rivaz, A., Azizian, M., and Soltani, M. (2019). Various mathematical models of tumor growth with reference to cancer stem cells: A Review. *Iranian Journal of Science and Technology, Transaction A: Science*, 43(2), 687–700. <https://doi.org/10.1007/s40995-019-00681-w>
- Ruggiero, C., De Pascale, S., and Fagnano, M. (1999). Plant and soil resistance to water flow in faba bean (*Vicia faba* L. major Harz.). *Plant and Soil*. <https://doi.org/10.1023/A:1004690101953>
- Sachs, R. K., Hlatky, L. R., and Hahnfeldt, P. (2001). Simple ODE models of tumor growth and anti-angiogenic or radiation treatment. *Mathematical and Computer Modelling*, 33(12-13), 1297-1305. [https://doi.org/10.1016/S0895-7177\(00\)00316-2](https://doi.org/10.1016/S0895-7177(00)00316-2)
- Sethanan, K., Pitakaso, R., Srichok, T., Khonjun, S., Thannipat, P., Wanram, S., Boonmee, C., Gonwirat, S., Enkvetchakul, P., Kaewta, C., and Nanthasamroeng, N. (2023). Double AMIS-ensemble deep learning for skin cancer classification. *Expert Systems with Applications*, 234. <https://doi.org/10.1016/j.eswa.2023.121047>
- Stare, A., Hvala, N., and Vrecko, D. (2006). Modeling, identification, and validation of models for predictive ammonia control in a wastewater treatment plant--a case study. *ISA Transactions*, 45(2), 159–174. [https://doi.org/10.1016/S0019-0578\(07\)60187-6](https://doi.org/10.1016/S0019-0578(07)60187-6)
- Stirzaker, R. J., and Passioura, J. B. (1996). The water relations of the root-soil interface. *Plant, Cell and Environment*, 19(2), 201-208. <https://doi.org/10.1111/j.1365-3040.1996.tb00241.x>
- Sutherland, R. M. (1988). Cell and environment interactions in tumor microregions: The spheroid model. *Science*, 240(4849), 177–184.
- Talkington, A., and Durrett, R. (2015). Estimating tumor growth rates in vivo. *Bulletin of Mathematical Biology*, 77, 1934–1954. <https://doi.org/10.1007/s11538-015-0110-8>

- Tuzet, A., Perrier, A., and Leuning, R. (2003). A coupled model of stomatal conductance, photosynthesis and transpiration. *Plant, Cell and Environment*, 26(7), 1097–1116. <https://doi.org/10.1046/j.1365-3040.2003.01035.x>
- Vallverdú, J., Castro, O., Mayne, R., Talanov, M., Levin, M., Baluška, F., Gunji, Y., Dussutour, A., Zenil, H., and Adamatzky, A. (2018). Slime mould: The fundamental mechanisms of biological cognition. *BioSystems*, 165, 57–70. <https://doi.org/10.1016/j.biosystems.2017.12.011>
- van Bavel, C. H. M. (1996). Water relations of plants and soils. *Soil Science*, 161(4), 257-260. <https://doi.org/10.1097/00010694-199604000-00007>
- Varalta, N., Gomes, A. V., and Camargo, R. F. (2014). A prelude to the fractional calculus applied to tumor dynamic. *Tendências Em Matemática Aplicada e Computacional*, 15(2), 211–221. <https://doi.org/10.5540/tema.2014.015.02.0211>
- Verfaillie, C. M. (2002). Adult stem cells: Assessing the case for pluripotency. *Trends in Cell Biology*, 12(11), 502–508. [https://doi.org/10.1016/S0962-8924\(02\)02386-3](https://doi.org/10.1016/S0962-8924(02)02386-3)
- West, J., and Newton, P. K. (2019). Cellular interactions constrain tumor growth. *Proceedings of the National Academy of Sciences of the United States of America*, 116(6), 1918–1923. <https://doi.org/10.1073/pnas.1804150116>
- Yang, J., Virostko, J., Hormuth, D. A., Liu, J., Brock, A., Kowalski, J., and Yankeelov, T. (2021). An experimental-mathematical approach to predict tumor cell growth as a function of glucose availability in breast cancer cell lines. *PloS one*, 16(7), e0240765. <https://doi.org/10.1371/journal.pone.0240765>
- Young, H. E., and Black, A. C. (2004). Adult stem cells. *Anatomical Record - Part A: Discoveries in Molecular, Cellular, and Evolutionary Biology*, 276(1), 75-102 Wiley-Liss Inc. <https://doi.org/10.1002/ar.a.10134>
- Zhang, C., Jia, D., Li, Z., Wu, N., He, Z., Jiang, H., and Yan, Q. (2024). Esophageal cancer detection framework based on time series information from smear images. *Expert Systems with Applications*, 238. <https://doi.org/10.1016/j.eswa.2023.122362>
- Zhuang, J., Yu, G. R., and Nakayama, K. (2014). A series RCL circuit theory for analyzing non-steady-state water uptake of maize plants. *Scientific Reports*, 4(1), 1–7, 6720. <https://doi.org/10.1038/srep06720>
- Zweifel, R., Steppe, K., and Sterck, F. J. (2007). Stomatal regulation by microclimate and tree water relations: interpreting ecophysiological field data with a hydraulic plant model. *Journal of Experimental Botany*, 58(8), 2113–2131. <https://doi.org/10.1093/jxb/erm050>